สำนักงานวิทยทรัพยากร
จุฬาลงกรณ์มหาวิทยาลัย

CHAPTER II

CHEMICAL CONSTITUENTS AND BIOLOGICAL ACTIVITIES OF THE HEARTWOODS OF *Dalbergia oliveri*

From the preliminary results for biological activities of the extracts of four selected plants, *D. oliveri* was selected for further investigation on chemical constituents and their biological activities since its CH_2Cl_2 and MeOH extracts exhibited excellent radial scavenging effect on DPPH radical.

2.1 INTRODUCTION

2.1.1 Botanical Characteristics of *Dalbergia oliveri* Gamble [44-46]

Family Name: Leguminosae-Papilionoideae

Common Name: Rosewood, Black-wood, Tamalin

Synonyme: *Dalbergia bariensis* Pierre, *Dalbergia dongnaiensis* Pierre, *Dalbergia duperreana* Pierre

Origin: Burma & Thailand

In Thailand *D. oliveri* has been known as Ching Chan. Orther names are Pruduu chingchan, Duu sadaen, Geddaeng, Emeng and orther. The botanical characteristics can be described as follows:

Tree: deciduous tree to 20 (rarely 30) m with delicate foliage and open, spreading crown when mature

Bark: dark gray, rather thick, scaly and flaking in small piece, inner bark yellow, heartwood dark red

Leaves: 15-30 cm, 5-7 (10) pairs of leaflets, 3-8 x 1-3 cm, end leaflet only slightly larger than other, blunt or slightly pointed at both ends, vein network clear. Young leaves pale pink with silky hairs, mature leaves dark grey-green, smooth.

Flowers: ±1.2 cm, purple in bud, later lilac or white, in branched clusters at or near end of twigs, 10-15 cm. Calyx tube 4-5 nm, dull purple, smooth or nearly so, lower tooth much longer than others. Top petal rounded, as wide as long, bottom petal slightly shorter. Stamens in 2 clusters.

Fruit: 9-14 x 2.5-4 cm, narrow and pointed at both ends, smooth, pale brown when dry, much thicker near seeds.

Seed: usually 1, sometimes 2 or 3 seeds, reddish brown.

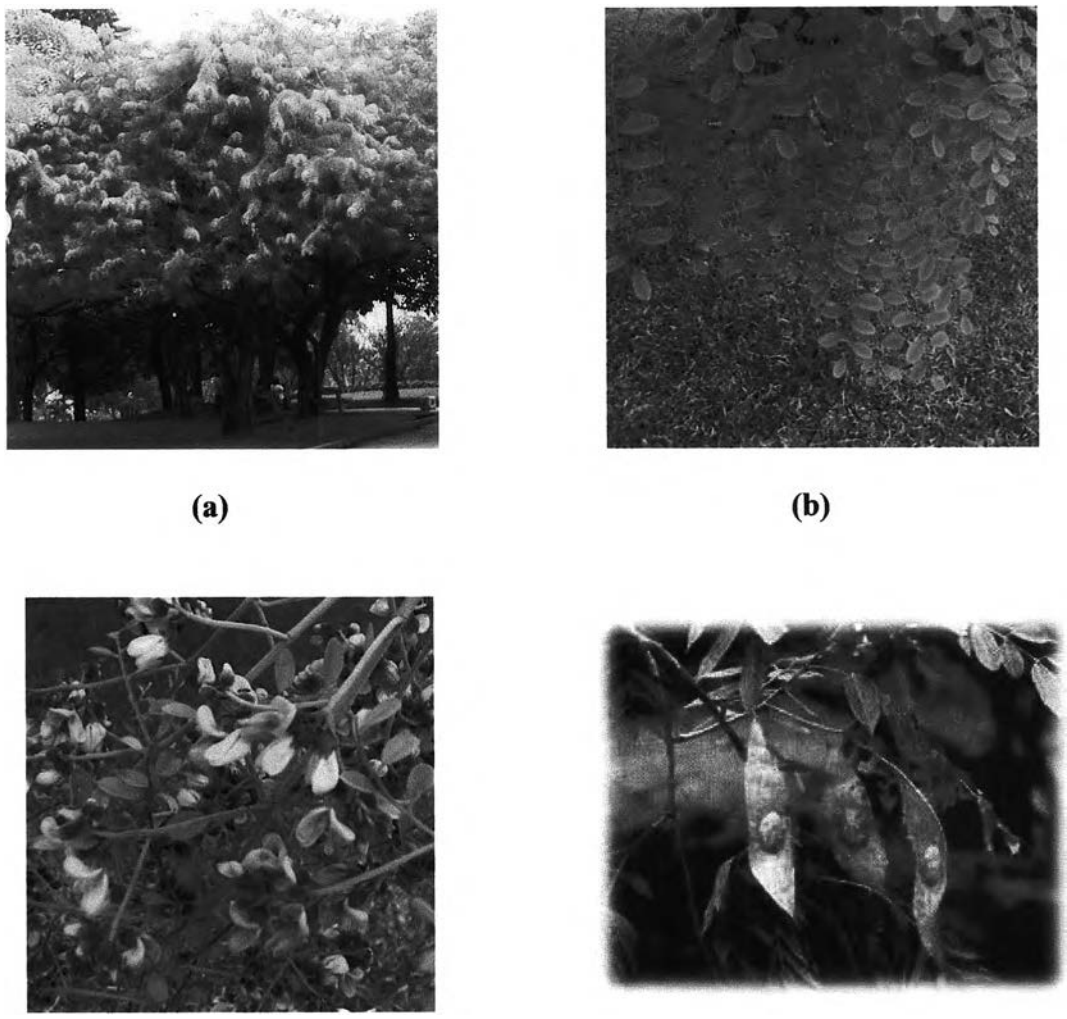

(a) **(b)** **(c)** **(d)**

Figure 2.1 (a) Tree, (b) leaves, (c) flowers and (d) fruit and seeds of *Dalbergia oliveri*

2.1.2 Chemical Constituents and Literature Reviews on *Dalbergia* Genus

Literature surveys of chemical constituents of the plants belonging to *Dalbergia* genus are accumulated in the Table 2.1 and the structures of isolated compounds are shown in Figure 2.2.

Table 2.1 Compounds from the heartwoods of *Dalbergia* Genus

Scientific Name	Compounds	Ref.
Dalbergia retusa	retusin (**1**), 8-methoxyretusin (**2**)	47
Dalbergia odorifera	formononetin (**3**), liquiritigenin (**4**), medicarpin (**5**), (*3R*)-vestitol (**6**), (*3R*)-claussequinone (**7**), bowdichione (**8**), isoliquiritigenin (**9**), (*3R*)-5'-methoxyvestitol (**10**), (*3R*)-3',8-dihydroxyvestitol (**11**), (*3R*)-2',3',7-trihydroxy-4'-methoxyisoflavanone (**12**), 3'-methoxydaidzein (**13**), 2'-methoxyisoliquiritigenin (**14**), (*3R,4R*)-*trans*-2',3',7-trihydroxy-4'-methoxy-4-[(*3R*)-2',7-dihydroxy-4'-methoxyisoflavan-5'yl]isoflavan (**15**), (*3R,4R*)-*trans*-2',7-dihydroxy-4'-methoxy-4-[(*3R*)-2',7-dihydroxy-4'-methoxyisoflavan-5'-yl]isoflavan (**16**), (*3R,4R*)-*trans*-2',7-dihydroxy-4',5'-dimethoxy-4-[(*3R*)-2',7-dihydroxy-4'-methoxyisoflavan-5'-yl]isoflavan (**17**), (*3R,4R*)-*trans*-3',7-dihydroxy-2',4'-dimethoxy-4-[(*3R*)-2',7-dihydroxy-4'-methoxyisoflavan-5'-yl]isoflavan (**18**)	48
Dalbergia nitidula	(*3S*)-6-(3-phenyl-5-hydroxy-6-methoxybenzo[b]furan-2-ylmethyl)vestitol (**19**), 4',5',7-trihydroxy-2'-methoxyisoflavone (**20**)	49
Dalbergia louvelii	isoliquiritigenin, 1-(3-hydroxyphenyl)-3-(4-hydroxy-2,5-dimethoxyphenyl)propane (**21**), spirolouveline (**22**), (*3R*)-7,2'-dihydroxy-4',5'-dimethoxyisoflavanone (**23**), 3-(2,4-dihydroxy-5-methoxy)phenyl-7-hydroxycoumarin (**24**), (*R*)-4"-methoxydalbergione (**25**), obtusafuran (**26**), 7,4'-dihydroxy-3'-methoxyisoflavone (**27**),	50
Dalbergia odorifera	liquiritigenin, formononetin, medicarpin, violanone (**28**), butin (**29**), (*3R*)-4'-methoxy-2',3,7-trihydroxyisoflavone (**30**), melanettin (**31**), dalbergin (**32**), vistitone (**33**), sativanone (**34**)	51

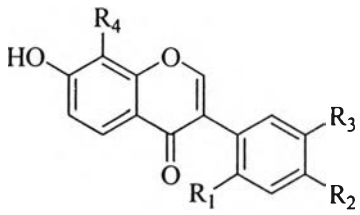

(**1**) $R_1 = R_3 = H$, $R_2 = OMe$, $R_4 = OH$

(**2**) $R_1 = R_3 = H$, $R_2 = OMe$, $R_4 = OMe$

(**13**) $R_1 = R_4 = H$, $R_2 = OH$, $R_3 = OMe$

(**20**) $R_1 = OMe$, $R_2 = R_3 = OH$, $R_4 = H$

(**27**) $R_1 = H$, $R_2 = OH$, $R_3 = OMe$, $R_4 = H$

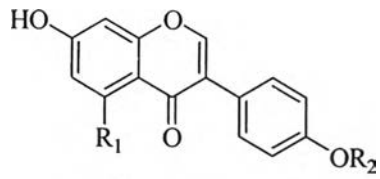

(**3**) $R_1 = H$, $R_2 = CH_3$

(**42**) $R_1 = OH$, $R_2 = CH_3$

(**43**) $R_1 = OH$, $R_2 = H$

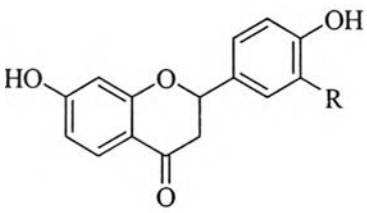

(**4**) R = H

(**29**) R = OH

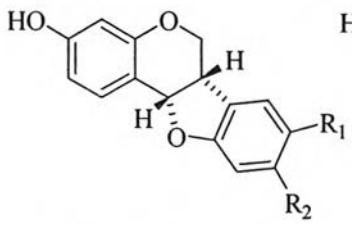

(**5**) $R_1 = H$, $R_2 = OMe$

(**35**) $R_1R_2 = -OCH_2O-$

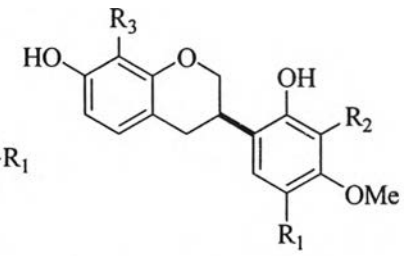

(**6**) $R_1 = R_2 = R_3 = H$

(**10**) $R_1 = OMe$, $R_2 = R_3 = H$

(**11**) $R_1 = H$, $R_2 = R_3 = OH$

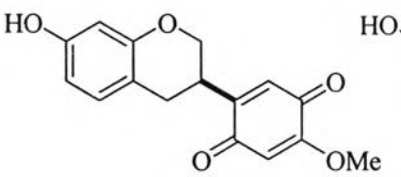

(**7**)

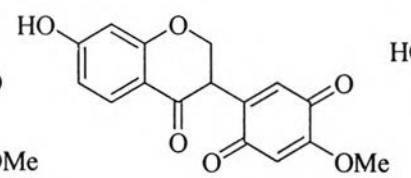

(**8**)

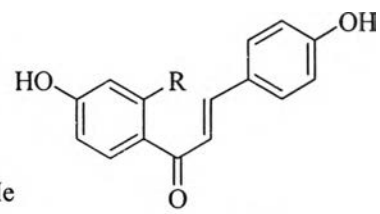

(**9**) R= OH

(**14**) R= OMe

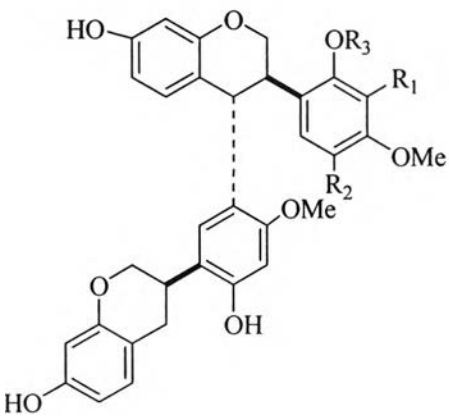

(**15**) $R_1 = OH$, $R_2 = R_3 = H$

(**16**) $R_1 = R_2 = R_3 = H$

(**17**) $R_1 = R_3 = H$, $R_2 = OMe$

(**18**) $R_1 = OH$, $R_2 = H$, $R_3 = Me$

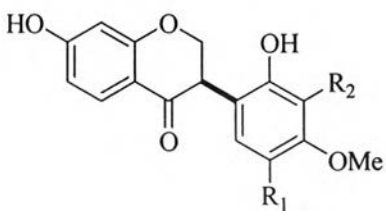

(**12**) $R_1 = H$, $R_2 = OH$

(**23**) $R_1 = OMe$, $R_2 = H$

Figure 2.2 Chemical constituents of the heartwoods of *Dalbergia* genus

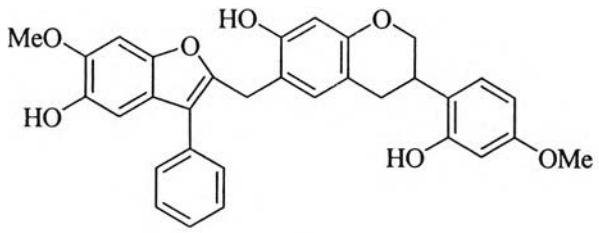

(19)

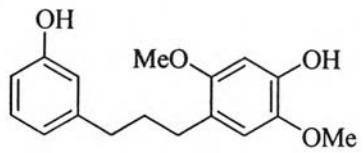

(21)

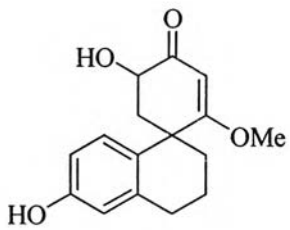

(22)

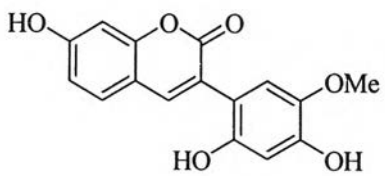

(24)

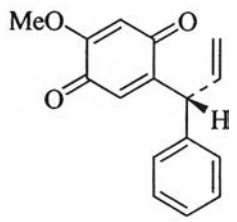

(25)

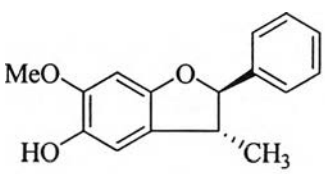

(26)

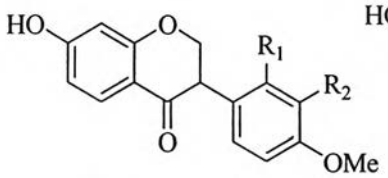

(28) R_1 = OMe, R_2 = OH

(33) R_1 = OH, R_2 = H

(34) R_1 = OMe, R_2 = H

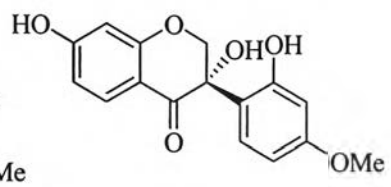

(30)

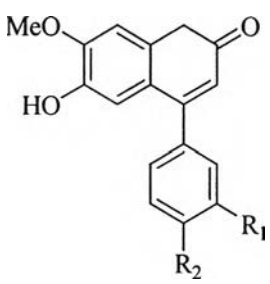

(31) R_1 = H, R_2 = OH

(32) R_1 = R_2 = H

Figure 2.2 (continued)

2.1.3 Chemical Constituents and Literature Reviews on *Dalbergia oliveri* Gamble

From the literature reviews, there are a few reports on the chemical constituents of *D. oliveri* which can be summarized as follows:

In 1972, Donnelly and coworkers isolated 11 natural products from acetone extract of the heartwoods of *D. oliveri* and characterized as 3-hydroxy-9-

methoxypterocarpan (**5**), 3-hydroxy-8,9-methylenedioxypterocarpan (**35**), 7-hydroxy-12-methoxycoumestone (**36a**), 7-hydroxy-11,12-methylenedioxycoumestone (**36b**), 2',7-dihydroxy-4'-methoxy-3-phenylcoumarin (**37a**), 2',7-dihydroxy-4',5'-methylene-dioxy-3-phenylcoumarin (**37b**), (±)-mucronulatol (**38**), (±)-violanone (**28**), formononetin (**3**), (+)-liquiritigenin (**4**) and 2',4',4-trihydroxychalcone (**39**) [43].

In 2003, Ito, *et al.* reported that olibergi A (**40**) and B (**41**), formononetin, biochanin A (**42**) and genistein (**43**) were obtained from the ethanol extract of the stem barks of *D. oliveri*. They were inhibitor of Epstein-Barr virus early antigen activation induced by 12-*o*-tetradecanoylphorbol-13-acetate in Raji cells [52].

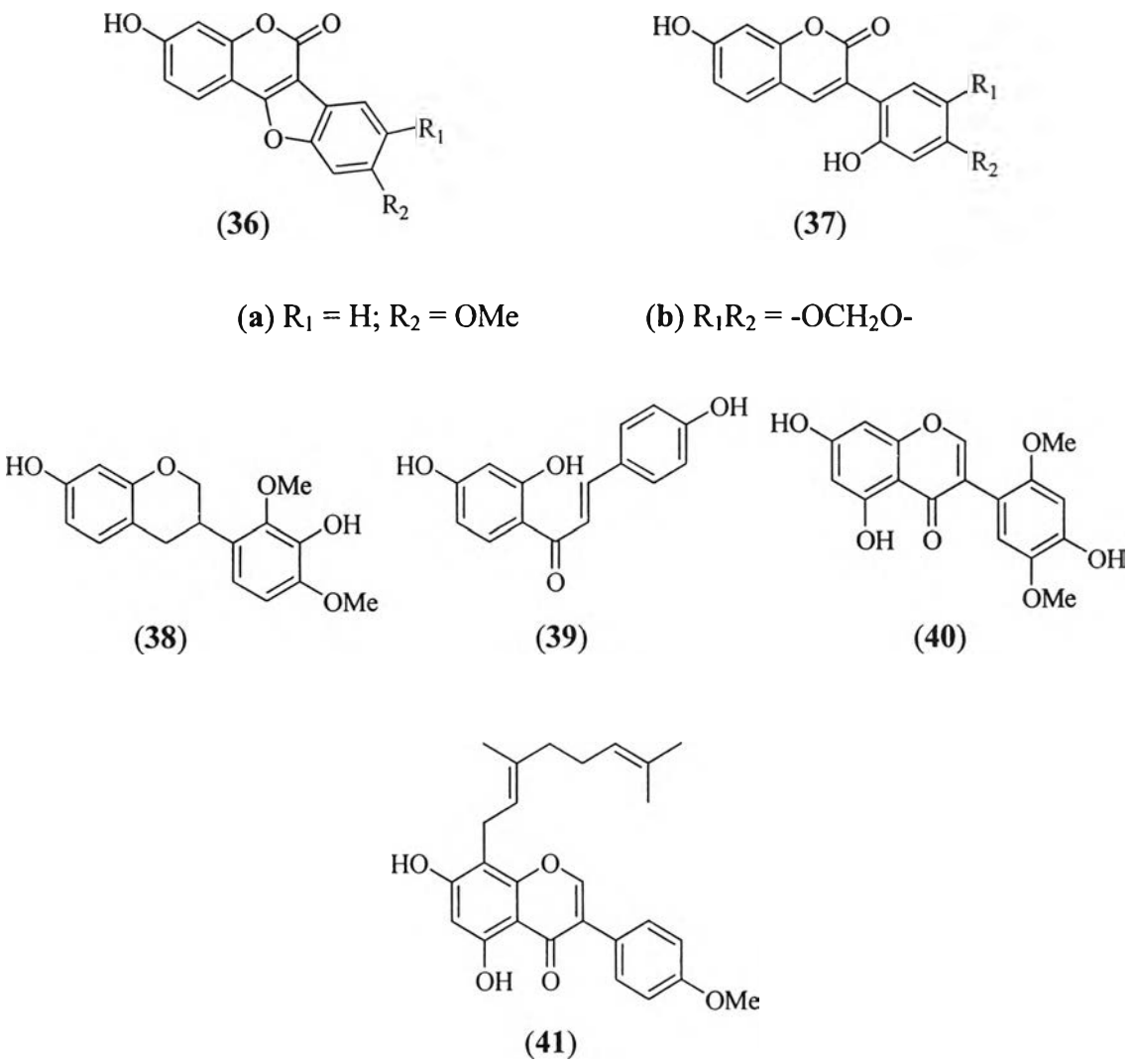

Figure 2.3 Chemical constituents of *Dalbergia oliveri*

2.1.4 The Goal of This Research

The attractive preliminary results of *D. oliveri* heartwood extracts as aforementioned in Section 1.1.3 of Chapter I call for intensive investigation. Thereby, the goal of this chapter can be summarized as:

1. To extract and isolate the chemical constituents from the heartwoods of *D. oliveri*
2. To elucidate the structures of isolated compounds
3. To investigate biological activity of isolated compounds

2.2 EXPERIMENTAL

2.2.1 Plant Material

The heartwoods of *D. oliveri* were collected from Singburi Province, Thailand, in November 2003.

2.2.2 Instruments and Equipment

The ^{1}H and ^{13}C NMR spectra (both 1D and 2D) were performed in deuterated chloroform or otherwise stated with tetramethylsilane as an internal reference on Fourier transform nuclear magnetic resonance spectrophotometer of Varian model Mercury+400. The Fourier transform-infrared spectra (FT-IR) were recorded on Nicolet IMPACT 410 FT-IR spectrometer. Mass spectrometry (MS) analysis was conducted on JEOL JMX_SX102/SX102. X-ray data collection performed at room temperature with Bruker Axs AMART diffractometer equipped with CCD area detector using graphite-monochromated Mo Kα radiation. Specific rotations were measured on a Perkin-Elmer 341 polarimeter. Melting points were determined with a Fisher-Johns melting point apparatus and are uncorrected. TLC was performed on an aluminium sheet precoated with silica gel (Merck's Kieselgel 60 PF_{254}). Column chromatography was performed on silica gel (Merck's Kieselgel 60 G) cat No. 7734, flash chromatography was preceded on silica gel (Merck's Kieselgel 60 G) cat No. 9385 and quick chromatography was performed on silica gel (Merck's Kieselgel 60 G) cat No. 7731.

2.2.3 Chemical Test

- Liebermann-Burchard's Test

The sample was dissolved in dry chloroform 0.5 mL, then slowly added 2-3 drops of acetic anhydride followed by one drop of concentrated sulfuric acid. Development of the color suggests the presence of steroids or triterpenoids. If the solution was dark blue or greenish blue, the sample may contain steroidal nucleus, whereas if the solution turned reddish or purplish the sample should be triterpenoidal compound.

2.2.4 Extraction of *Dalbergia oliveri* Gamble

Four kilograms of dried and powder heartwoods of *D. oliveri* were extracted with hexane by soaking at room temperature for seven days. The obtained hexane extract was filtered and then evaporated under vacuum. This process was repeated for three times to obtain hexane extract as an orange brown oil (4.27 g). The marc was then extracted with CH_2Cl_2, EtOAc and MeOH, respectively employing the same procedure described above. After the solvent was removed, three extracts: CH_2Cl_2 extract as black-brown sticky gum (184.84 g), EtOAc extract as a black-brown sticky gum (150.49 g) and MeOH extract as black-brown gum (296.89 g) were obtained. The extract procedure was summarized as shown in Scheme 2.1.

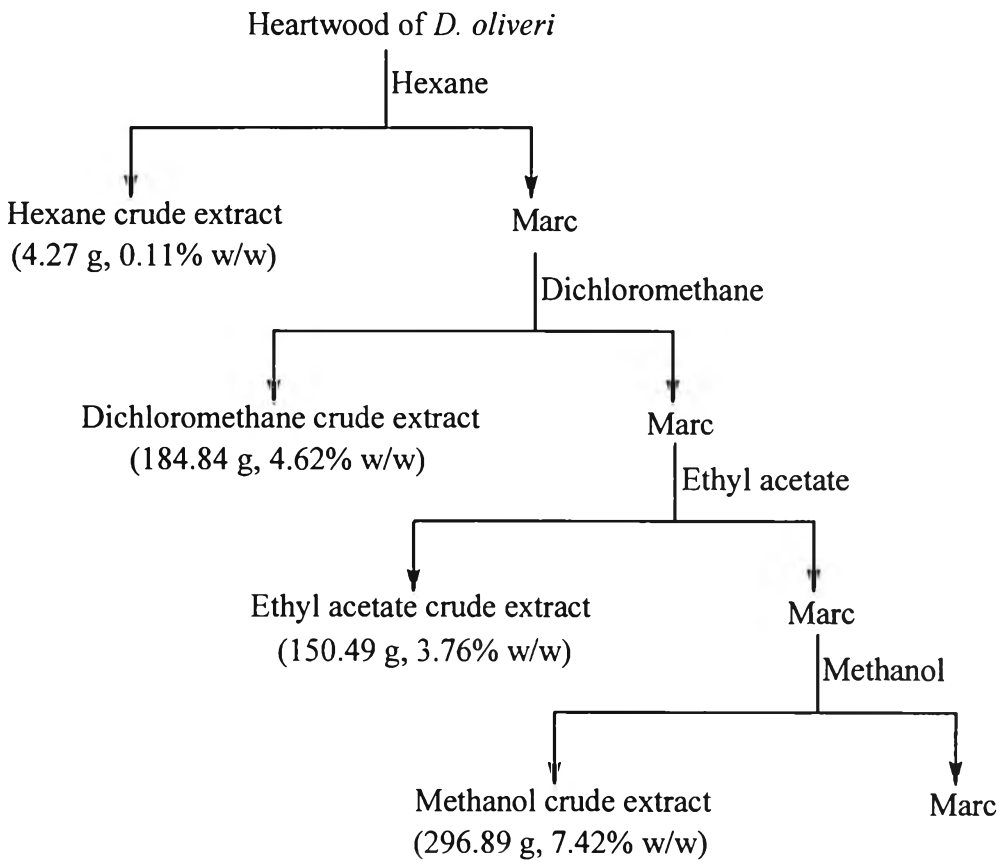

Scheme 2.1 The extraction procedure of the heartwoods of *D. oliveri*

2.2.5 Bioassay Experiments

2.2.5.1 Scavenging Effect on DPPH Radical [42]

2,2-Diphenyl-1-picryhydrazyl (DPPH) radical is a stable radical with a purple color (λ_{max} 517 nm). Scavenging effect toward DDPH radical consisted of two assays for qualitative and quantitative analysis. The assay for qualitative analysis employed TLC autographic method while spectrophotometric assay was used for quantitative analysis. The different color between radical form (purple) and non-radical form (colorless) of DPPH was used for this regarding. Upon reduction by a scavenger, the extensive conjugation is disrupted and the compound turns yellow. The structure of DPPH radical and non-radical forms are illustrated as shown below.

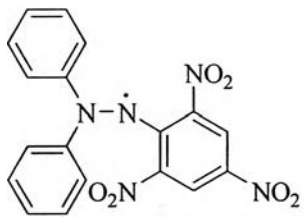

DPPH radical form

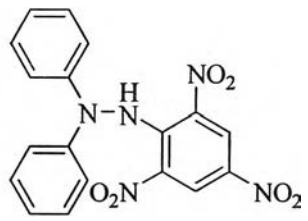

DPPH non- radical form

Spectrophotometric Assay

Samples of various concentrations (1, 0.5, 0.25, 0.125, 0.0625 mM, 0.5 mL) were added to a 1 mL MeOH solution of DPPH radical (final concentration of DPPH was 0.2 mM). The mixture was shaken vigorously and then left for 30 minutes. The absorbance of the resulting solution was measured at λ 517 nm with a spectrophotometer. All tested and analyses were run in three replicates and averaged calculated the percentage of radical scavenging by the following equation.

$$\text{The percentage of radical scavenging} = (1 - A_{sample}/A_{control}) \times 100$$

A_{sample} = Absorbance of sample solution with DPPH

$A_{control}$ = Absorbance of only DPPH and used solvent

2.2.5.2 Antifungal Test [53, 54]

- TLC Screening Assay

Direct detection of TLC plate was applicable to microorganisms that could growth directly on TLC plate and suitable precautions were required. Each isolated compound was spotted on silica gel TLC and developed with suitable solvent system, after that the plates were dried for complete removal of solvents. The chromatograms were sprayed with a spore suspension of *Fusarium oxysporum* or *Colletotrichum gloeosporioides*. After incubation in an incubator at 25°C for 48 h, the plate was stained with 1% (v/v) lactophenol cotton blue in 5% (v/v) acetic acid for 10 minutes. The active components appeared as clear zone against blue background.

- Conidia Suspension Preparation

Conidial suspension distilled preparation of three phytopathogenic fungi: *Alternaria brassicicola* and *Fusarium oxysporum* was prepared from 7-to-14-day old cultures grown on PDA by flooding plates with 10 mL of sterile distilled water and scrapping the colonies on the agar surface with a glass rod. Aqueous conidial suspensions were filtered through steriled cotton wool to remove mycelia. Conidia concentrations in the suspensions were determined with a haemocytometer and then adjusted with steriled distilled water to the required concentration. The conidial suspensions were used for conidial germination inhibition and TLC bioautographic assay.

- Minimum Inhibition Concentration Assay

A. brassicicola and *F. oxysporum* grew on PDA for 7 days were used to prepare the conidial suspension as previous described, estimated by haemocytometer and diluted to the concentration of approximately 10^5 conidia/mL. Each isolated compound was determined the antifungal activity on TLC plate. Three pieces of TLC plates were prepared as follows: on each TLC, various concentrations (final concentrations were 10, 5, 1, 0.5, 0.1 μg/spot/1 μL) of isolated compound to be tested was applied and then developed with the appropriate solvent system. After the solvent was completely evaporated, the plate was marked after visualizing the spot position by UV. Conidia of *A. brassicicola* and *F. oxysporum* suspended in PDB were sprayed directly onto each piece of the previously developed plate and the other piece of the developed plate, no fungi suspension was applied. 10% Sulfuric acid in ethanol was sprayed, followed by heating to direct those compounds with no UV absorption. After incubation in an incubator at 25°C for 48 h, the plates were stained with 1% (v/v) lactophenol cotton blue in 5% (v/v) acetic acid for 10 minutes. A clearly visible growth inhibition zone was observed against a blue background to display antifungal activity. All treatments were performed replicatedly three times.

หอสมุดกลาง สำนักงานวิทยทรัพยากร
จุฬาลงกรณ์มหาวิทยาลัย

2.2.5.3 Antimicrobial Activity Test [55, 56]

- Micro-organisms and Growth Condition

Three references strain from Pasteur Institute (Paris) were used: *Escherichia coli* CIP 54127 and *Staphylococcus aureus* CIP 53124 were cultivated 24 h in LB broth (Difco) at 37°C and *Saccharomyces cerevisiae* CIP 28383 was cultivated 24 h in YPD broth (Difco) at 28°C.

- Minimum Inhibition Concentration Assay

Bacteria culture absorbance was adjusted to 0.01 at 600 nm with LB broth. In the case of yeasts, the absorbance was adjusted with YPD broth. Tested compounds were diluted at different concrentrations. After 24 h of incubation in described growth conditions, absorbance at 600 nm of each culture was determined with a multiplate spectrophotometer (IEMS, Labsystem). The MIC (minimum inhibition concentration) was evaluated as the microbial agent concentration inhibition 80 % of absorbance regarding to the reference (no agent added).

2.2.5.4 Cytotoxicity Test against HepG2 [57]

The HepG2 (human hepatocellular carcinoma) was kindly provided by animal cell biotechnology laboratory, national center for genetic engineering and biotechnology national science and technology development agency (BIOTEC). The HepG2 cell line was maintained in culture flasks in RPMI 1640 culture media (Gibco, Grand Island, NY) containing 10% fetal bovine serum (FBS), 2 mM glutamine and 1% antibiotic/antimyotic solution (Gibco). Cells were batch cultured for 10 days, then seeds at concentration of 10,000 cells/well in fresh media in 96-well microtiter plastic plates in 5% CO_2 at 37°C for a day.

- Cytotoxicity Test

The cells were exposed to different concentrations of samples (100, 50, 20, 10, 5, 0.5, 0.1 and 0.01 μg/mL) at final volume of 100 μg/well. Eight-fold serial dilution of samples was carried out in the plate with four replicate wells per concentration. After 24 h of incubation with chemicals, live cells were visualized by MTT assay.

- MTT Assay

The MTT assay based on the method of Oka *et al.* [58] was measured the metabolism of 3-(4,5-dimethylthiazol-2-yl)-2,5-biphenyl tetrazolium bromide to form an insoluble formazan precipitate by mitochondrial dehydrogenases only present in viable cells. 20 μL of MTT solution was added to 100 μL medium in each well of 96-well plate, and the plate was incubated at 37°C for 4 h. The medium was then removed by aspiration, 200 μL of DMSO added to each well to detach the cells and the plate at room temperature to help release the tetrazolium salt. Finally 20 μL of Sorenson's buffer was added per well, the plate was shaken for a further 5 min and the absorbance at OD 570 nm was measured using microplate reader. Negative (without cells) and positive (without test chemicals) controls were also incubated with each plate. The endpoint was determined from the exponential curve of viability *versus* concentration as IC_{50}, which represented the concentration of compound that killed 50% of cells.

2.2.5.5 Cytotoxicity Test against Diamondback Moth

- Leaf Disk Dip Bioassay

The leaf disk dip bioassay for diamondback moth, *Plutella xylostella*, as described by Tabashnik *et al.* [59] and Pimsamarn *et al.* [60] was adapted in the present study. Chinese kale leaves (growth under xenobiotic free condition) were truly washed with distilled water, and dried for 1 h. Leaf disks (3 cm diameters) were cut with a metal punch and then dipped in various test sample concentrations (10, 20, 40, 80, 160 and 320 ppm) for 10 sec. The leaf disks were placed slanting over blotting paper in a tray for 2 min to drain excess substances. The test substances were dried at room temperature for 1 h. Ten larvae (3rd instar) were released on each disk in an individual round plastic box (5 cm diameters, 10 replications). The control was prepared by using only a proper solvent. After 48 h, the died diamondback moths were counted. The curve between the died diamondback moths and the concentration of each sample was plotted. LC_{50} and LC_{95} were evaluated as the agent concentration that killed 50% and 95%, respectively of diamondback moths regarding to the reference (no agent added).

2.2.5.6 Cytoxicity Test against Mosquito Larvae

- Aqueous Dispersion Test [61]

Aqueous dispersion test was carried out for larvicidal activity of mosquito larvae, *Aedes aegypti*. Twenty forth-instar mosquito larvae were placed in 50 mL of degassed distilled water with 500 μL of DMSO for control. For treatments, samples were prepared for 6 concentrations (10, 20, 40. 80, 160 and 320 ppm). Each cup was left at room temperature. Each treatment was done with ten replicates. During aqueous dispersion test, food was not given to the larvae. After 48 h mortality was recorded. The curve between the died mosquito larvae and the concentration of each sample was plotted. LC_{50} and LC_{95} were evaluated as the agent concentration that killed 50% and 95%, respectively of mosquito larvae regarding to the reference (no agent added).

2.3 RESULTS AND DISCUSSION

2.3.1 The Results of the Extraction of the Heartwoods of *D. oliveri*

The crush dried heartwoods of *D. oliveri* was extracted according to the procedure described in Section 2.2.4. The results of extraction of the heartwoods of *D. oliveri* are summarized as shown in Table 2.2.

Table 2.2 The results of the extraction of the heartwoods of *D. oliveri*

Crude extract	Weight (g)	Percentage yield (% w/w)
Hexane	4.27	0.11
Dichloromethane	184.84	4.62
Ethyl acetate	150.49	3.76
Methanol	296.84	7.42

From the extraction results, it was signified that the MeOH extract gave the best yield 296.84 g or 7.42 % (w/w), whereas the hexane crude extract gave the lowest yield 4.27 g or 0.11% (w/w).

Hexane, CH_2Cl_2, EtOAc and MeOH extracts of the heartwoods of *D. oliveri* were preliminarily screened for radical scavenging effect against DPPH by TLC autographic assay to affirm the preliminary results as discussion in Section 1.1.3. The CH_2Cl_2 and MeOH extracts of *D. oliveri* exhibited excellent radial scavenger properties toward DPPH. The TLC plates containing spots of each extract were developed in appropriate solvent before being dried and sprayed with DPPH reagent. The active substances were detected as yellow spots on a purple background. The results of scavenging effect on DPPH by TLC assay are presented in Figure 2.4.

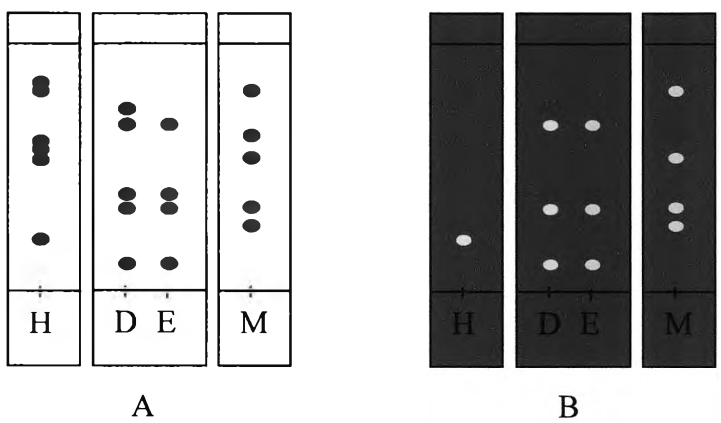

Figure 2.4 TLC autographic assay for DPPH radical scavenger for the extracts of the heartwoods of *D. oliveri*

(A) TLC chromatogram before spraying with DPPH reagent

(B) TLC chromatogram after spraying with DPPH reagent

H: Hexane (system: 20% EtOAc:Hexane) , D: Dichloromethane and E: Ethyl acetate (system: 60% EtOAc:Hexane) and M: Methanol (system: 80% EtOAc:Hexane) extracts; ( ) referred TLC appropriated solvent system

From the results as shown in Figure 2.4, all extracts exposed significant radical scavenging effect toward DPPH. Thus these extracts were rationalized for further investigation on chemical constituents and their biological activities.

2.3.2 The Separation of CH_2Cl_2 Extract

The portion of CH_2Cl_2 extract (140 g) as a dark brown material was fractioned using silica gel (< 45 μm, cat No. 7731) column chromatography eluting by gradient with an increase polarity of hexane, EtOAc in hexane, EtOAc and finally MeOH in EtOAc, respectively. The eluted solution was collected approximately 2000 mL. Every fraction was collected, concentrated to a small volume and then monitored by

TLC. The fractions which contained similar components were combined. The results of separation are shown in Scheme 2.2 and Table 2.3.

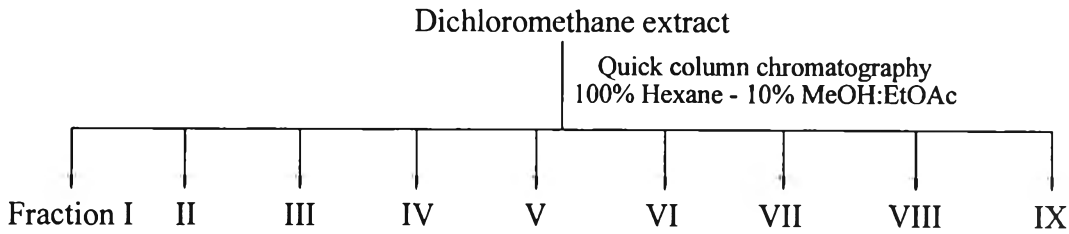

Scheme 2.2 The separation of CH_2Cl_2 extract

Table 2.3 The separation of CH_2Cl_2 extract

Fraction	Solvent system	Remarks	Weight (g)
I	100% Hexane-10% EtOAc:Hexane	Yellow oil	2.55
II	15% EtOAc:Hexane	Brown yellow solid	31.99
III	20% EtOAc:Hexane	Brown syrup	11.69
IV	30% EtOAc:Hexane	Brown syrup	7.52
V	40% EtOAc:Hexane	Brown syrup	5.54
VI	50% EtOAc:Hexane	Dark brown syrup	14.12
VII	60% EtOAc:Hexane	Dark brown syrup	8.85
VIII	80% EtOAc:Hexane	Dark brown syrup	24.60
IX	100% EtOAc-10% MeOH:EtOAc	Dark brown syrup	4.88

As the results, the separation of CH_2Cl_2 extract using gradient eluent started form 100% hexane until 10% MeOH in EtOAc yielded 9 fractions (I-IX).

Separation of Fraction I

Fraction I (2.55 g) was reseparated by silica gel column chromatography eluting with 100% hexane to 20% EtOAc in hexane as solvent. White crystal assigned as **D1** was afforded after washing with cooled hexane and yellow needle crystal designated as **D2** was obtained after recrystalization with acetone. The results of separation are shown below.

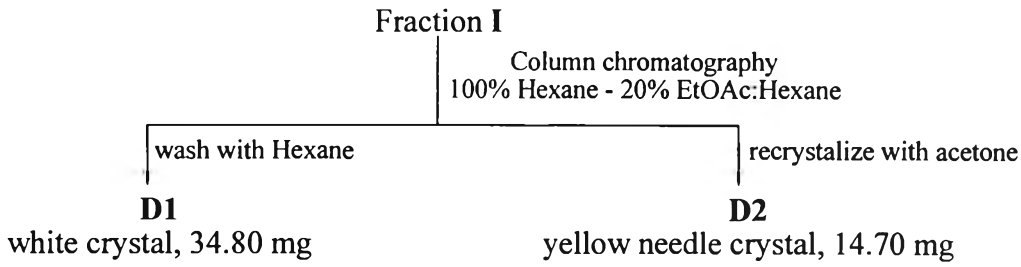

Structural elucidation of D1

D1 was obtained as white crystal (34.80 mg) after washing with cold hexane. Its melting point was 131.5-132.0°C (lit [62], 133-144°C) with R_f 0.36 using 50% EtOAc in hexane as a solvent system. It was soluble in acetone, $CHCl_3$ and MeOH but not in hexane.

The IR spectrum (Figure 2.5) clearly confirmed the presence of hydroxyl group at 3346-3572 cm^{-1} due to -OH stretching vibration, carbonyl group at 1684 cm^{-1} due to C=O stretching vibration and C=C stretching vibration of alkene and benzene moiety at 1626 and 1420 cm^{-1}.

The ^{1}H-NMR ($CDCl_3$) spectrum of **D1** (Figure 2.6) revealed two aromatic proton signals at δ 7.46 (3H, m, H-3, H-4 and H-5) and 7.60 (2H, m, H-2 and H-6). Two olefinic protons could be detected at δ 6.51 (1H, d, J = 16.0 Hz, -CH=C<u>H</u>COOH) and 7.84 (1H, d, J = 16.0 Hz, -C<u>H</u>=CHCOOH). Further support for the assignment as a *trans* alkene was provided by the coupling constant of alkene as 16 Hz [62].

The ^{13}C-NMR ($CDCl_3$) spectrum of **D1** (Figure 2.7) displayed seven carbon signals which could be assigned for a carbonyl group at δ 172.3 and four aromatic carbon signals at δ 128.4 (2C, C-2, C-6), 129.0 (2C, C-3, C-5), 130.8 (C-4), 134.0 (C-1) and two olefinic carbon signals at δ 117.3 (-CH=<u>C</u>HCOOH) and 147.1 (-<u>C</u>H=CHCOOH).

According to the physical data, ^{1}H-, ^{13}C-NMR and IR spectra compared with literature, it could be confirmed that the structure of **D1** was 3-phenylpropenoic acid or *trans*-cinnamic acid.

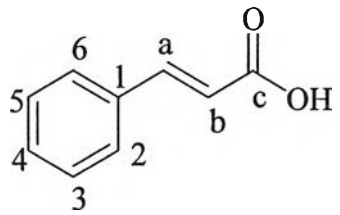

trans-cinnamic acid

The ^{1}H-, ^{13}C-NMR chemical shift assignment of **D1** compared with *trans*-cinnamic acid [63, 64] are presented in Table 2.4.

Table 2.4 The ^{1}H-, ^{13}C-NMR chemical shift assignment of **D1** compared with *trans*-cinnamic acid [63, 64]

Position	Chemical shift (ppm)			
	D1		*trans*-cinnamic acid	
	^{13}C	^{1}H	^{13}C [64]	^{1}H [63]
1	134.0	-	130.1	-
2, 6	128.4	7.59-7.61 (2H, m)	128.0	7.45 (5H, m)
3, 5	129.0	7.45-7.46 (3H, m)	128.9	
4	130.8		134.4	
a	147.1	7.84 (1H, d, J = 16.0 Hz)	144.2	7.80 (1H, d, J = 16.5 Hz)
b	117.3	6.51 (1H, d, J = 16.0 Hz)	119.2	6.55 (1H, d, J = 16.5 Hz)
c	172.3	-	168.0	-

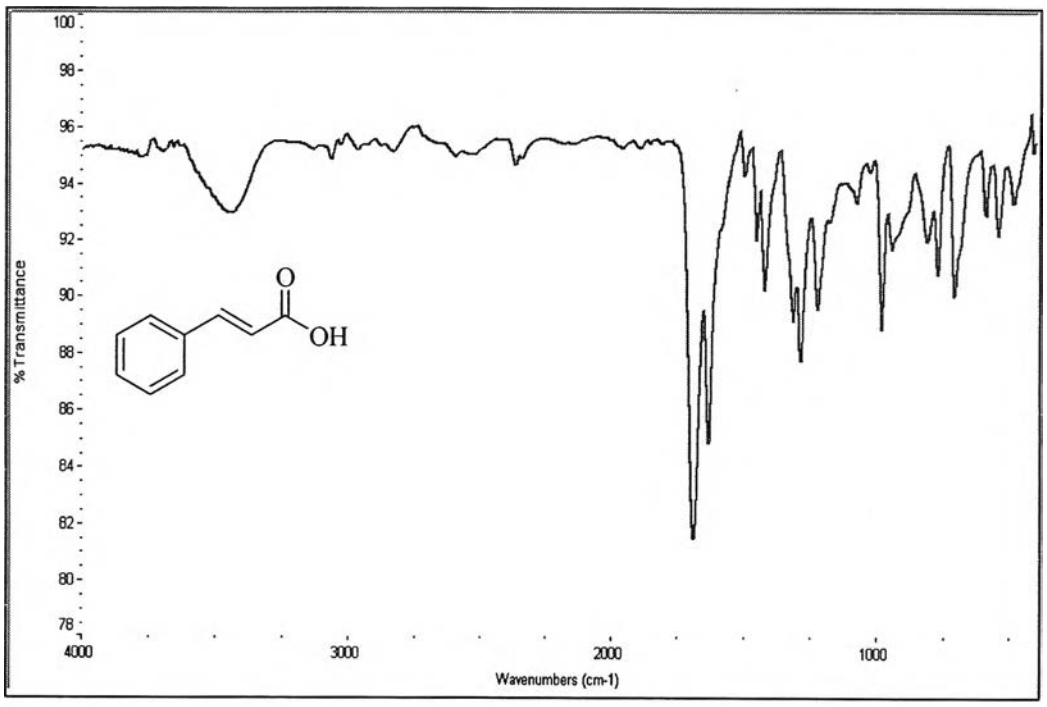

Figure 2.5 The IR spectrum of **D1**

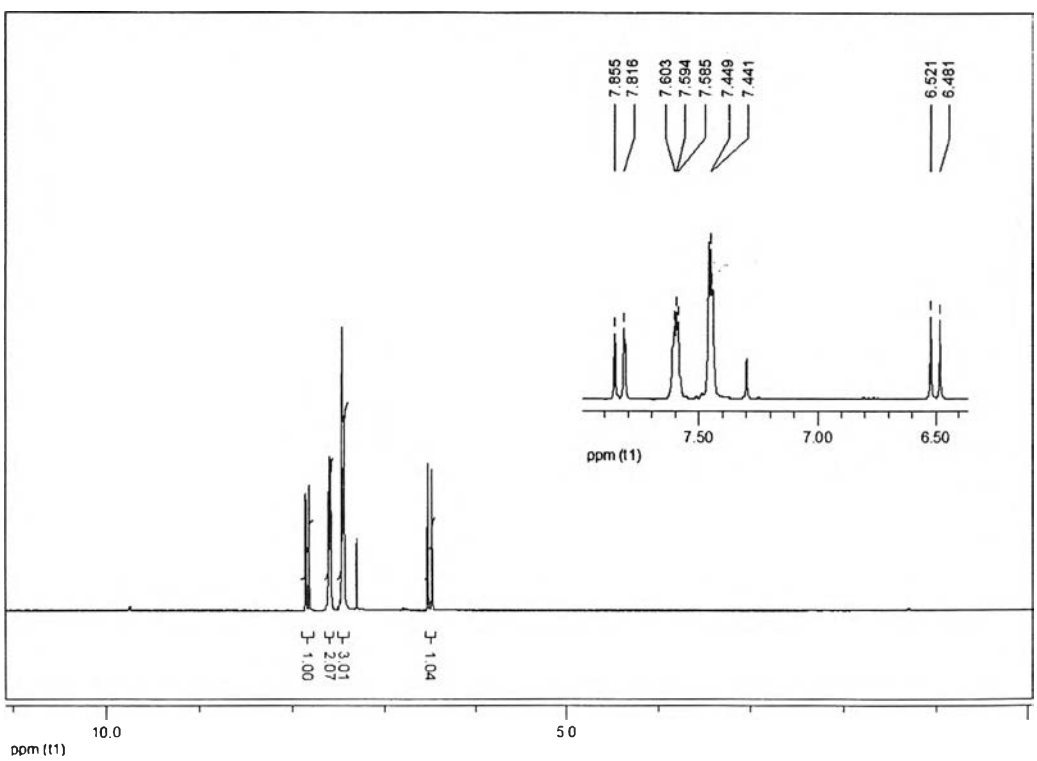

Figure 2.6 The ^{1}H-NMR spectrum of **D1**

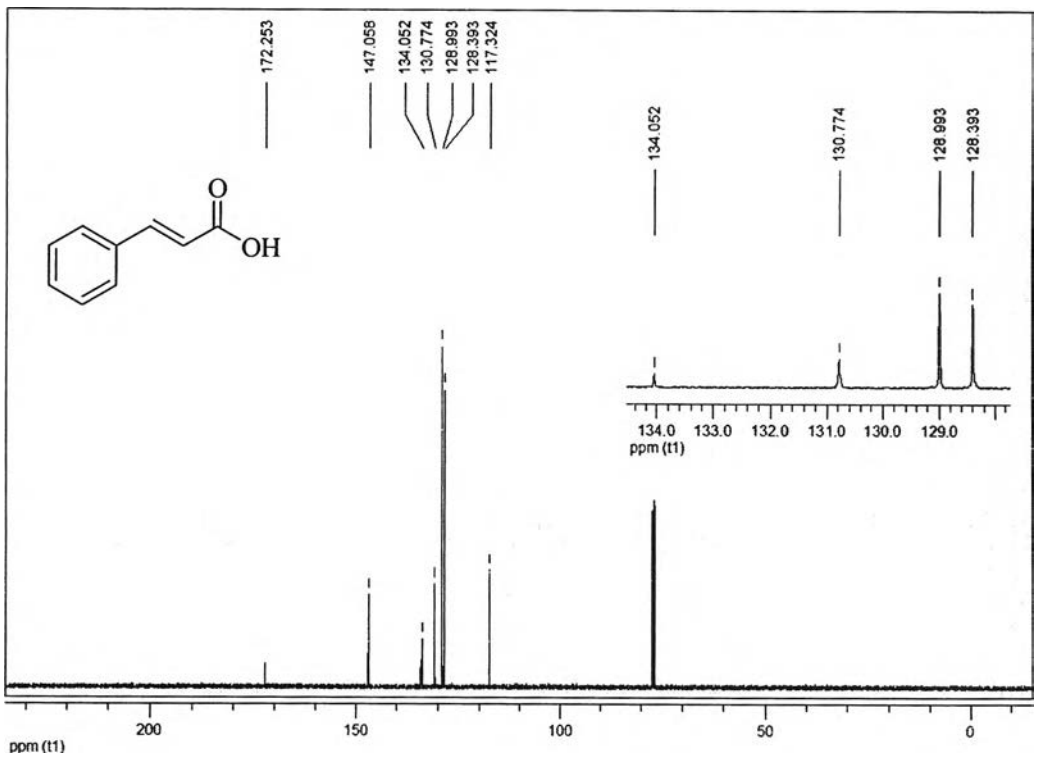

Figure 2.7 The ^{13}C-NMR spectrum of **D1**

Structural elucidation of D2

After recrystalization with acetone, **D2** as yellow needle crystal (14.70 mg) was obtained. It exhibited a single spot on TLC with R_f value 0.47 (20% EtOAc - hexane) and m.p. 162.0-162.5°C (lit [65], 168-169°C).

The electron impact mass spectrum (EI-MS) (Figure 2.8) showed the molecular ion peak at m/z 298 [M^+] along with fragment ion peaks at m/z 175, 162 and 148. Molecular formula was determined to be $C_{17}H_{14}O_5$ on the basis of ^{1}H-, ^{13}C-NMR and mass spectral data. The significant ions observed in the mass spectrum of **D2** [66] was presented in Scheme 2.3.

The IR spectrum (Figure 2.9) displayed the characteristic absorption peaks of C=C bond of an aromatic ring at 1622 and 1473 cm^{-1}. The C-H stretching vibration of CH and CH_2 was observed at 2891 cm^{-1}. Other signals were tentatively assigned at 1273, 1203, 1149, 1111, 1034 and 933 cm^{-1}.

The ^{1}H-NMR ($CDCl_3$) spectrum of **D2** (Figure 2.10) revealed typical center four proton signals of pterocarpan type skeleton [67]. The proton on C-6 showed both double doublet at δ 3.69 (J_{ax} = 10.9 and 10.9 Hz) and 4.25 (J_{eq} = 4.8 and 10.9 Hz) with range of signal reported for an axial and equatorial protons, respectively. In

addition, the protons of C-11a and -6a position exhibited as doublet at δ 5.52 (J = 6.7 Hz) and multiplet at δ 3.52, respectively. Furthermore, the characteristic methylenedioxy proton signal at δ 5.95 (2H, 2 overlapping d) [68] and that of a methoxy group at δ 3.83 could manifestly visualized. The assignment of a *cis* ring juncture in this compound was endorsed by J_{H6a}-H_{11a} = 6.7 Hz (J_{H6a}-H_{11a} ≈ 6-7 Hz, [68]).

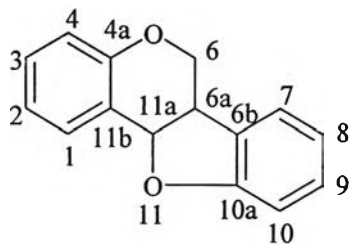

pterocarpan skeleton

The ^{13}C-NMR ($CDCl_3$) spectrum of this compound (Figure 2.11) indicated the central three-carbon unit of pterocarpan type which could be observed at δ 66.5, 40.2 and 78.5 associated with C-6, C-6a and C-11a, respectively. The carbon signal at δ 101.3 was attributed for a methylenedioxy carbon. In addition, seven quaternary carbons at δ 161.0 (C-3), 156.6 (C-4a), 154.3 (C-10a), 148.1 (C-8), 141.7 (C-9), 117.9 (C-6b) and 112.3 (C-11b), five methine carbons at δ 131.8 (C-1), 109.2 (C-2), 104.8 (C-7), 101.6 (C-4) and 93.9 (C-10) and a methoxy carbon at δ 55.4 were obviously detected.

The NOE DIFF experiments (Figures 2.12-2.14) were performed to acquire for addition information. Irradiation of the proton signal at δ 5.52 (H-11a) caused the enhancement of the proton signal at δ 7.44 (H-1) and 3.49-3.54 (H-6a) which confirmed a *cis* ring juncture. Similarly, the irradiation of the proton signal at δ 3.49-3.54 (H-6a) caused the enhancement of the proton signal at δ 4.25 (H-6*eq*), 5.52 (H-11a) and 6.76 (H-7). The position of the methoxy group was also confirmed by this technique to be posed at C-3. To illustrate this, the irradiation of the methoxy proton signal at δ 3.83 caused the enhancement of the proton signal at δ 6.51 (H-4) and 6.68 (H-2). The NOE DIFF correlation of **D2** is shown below:

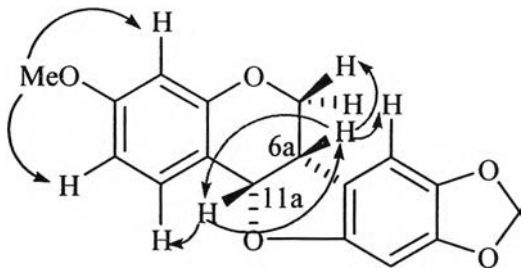

The sign of optical rotation of **D2** was $[\alpha]_D$ +20.7° (c 0.15 in acetone, at 20°C).

D2 contained two chiral centers at C-6a and C-11a which were considered to posses either *R,R* or *S,S* configurations from the stereochemical environment around the C-6a and C-11a [69]. It has been generally accepted that the absolute configuration of pterocarpans may be presumed from the sign of the optical rotation [69]. That is, the levorotatory pterocarpans have *6aR,11aR* configuration, whereas the dextrorotary ones have *6aS,11aS* configuration. In the case of **D2**, the specific rotation of **D2** was found to be +20.7°, so that the absolute configuration of **D2** was presumed to be *6aS* and *11aS*.

Gathering from the above data, **D2** was deduced to be (+)-3-methoxy-8,9-methylenedioxypterocarpan or (+)(*6aS,11aS*)-pterocarpin. The structure is shown below.

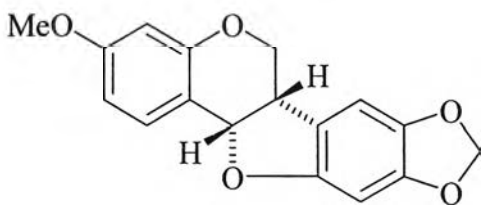

(+)(*6aS,11aS*)-pterocarpin

The ^{1}H-, ^{13}C-NMR chemical shift assignments of **D2** compared with (-)-pterocarpin [70] are presented in Table 2.5.

Table 2.5 The ^{1}H-, ^{13}C-NMR chemical shift assignments of **D2** compared with (-)(*6aR,11aR*)-pterocarpin [70]

Position	Chemical shift (ppm)			
	D2		(-)(*6aR,11aR*)-pterocarpin	
	^{13}C	^{1}H	^{13}C	^{1}H
1	131.8	7.44 (d, *J* = 8.5 Hz)	131.8	7.40 (d, *J* = 8.5 Hz)
2	109.2	6.68 (dd, *J* = 2.5, 8.5 Hz)	109.2	6.64 (dd, *J* = 2.5, 8.5 Hz)
3	161.0	-	161.0	-
4	101.6	6.51 (d, *J* = 2.5 Hz)	101.6	6.47 (d, *J* = 2.5 Hz)
4a	156.6	-	156.6	-
6	66.5	3.69 (dd, *Jax* = 10.9, 10.9 Hz)	66.5	3.66 (dd, *Jax* = 11.0, 11.0 Hz)
		4.25 (dd, *Jeq* = 4.8, 10.9 Hz)		4.23 (dd, *Jeq* = 5.0, 11.0 Hz)
6a	40.2	3.49-3.54 (m)	40.2	3.48 (ddd, *J* = 5.0, 6.8, 11.0 Hz)
6b	117.9	-	117.9	-
7	104.8	6.76 (s)	104.8	6.72 (s)
8	148.1	-	148.1	-
9	141.7	-	141.7	-
10	93.9	6.47 (s)	93.9	6.44 (s)
10a	154.2	-	154.2	-
11a	78.5	5.52 (d, *J* = 6.7 Hz)	78.5	5.49 (d, *J* = 6.8 Hz)
11b	112.3	-	112.3	-
OCH_2O	101.3	5.95 (2 overlapping d)	101.3	5.89 (d, *J* = 1.6 Hz, OC*H*HO) 5.92 (d, *J* = 1.6 Hz, OCH*H*O)
OMe	55.4	3.83 (s)	55.4	3.79 (s)

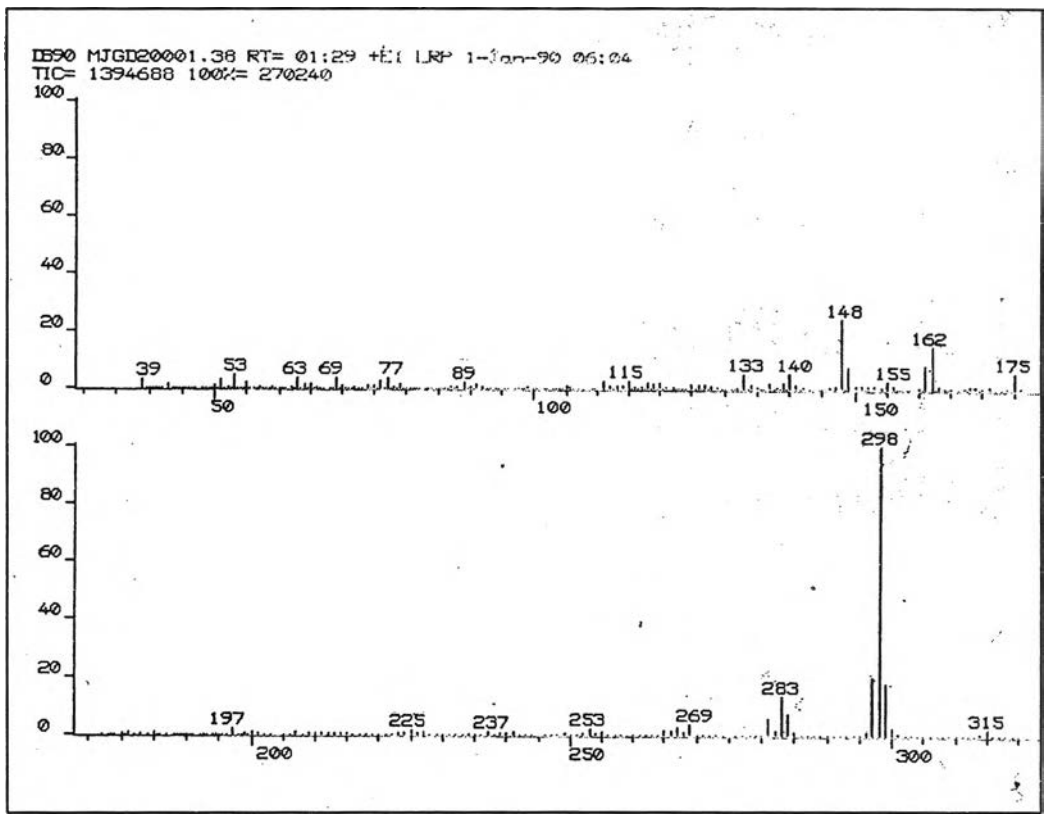

Figure 2.8 The mass spectrum of **D2**

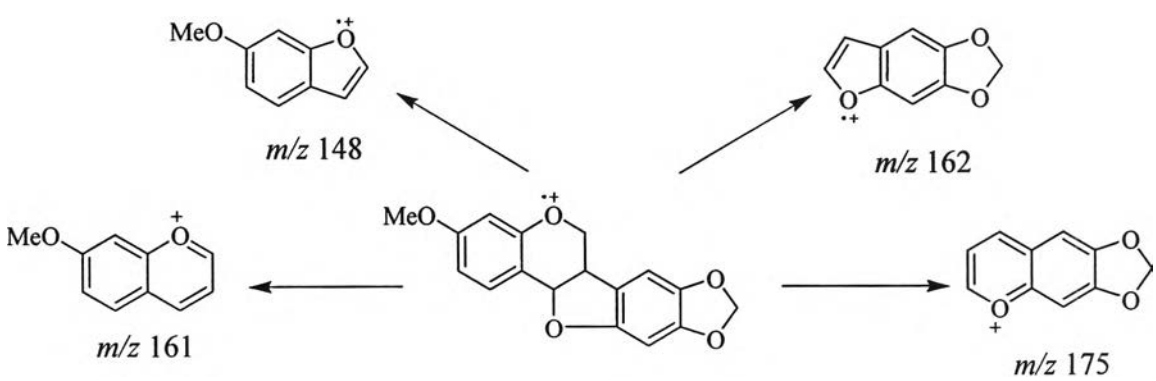

Scheme 2.3 The significant ions observed in the mass spectrum of **D2**

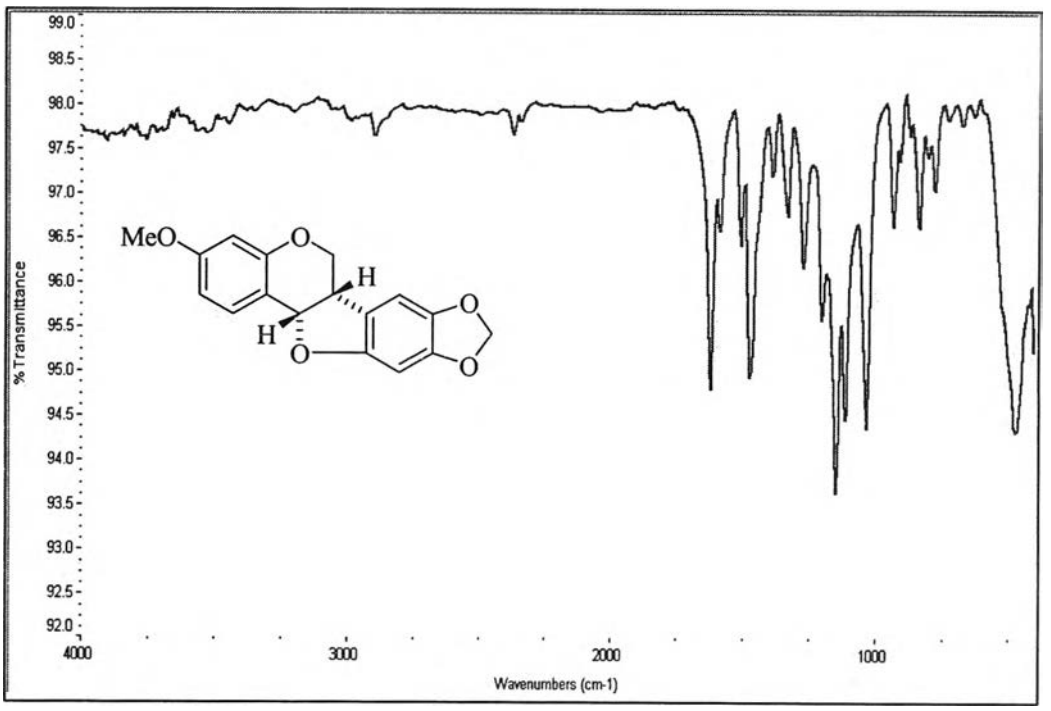

Figure 2.9 The IR spectrum of **D2**

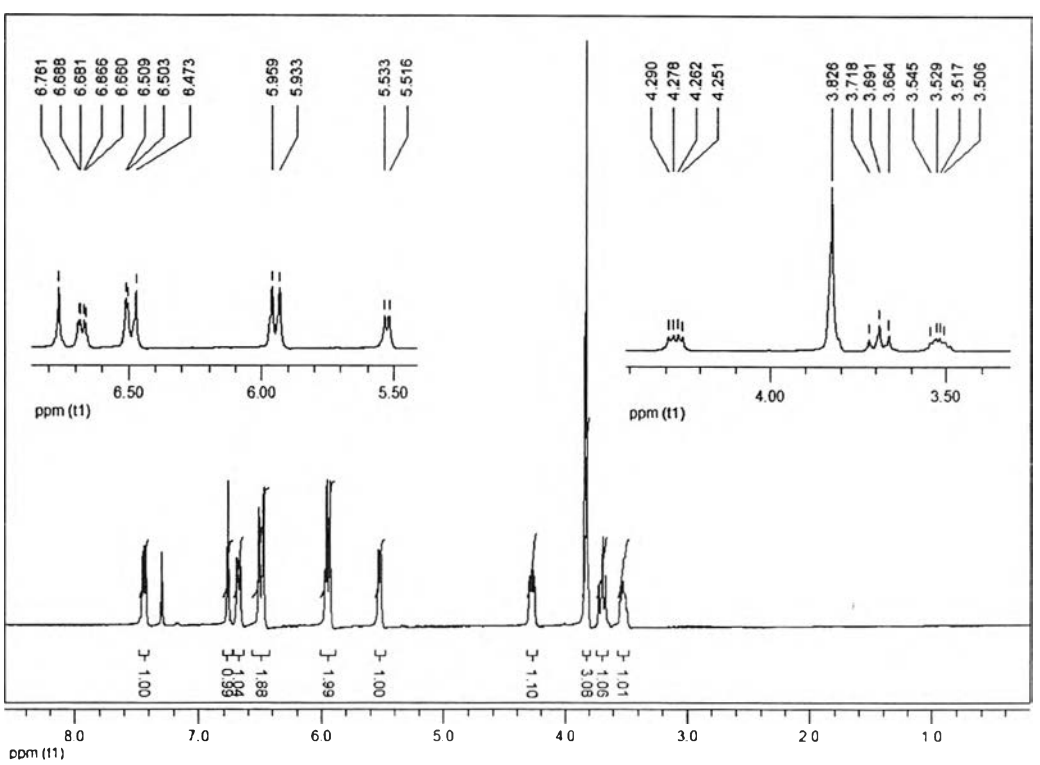

Figure 2.10 The ^{1}H-NMR spectrum of **D2**

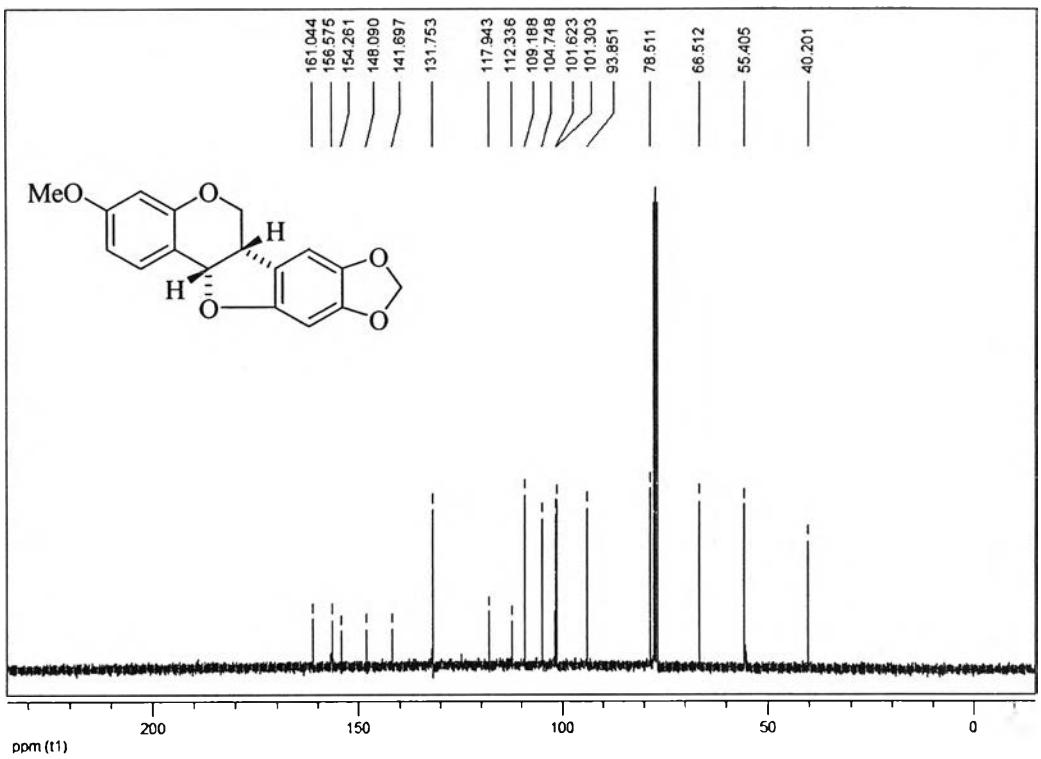

Figure 2.11 The ^{13}C-NMR spectrum of **D2**

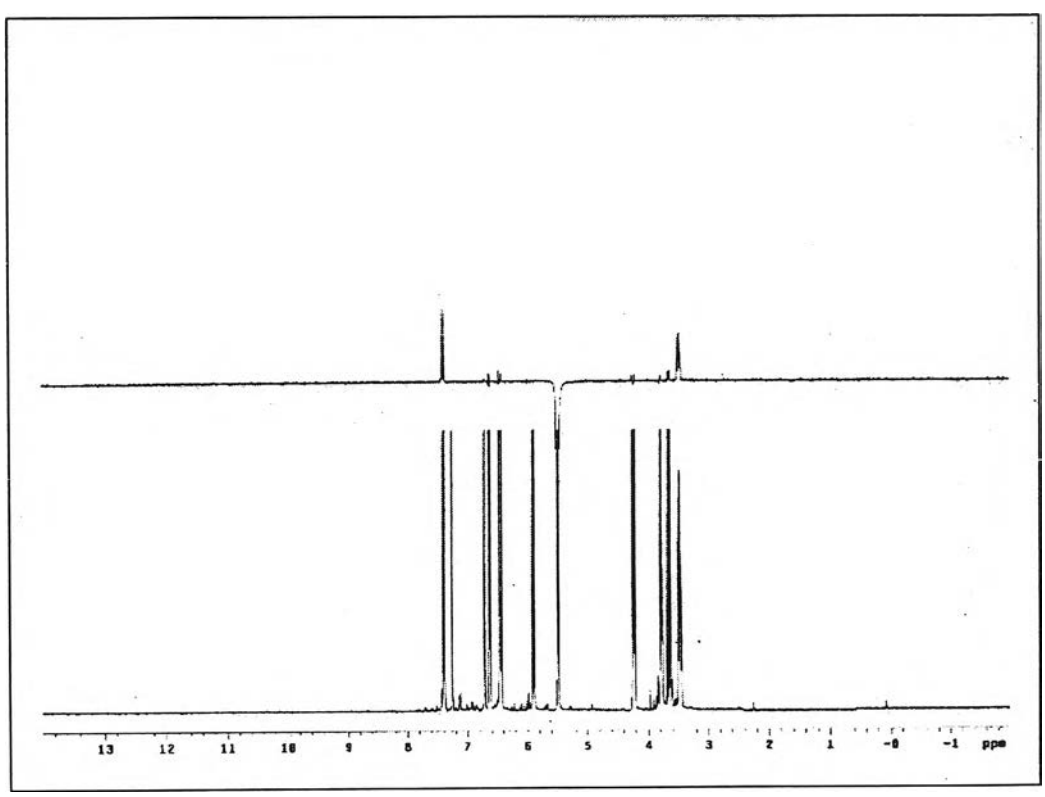

Figure 2.12 NOE DIFF of **D2** (irradiated at δ 5.52)

I2519621X

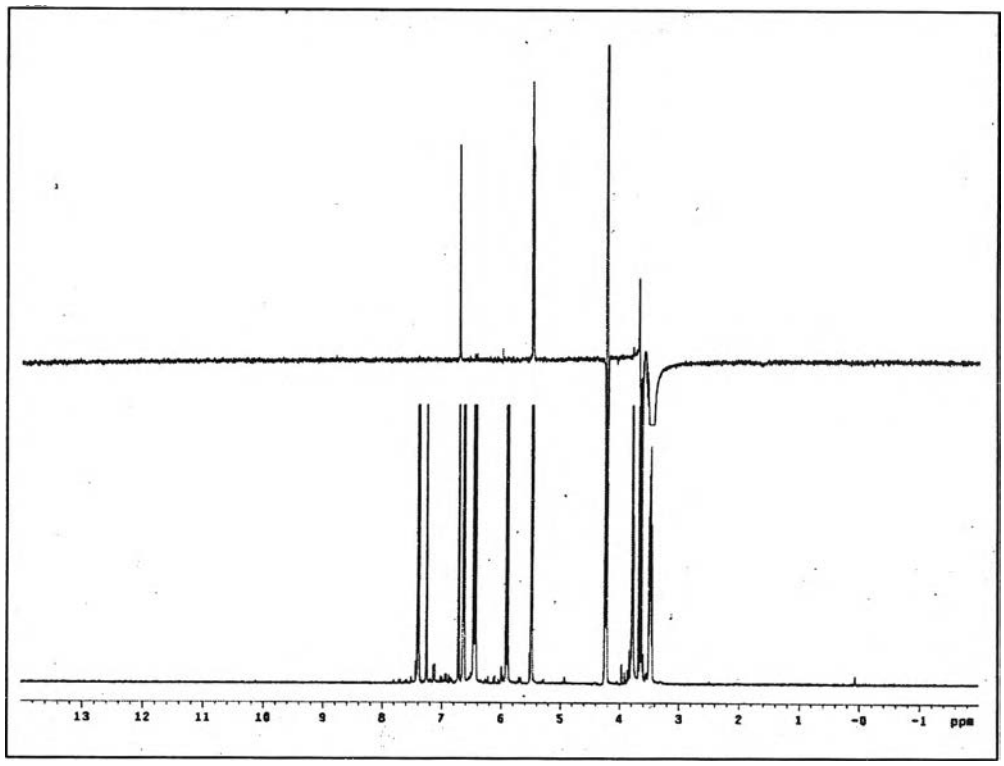

Figure 2.13 NOE DIFF of **D2** (irradiated at δ 3.49-3.54)

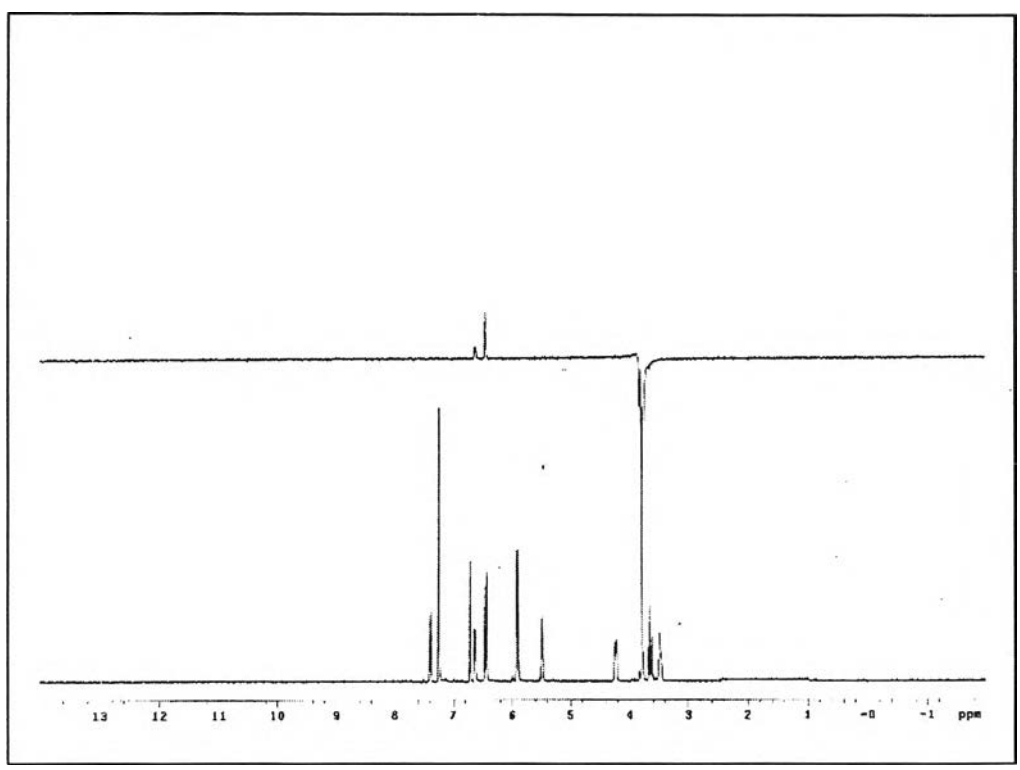

Figure 2.14 NOE DIFF of **D2** (irradiated at δ 3.83)

Separation of Fraction III

Fraction III (11.69 g) was subjected to silica gel column chromatography eluting with 10% EtOAc in hexane to 60% EtOAc in hexane to give white needle crystal designated as **D3** and fraction III-II. The fraction III-II was further separated with silica gel column chromatography eluting with 10% EtOAc in hexane to 100% EtOAc to afford **D3** (fraction III-II-I) and fraction III-II-II. The fraction III-II-II was further separated by sephadex LH20 column chromatography eluting with 50% MeOH in CH_2Cl_2 and followed with flash column chromatography using 30% EtOAc in hexane to 50% EtOAc in hexane to furnish **D4**. It should be noted that each fraction was monitored by TLC and fractions which showed similar pattern were combined.

The results of separation fraction III are presented as follows:

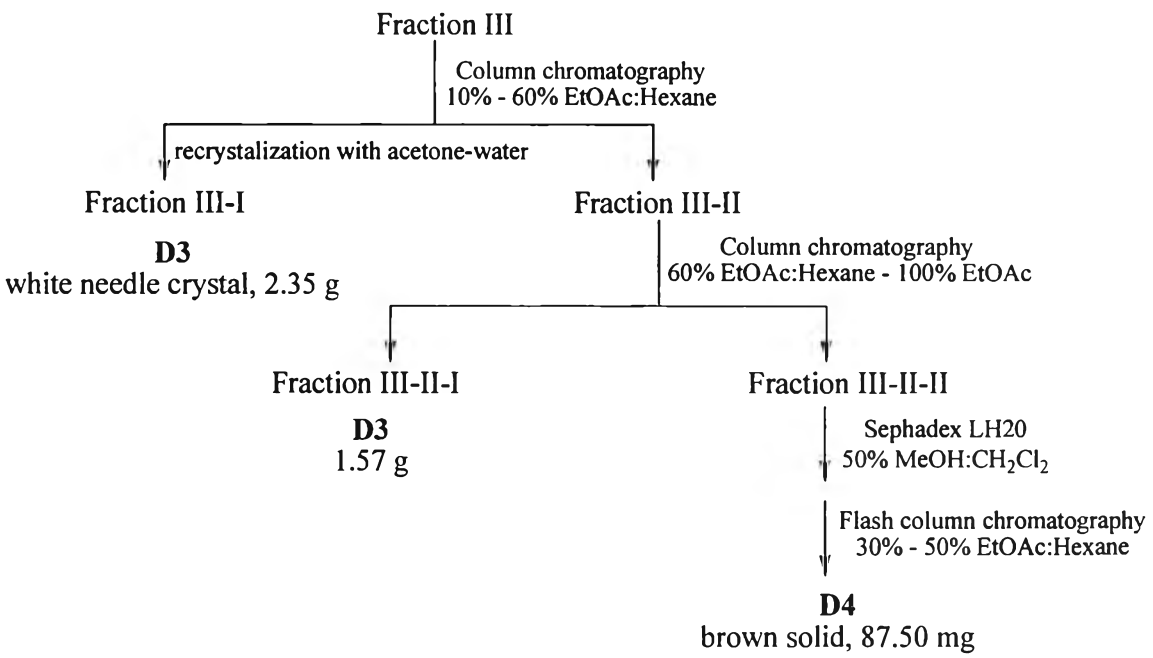

Structural elucidation of D3

D3, constituting as a major composition of CH_2Cl_2 crude extract of the heartwoods from *D. oliveri*, was achieved as white needle crystal (3.92 g) after recrystallization with acetone-water and gave a single spot on TLC. The R_f value of **D3** was 0.54 (40% EtOAc in hexane), m.p. 132.0-133.5°C (lit [38], 128-129°C).

The molecular composition was defined as $C_{16}H_{14}O_4$ by the electron impact mass spectrum (EI-MS) analysis (Figure 2.15). The molecular ion peak was observed at m/z 270 [M^+] along with other fragment ion peaks at m/z 161, 148 and 147. The

significant ions observed in the mass spectrum of **D3** [66] was proposed as shown in Scheme 2.4.

The IR spectrum of this compound (Figure 2.16) displayed the absorption band of an aromatic ring at 1626 and 1494 cm^{-1}. The C-H stretching vibration of CH and CH_2 was observed at 2918 and 2864 cm^{-1}. Other signals were observed at 1369, 1256, 1210, 1167, 1112, 1081, 1042 and 949 cm^{-1}.

The ^{1}H-NMR ($CDCl_3$) spectrum of **D3** (Figure 2.17) showed the characteristic chemical shifts and coupling pattern at δ 3.55 (1H, m, H-6a), 3.65 (1H, dd, J = 10.9 and 10.9 Hz, H-6*ax*), 4.26 (1H, dd, J = 4.8, 10.9 Hz, H-6*eq*) and 5.23 (1H, d, J = 6.7 Hz, H-11a) which were reminisced of a pterocarpan skeleton. The signal belonged to a methoxy group could indeed clearly detected at δ 3.80. The coupling constant of H-6a and H-11a was 6.7 Hz which confirmed the assignment of a *cis* ring juncture in this compound (J_{H6a}-H_{11a} ≈ 6-7 Hz, [68]).

The ^{13}C-NMR ($CDCl_3$) spectrum of **D3** (Figure 2.18) displayed typical central three-carbon unit of pterocarpan type skeleton which could be assigned at δ 66.5, 39.5 and 79.7 corresponded with C-6, C-6a and C-11a, respectively. In addition, the carbon signal at δ 55.6 was attributed for a methoxy group. Other carbon signals are assigned as tabulated in Table 2.6.

The assignment of a *cis* ring juncture in this compound was also confirmed by the NOE difference technique (Figures 2.19-2.20). The irradiation of the proton signal at δ 5.53 (H-11a) resulted in the enhancement of the proton signal at δ 3.55 (H-6a) and 7.40 (H-1) and that of the proton signal at δ 3.52-3.58 (H-6a) caused the enhancement of the proton signal at δ 3.65 (H-6*ax*), 4.26 (H-6*eq*), 5.53 (H-11a) and 7.16 (H-7). The position of the methoxy group could also be confirmed by this technique to be suited at C-9 position, *i.e.* the irradiation of the methoxy proton signal at δ 3.80 caused the enhancement of the proton signal at δ 6.50 (H-8 and H-10) (Figure 2.21). The NOE DIFF correlation of **D3** is shown below:

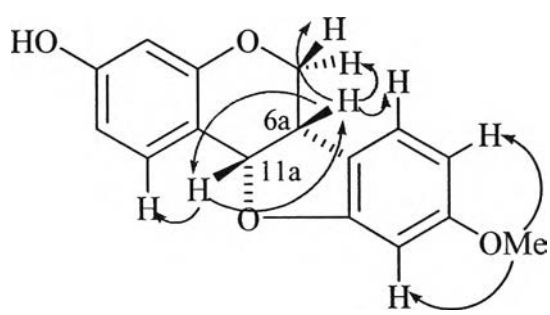

Additionally, the structure of **D3** was confirmed by single crystal X-ray diffraction analysis. A single crystal of this compound was prepared by carefully recrystallization in acetone. The formula per asymmetric unit is $C_{16}H_{14}O_4$ (Table A1). Atomic coordinates (x 10^4) and equivalent isotropic displacement parameters (A^2 x 10^3), the bond distances and bond angles of **D3** were also shown in Appendices. A completion of all X-ray data led to the elucidation of the structure of **D3** (Figure 2.22).

The specific rotation of **D3** as $[\alpha]_D$ + 223.1° (c 0.16 in acetone, at 20°C) firmly indicated the absolute configuration to be the same *6aS,11aS* as that of **D2**.

Based on these spectroscopic observation and single crystal X-ray diffraction analysis, the chemical structure of **D3** was found to be (+)-3-hydroxy-9-methoxypterocarpan or named (+)(*6aS,11aS*)-medicarpin. The structure is shown below.

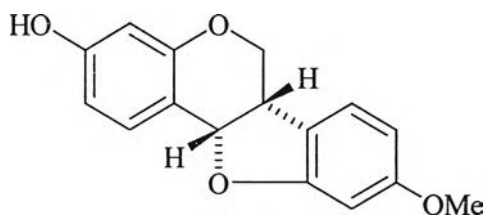

(+)(*6aS,11aS*)-medicarpin

The ^{1}H- and ^{13}C-NMR chemical shift assignments of **D3** compared with medicarpin [38] is presented in Table 2.6.

Table 2.6 The ^{1}H-, ^{13}C-NMR chemical shift assignments of **D3** compared with medicarpin [38]

Position	Chemical shift (ppm)			
	D3		medicarpin	
	^{13}C	^{1}H	^{13}C	^{1}H
1	132.3	7.40 (d, *J* = 8.5 Hz)	132.6	7.41 (d, *J* = 8.4 Hz)
2	110.0	6.58 (dd, *J* = 2.4, 8.5 Hz)	102.2	6.58 (dd, *J* = 2.4, 8.4 Hz)
3	157.3	-	157.5	-
4	103.7	6.45 (d, *J* = 2.4 Hz)	104.1	6.44 (d, *J* = 2.4 Hz)
4a	156.5	-	157.1	-
6	66.5	3.65 (dd, *Jax* = 10.9, 10.9 Hz)	67.0	3.64 (dd, *Jax* = 10.9, 11.0 Hz)
		4.26 (dd, *Jeq* = 4.8, 10.9 Hz)		4.26 (dd, *Jeq* = 5.0, 11.0 Hz)
6a	39.5	3.52-3.58 (m)	39.9	3.55 (ddd, *J* = 5.1, 6.7, 11.0 Hz)
6b	119.2	-	119.5	-
7	124.9	7.16 (d, *J* = 8.8 Hz)	125.2	7.15 (d, *J* = 8.9 Hz)
8	106.6	6.50 (br)	106.8	6.48 (m)
9	161.0	-	161.1	-
10	96.9	6.50 (br)	97.3	6.48 (m)
10a	160.5	-	161.5	-
11a	79.7	5.53 (d, *J* = 6.7 Hz)	79.0	5.52 (d, *J* = 6.8 Hz)
11b	112.4	-	113.0	-
OMe	55.6	3.80 (s)	55.9	3.79 (s)

ax: axial; *eq*: equatorial

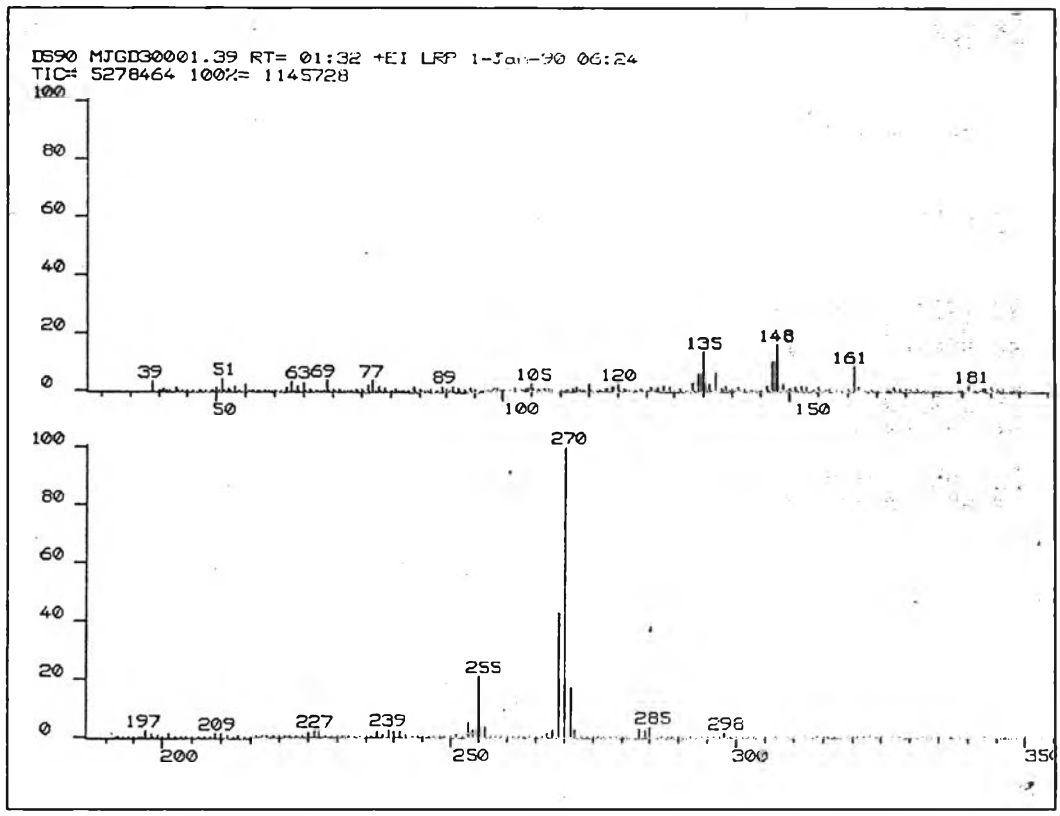

Figure 2.15 The mass spectrum of **D3**

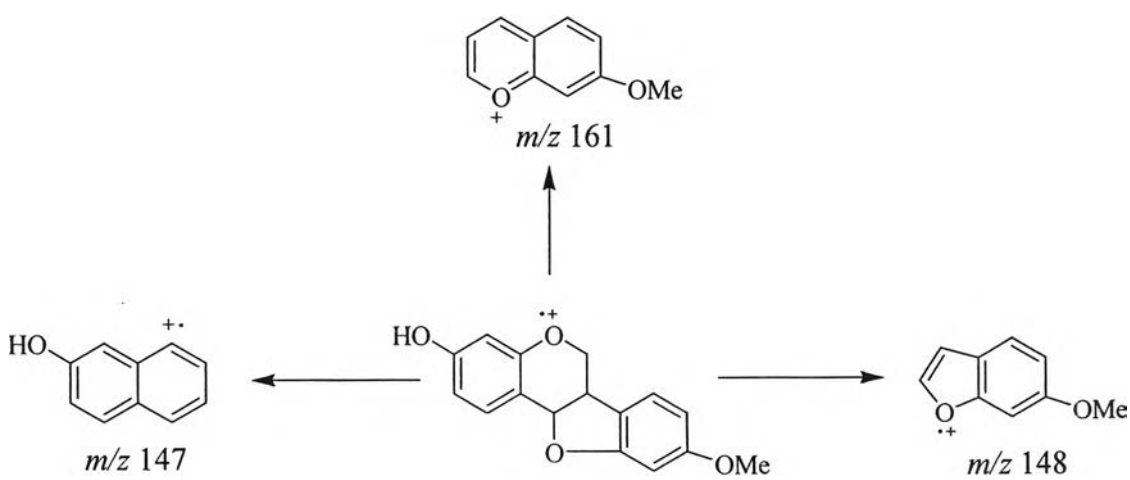

Scheme 2.4 The significant ions observed in the mass spectrum of **D3**

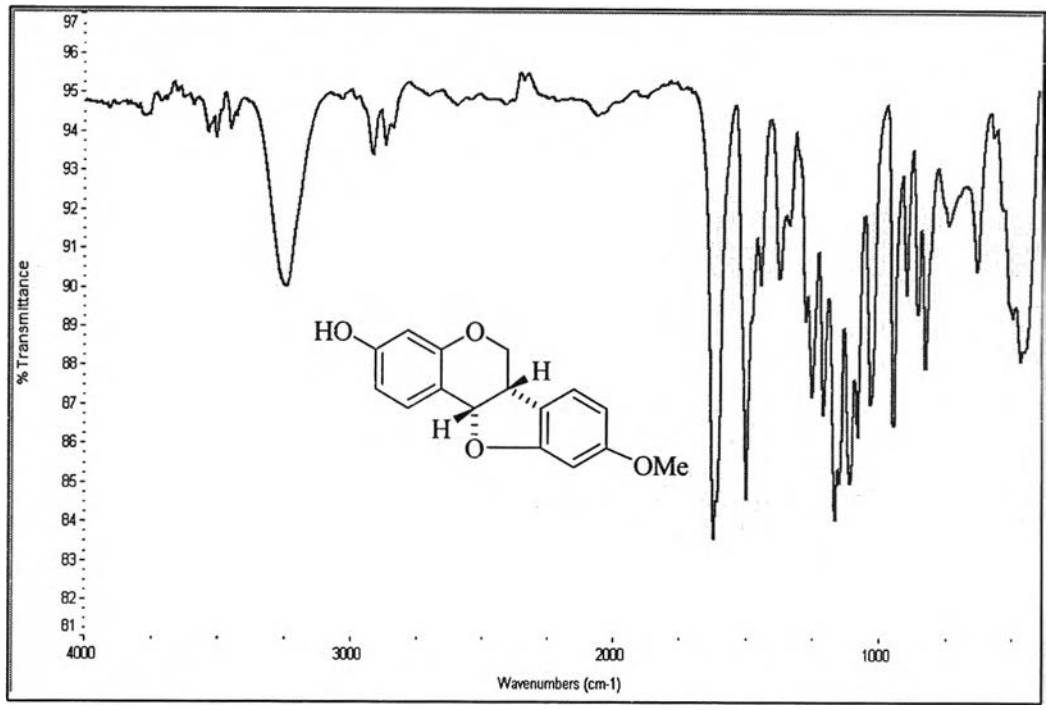

Figure 2.16 The IR spectrum of **D3**

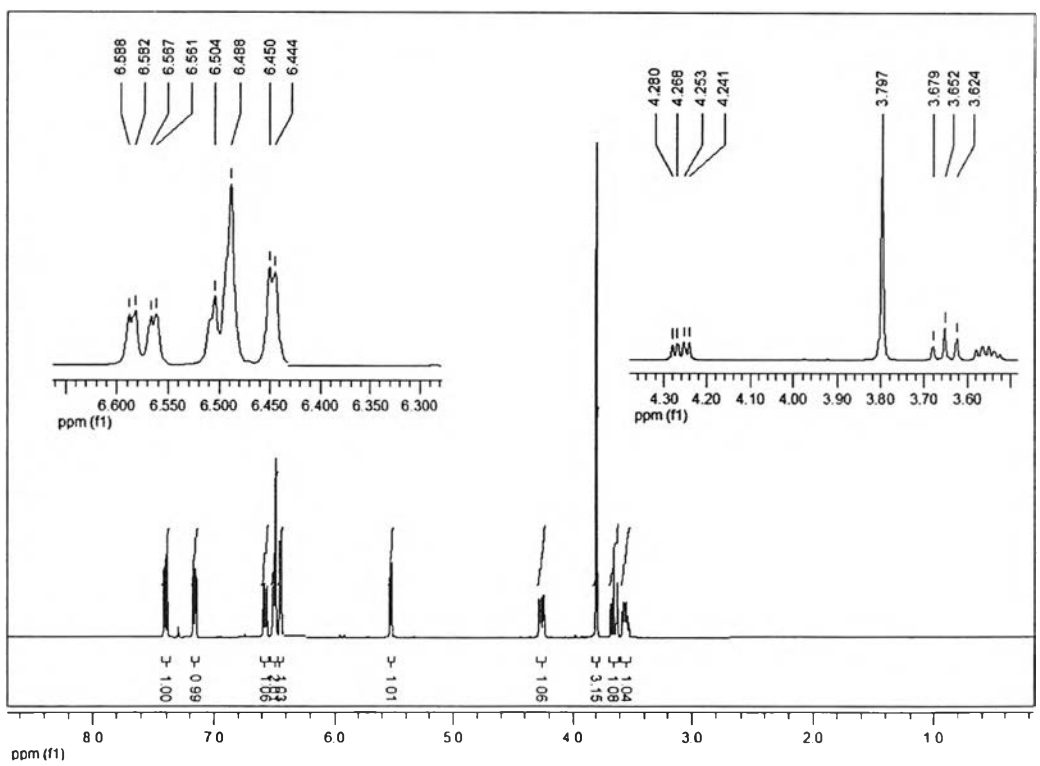

Figure 2.17 The ^{1}H-NMR spectrum of **D3**

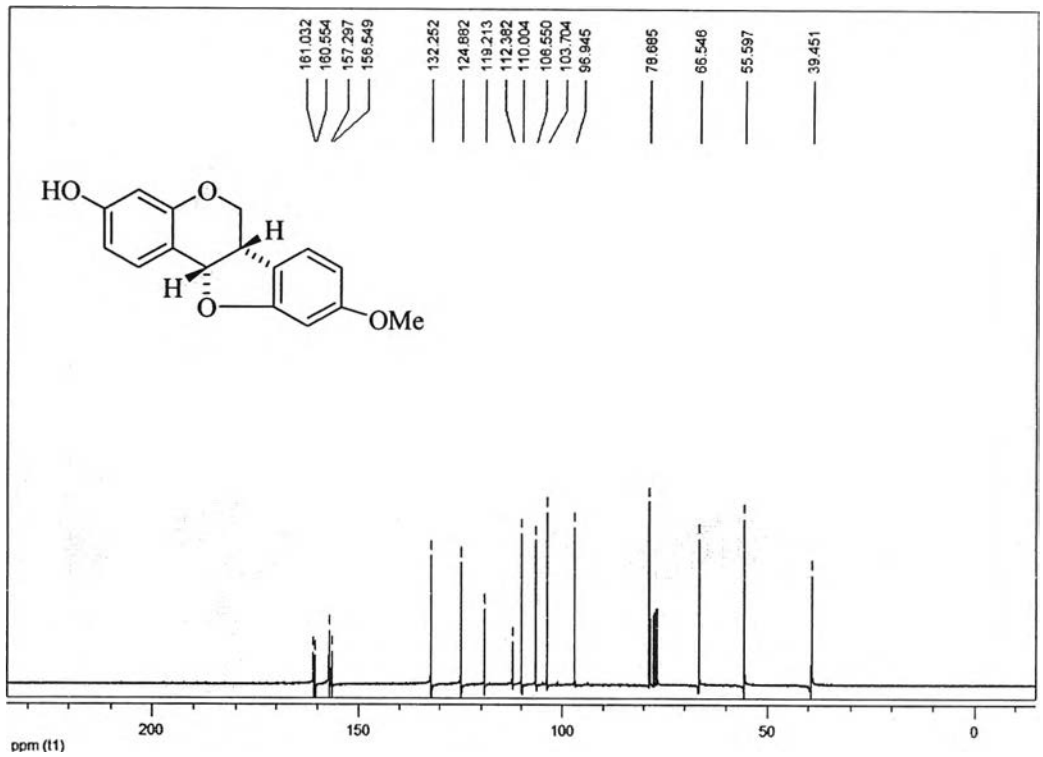

Figure 2.18 The ^{13}C-NMR spectrum of **D3**

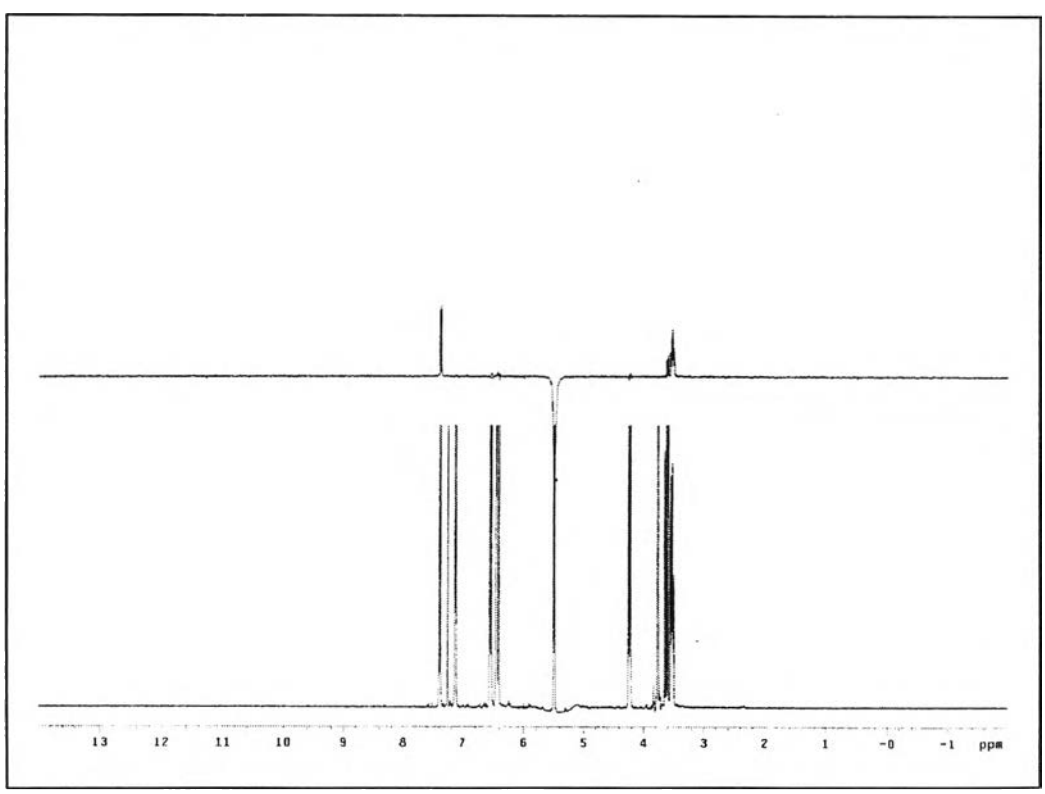

Figure 2.19 NOE DIFF of **D3** (irradiated at δ 5.53)

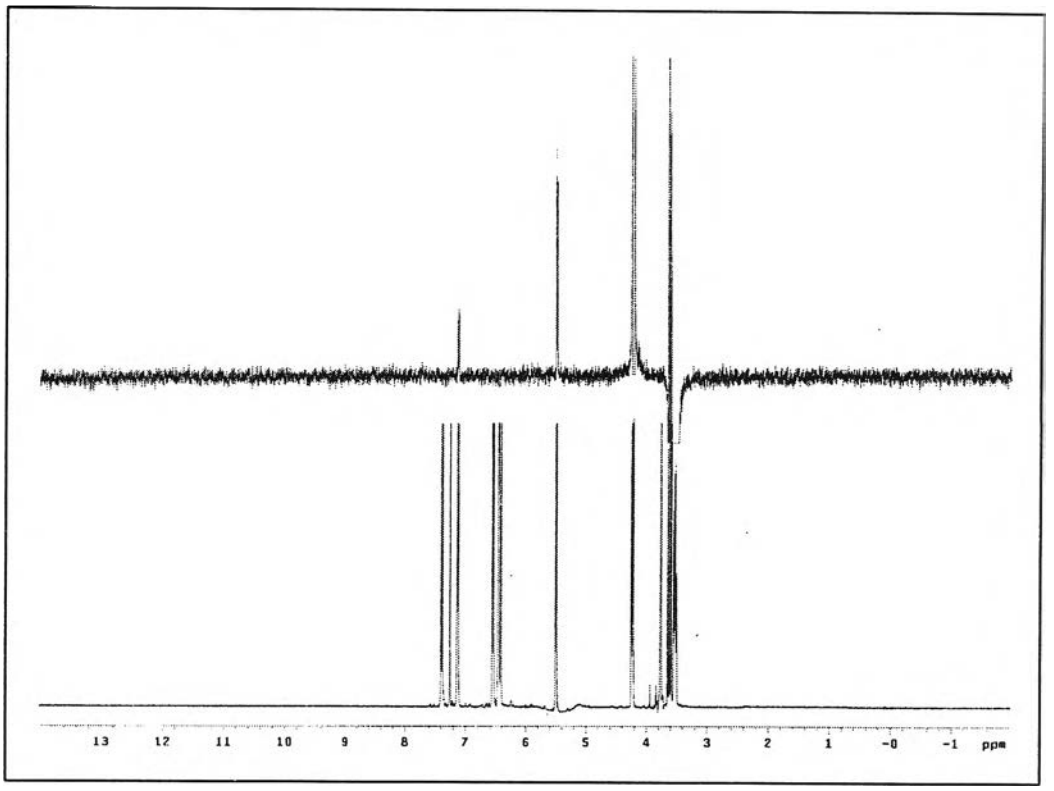

Figure 2.20 NOE DIFF of **D3** (irradiated at δ 3.52-3.58)

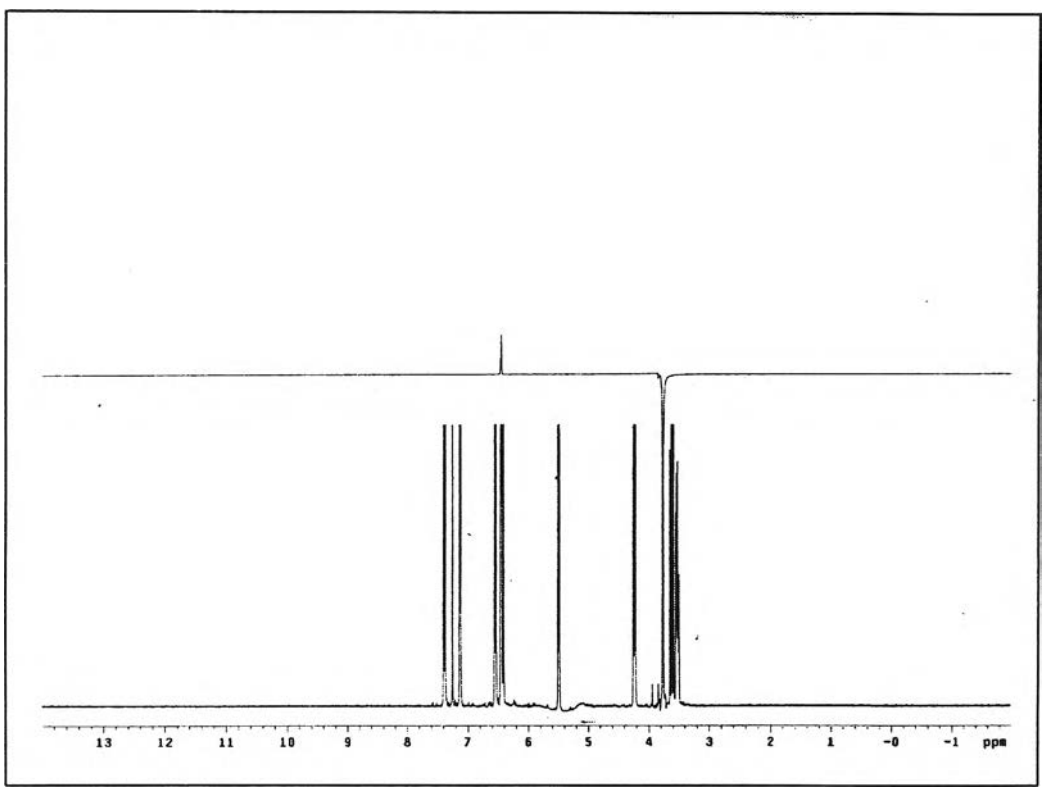

Figure 2.21 NOE DIFF of **D3** (irradiated at δ 3.80)

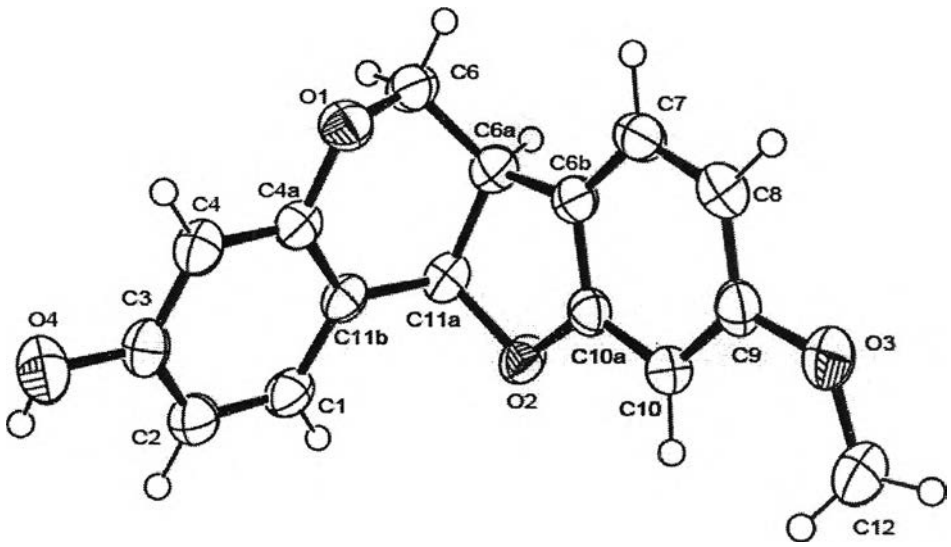

Figure 2.22 Computer-generated ORTEP drawing of **D3**

Structural elucidation of D4

D4 was isolated as brown solid with m.p. 188-190°C, and R_f value 0.56 (70% EtOAc in hexane). The molecular composition was defined as $C_{32}H_{28}O_8$ by the fast bombardment mass spectrometry analysis (FAB-MS).

The IR spectrum (Figure 2.23) exhibited the characteristic absorption peaks of hydroxyl group at 3155-3615 cm^{-1}, the C-H stretching vibration of CH and CH_2 at 2926, 2871 cm^{-1} and the C-H stretching of benzene ring at 1620, 1512 and 1481 cm^{-1}.

The ^{1}H-NMR (acetone-d_6) spectrum (Figure 2.24) showed the characteristics both of isoflavan and pterocarpan (isoflavan-pterocarpan type). This spectrum revealed the characteristic chemical shifts and coupling pattern at δ 3.49-3.51 (2H, m, H-6*ax*(E) and H-6a(E/F)), 4.14-4.16 (1H, m, H-6*eq*(E)) and 5.46 (1H, d, J = 6.2 Hz, H-11a(E/F)) which were reminisced of a pterocarpan skeleton. The coupling constant of H-6a(E/F) and H-11a(E/F) was 6.2 Hz which affirmed the assignment of a *cis* ring juncture in the pterocarpan part (J_{H6a}-H_{11a} ≈ 6-7 Hz, [68]). Moreover, it also showed the characteristic signals assignable to CH_2-CH-CH grouping of 3,4-diarylchroman system at δ 4.78 (1H, d, J = 8.4 Hz, H-4(C)), 3.73-3.75 (1H, m, H-3(C)), 4.14-4.16 (1H, m, H-2*ax*(C)) and 4.27 (1H, dd, J = 3.3, 10.5 Hz, H-2*eq*(C)) in an 4-aryl substituted isoflavan skeleton. The coupling constant of H-3 and H-4 in ring C was 8.4 Hz which confirmed the 3,4-*trans*- configuration in the isoflavan [71]. In addition, this spectrum further displayed the presence of two methoxy groups (δ 3.79 and 3.70)

and three hydroxyl groups (δ 8.33, 8.53 and 8.75 Hz). Other proton signals are tentatively assigned in Table 2.7.

The ^{13}C-NMR (acetone-d_6) spectrum (Figure 2.25) indicated the characteristic both of isoflavan and pterocarpan (isoflavan-pterocarpan type). This spectrum presented typical center three-carbon unit of pterocarpan type skeleton which could be assigned at δ 66.2, 39.7 and 78.3 coincided with C-6(E), C-6a(E/F) and C-11a(E/F), respectively. A set of three carbon signals at δ 37.9 (2C, C-3 and C-4) and 68.5 (C-2) in ring C was also present in this spectrum, clarifying that **D4** had an isoflavan skeleton. In addition, eight quaternary carbon signals attached to an oxygen function could be ascribed for the signals detected at δ 159.3 (C-4'(B)), 159.2 (C-10a(F/G)), 158.8 (C-3(D)), 158.6 (C-9(G)), 156.8 (C-4a(D/E)), 156.6 (C-7(A)), 156.0 (C-2'(B)) and 155.8 (C-8a(A/C)) and two signals belonging to methoxy groups were observed at δ 54.4 and 55.4. Other signals were detected as presented in Table 2.7.

According to the HMBC spectrum (Figure 2.26), it was manifested the correlations between C-4(C) (δ 37.9) and H-2*ax*(C), H-2*eq*(C), H-5(A), H-6'(B) and H-7(G) and between C-8(G) (δ 125.0) and H-3(C) and H-10(G). This affirmed the position of linkage in this molecule as [4(C), 8(G)]-linkage. Other correlations of **D4** are demonstrated in Table 2.7.

The specific rotation of **D4** was observed as $[\alpha]_D$ +116.1° (c 0.15 in acetone, at 20°C).

Additionally, the HSQC and COSY (Figures 2.27 and 2.28) spectra provided an additional information to endorse the proposed structure. The carbon and proton chemical shift assignments are shown in Table 2.7.

The NOE DIFF experiments were carried out. The irradiation of the proton signal at δ 3.49-3.51 (H-6*ax*(E) and H-6a(E/F)) caused the enhancement of the proton signal at δ 4.14-4.16 (H-6*eq*(E)), 5.46 (H-11a(E/F) and 6.93 (H-7(G) while the irradiation of the proton signal at δ 5.46 (H-11a(E/F) resulted in the enhancement of the proton signal at δ 3.49-3.51 (H-6a(E/F) and 7.32 (H-1(D). This confirmed that **D4** contained a *cis* ring juncture (Figures 2.29 and 2.30). The irradiation of the proton signal at δ 4.78 (H-4(C)) caused the enhancement of the proton signal at δ 3.73-3.75 (H-3(C)), 3.79 (OMe), 4.27 (H-2eq(C), 6.58 (H-5A), 6.93 (H-7(G) and 7.09 (H-6'(B) (Figure 2.31). In addition, the position of the two methoxy groups could also be confirmed by this technique. The irradiation of the proton signal at δ 3.70 resulted in the enhancement of the proton signal at δ 6.33-6.36 (H-5'(B)) and 6.44 (H-3'(B)) and

that of the proton signal at δ 3.79 caused the enhancement of the proton signal at δ 6.93 (H-7(G) and 6.49 (H-10(G) (Figures 2.32 and 2.33). Moreover, the position of three hydroxyl groups was also affirmed by this technique. To illustrate this, the irradiation of the proton signal at δ 8.33 resulted in the enhancement of the proton signal at δ 6.33-6.36 (H-6 and -8 (A)) and 6.58 (H-5(A)). The irradiation of the proton signal at δ 8.53 caused the enhancement of the proton signal at δ 6.44 (H-3'(B)) and that of the proton signal at δ 8.75 resulted in the enhancement of the proton signal at δ 6.59 (H-2(D)) and 6.38 (H-4(D)) (Figures 2.33, 2.35 and 2.36). The NOE DIFF correlation of **D4** is shown below:

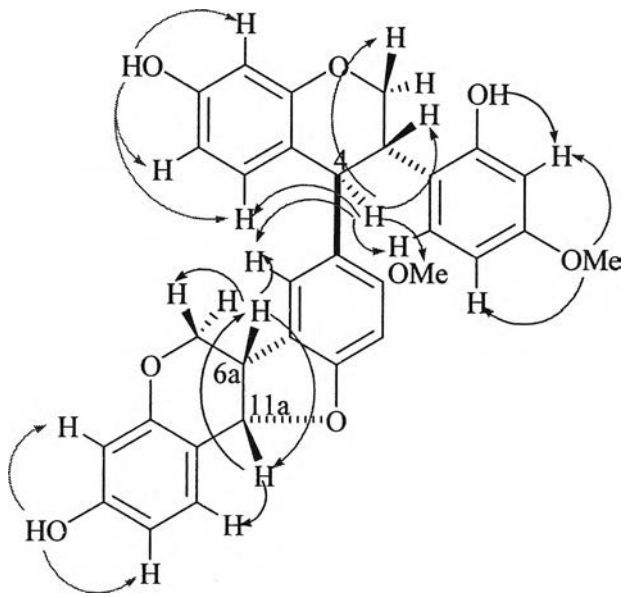

From the above-mentioned evidence, the structure of **D4** has been determined as (+)-3,4-*trans*-[3-hydroxy-9-methoxypterocarpan-8-yl]-2',7-dihydroxy-4'-methoxy-isoflavan which firstly isolated from natural product. The carbon and proton chemical shift assignments of **D4** compared with (*3S,4S*)-3,4-*trans*-4-[(6a*S*,11a*S*)-3,9-dimethoxypterocarpan-8-yl]-2',4',7-trimethoxyisoflavan (**44**) [71] are presented in Table 2.8. The structure of **D4** is shown below.

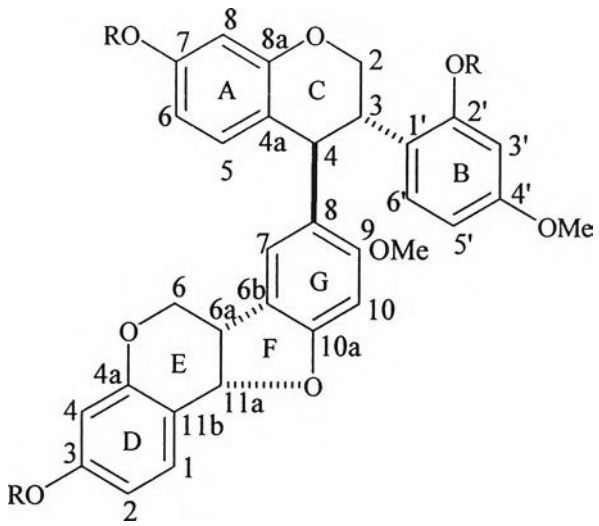

Compound **D4** R = H

44 R = Me

Table 2.7 The ^{1}H-, ^{13}C-NMR chemical shift assignments and 2D correlation of **D4**

Position (ring)	Type	Chemical shift (ppm)		COSY	HMBC
		^{13}C	^{1}H		
2(C)	CH_2	68.5	4.14-4.16 (m, H*ax*) 4.27 (dd, *J* = 3.3, 10.5 Hz, H*eq*)	H2*eq*(C), H2*ax*(C), H3(C)	H3(C), H4(C)
3(C)	CH	37.9	3.73-3.75 (m)	H4(C)	H6'(B), H4(C), H2*ax*(C), H2*eq*(C)
4 C)	CH	37.9	4.78 (d, *J* = 8.4 Hz)	-	H5(A), H2*ax*(C), H2*eq*(C), H7(G)
4a (A/C)	C	117.1	-	-	H6(A), H8(A), H4(C)
5 A)	CH	130.7	6.58 (d, *J* = 8.4 Hz)	H6(A)	H4(C)
6A)	CH	108.3	6.33-6.36 (m)	-	H5(A), H8(A), OH(8.33)
7(A)	C		-	-	H5(A), OH(8.33)
8(A)	CH	102.5	6.33-6.36 (m)		H6(A), OH(8.33)
8a (A/C)	C	155.8	-	-	H5(A), H8(A), H2*eq*(C), H4(C)
1'(B)	C	119.3	-	-	H3'(B), H5'(B), H2*ax*(C), H2*eq*(C), H3(C), H4(C), OH(8.53)
2'(B)	C	156.0	-	-	H3'(B), H6'(B), OH(8.53)
3'(B)	CH	101.4	6.44 (d, *J* = 2.5 Hz)		H5'(B), OH(8.53)
4'(B)	C	159.3	-	-	H3'(B), H4'(B), H6'(B), OMe (3.70)
5'(B)	CH	104.5	6.33-6.36 (m)	H6'(B)	H3'(B)
6' B)	CH	128.7	7.09 (d, *J* = 8.4 Hz)	-	H3(C)
1(D)	CH	132.2	7.32 (d, *J* = 8.4 Hz)	H2(D)	H11a(E/F)
2(D)	CH	109.6	6.59 (dd, *J* = 2.3 and 8.4 Hz)	-	H1(D), H4(D), OH(8.75)
3(D)	C	158.8	-	-	H1(D), H2(D), H4(D), OH(8.75)

Table 2.7 (continued)

Position (ring)	Type	Chemical shift (ppm)		COSY	HMBC
4(D)	CH	103.1	6.38 (d, J = 2.3 Hz)		H2(D), OH(8.75)
4a (D/E)	C	156.8	-	-	H1(D), H4(D), H6*ax*(E), H6*eq*(E), H11a(E/F)
6(E)	CH_2	66.2	3.49-3.51 (m, H*ax*)	H6*eq*(E), H6a(E/F)	H6*ax*(E), H6a(E/F), H11a(E/F)
			4.14-4.16 (m, H*eq*)		
6a (E/F)	CH	39.7	3.49-3.51 (m)	H11a(E/F)	H6*ax*(E), H6*eq*(E), H11a(E/F), H7G
6b (F/G)	C	118.9	-	-	H6*ax*(E), H6*eq*(E), H11a(E/F), H10(G)
7(G)	CH	125.1	6.93 (s)	-	H4(C), H6a(E/F)
8(G)	C	125.0	-	-	H(C), H10(G)
9(G)	C	158.6	-	-	H4(C), H7(G), H10(G), OMe (3.79)
10(G)	CH	94.0	6.49 (s)	-	OMe (3.79)
10a (F/G)	C	159.2	-	-	H6a(E/F), H11a(E/F), H7(G), H10(G)
11a (E/F)	CH	78.3	5.46 (d, J = 6.2 Hz)	-	H1(D), H6(E), H6*ax*(E/F), H6*eq*(E)
11b (D/E)	C	112.0	-	-	H2(D), H4(D), H6a(E/F), H11a(E/F)
9(G)	OMe	55.4	3.79 (s)	-	-
4'(B)	OMe	54.4	3.70 (s)	-	-
7(A)	OH		8.33 (s)	-	-
8(B)	OH		8.53 (s)	-	-
3(D)	OH		8.75 (s)	-	-

ax: axial; *eq*: equatorial

Table 2.8 The ^{1}H-NMR chemical shift assignments of **D4** compared with **44** [71]

Position (ring)	Chemical shift (ppm)	
	D4	**44**
2(C)	4.14-4.16 (m, H*ax*)	4.17-4.47 (m)
	4.27 (dd, *J* = 3.3 and 10.5 Hz, H*eq*)	
3(C)	3.73-3.75 (m)	3.69-3.88 (m)
4 (C)	4.78 (d, *J* = 8.4 Hz)	4.63 (d, *J* = 9.0 Hz)
5 (A)	6.58 (d, *J*= 8.4 Hz)	6.63 (d, *J*= 8.0 Hz)
6(A)	6.33-6.36 (m)	6.25-6.44 (m)
8(A)	6.33-6.36 (m)	6.25-6.44 (m)
3'(B)	6.44 (d, *J* = 2.5 Hz)	6.25-6.44 (m)
5'(B)	6.33-6.36 (m)	6.25-6.44 (m)
6' B)	7.09 (d, *J* = 8.4 Hz)	6.94 (d, *J* = 9.3 Hz)
1(D)	7.32 (d, *J* = 8.4 Hz)	7.34 (d, *J* = 8.5 Hz)
2(D)	6.59 (dd, *J* = 2.3, 8.4 Hz)	6.56 (dd, *J* = 2.5, 8.5 Hz)
4(D)	6.38 (d, *J* = 2.3 Hz)	6.25-6.44 (m)
6(E)	3.49-3.51 (m, H*ax*)	3.25-3.56 (m, H*ax*)
	4.14-4.16 (m, H*eq*)	3.95-4.09 (m, H*eq*)
6a(E/F)	3.49-3.51 (m)	3.25-3.56 (m)
7(G)	6.93 (s)	6.72 (s)
10(G)	6.49 (s)	6.25-6.44 (m)
11a(E/F)	5.46 (d, *J* = 6.2 Hz)	5.39 (d, *J* = 6.3 Hz)
OMe	3.70 (s)	3.59 (s)
OMe	3.79 (s)	3.66 (s)
OMe	-	3.72 (s)
OMe	-	3.75 (s)
OMe	-	3.75 (s)
OH	8.33 (s)	-
OH	8.53 (s)	-
OH	8.75 (s)	-

ax: axial; *eq*: equatorial

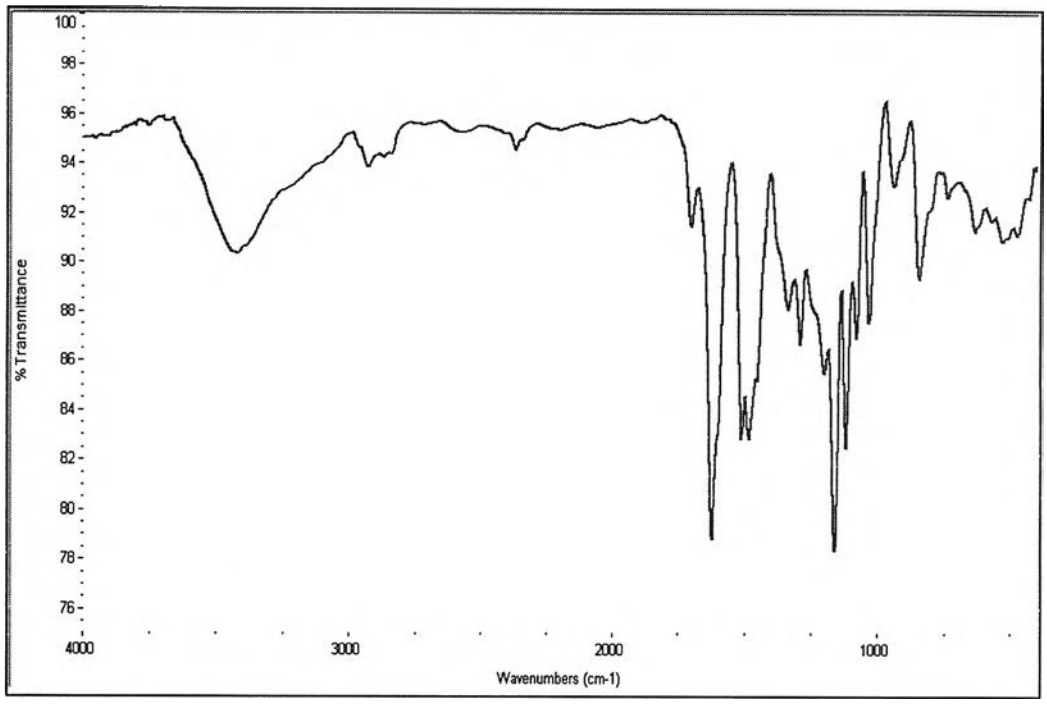

Figure 2.23 The IR spectrum of **D4**

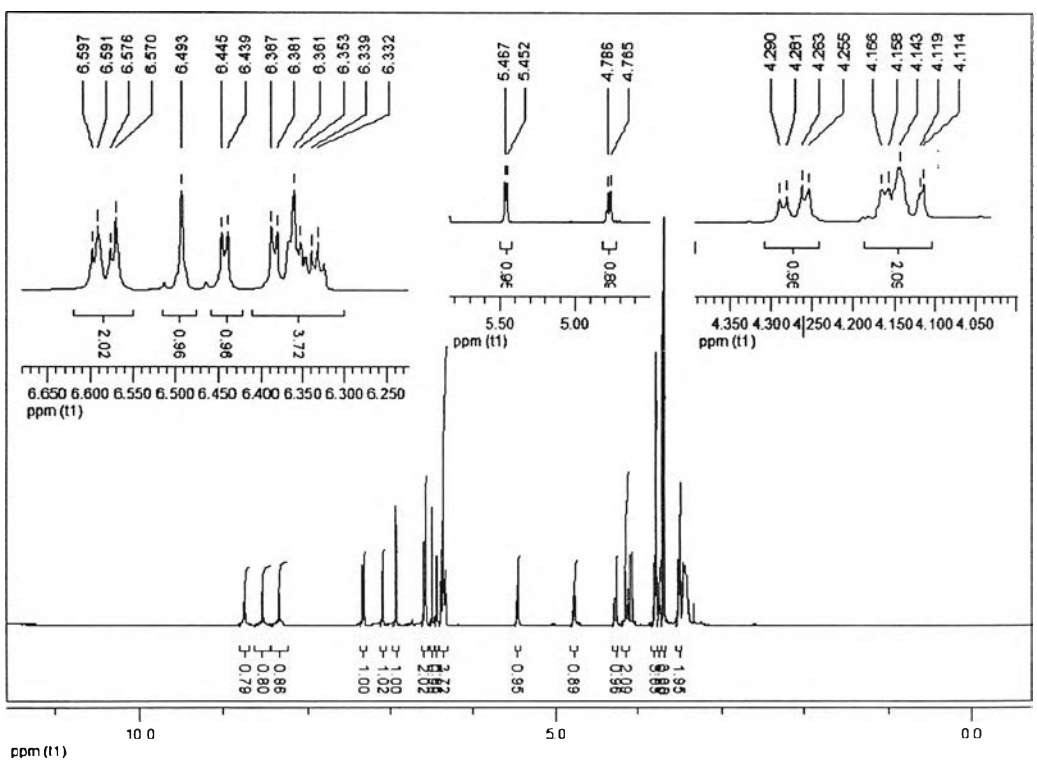

Figure 2.24 The ^{1}H-NMR spectrum of **D4**

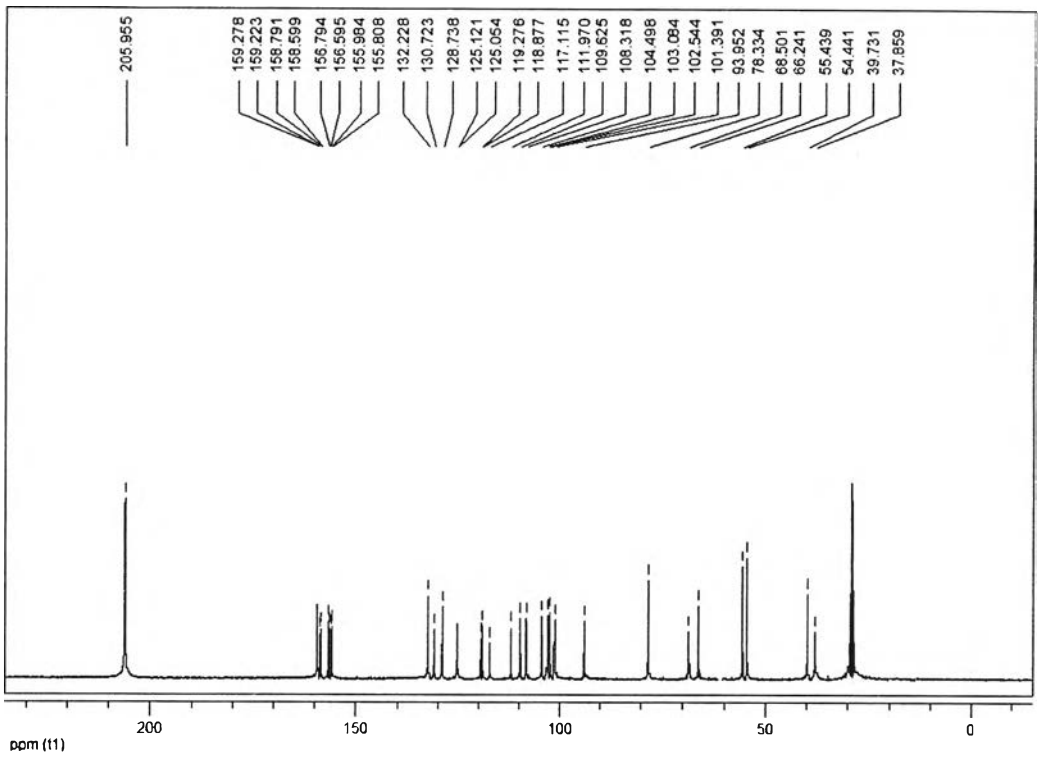

Figure 2.25 The ^{13}C-NMR spectrum of **D4**

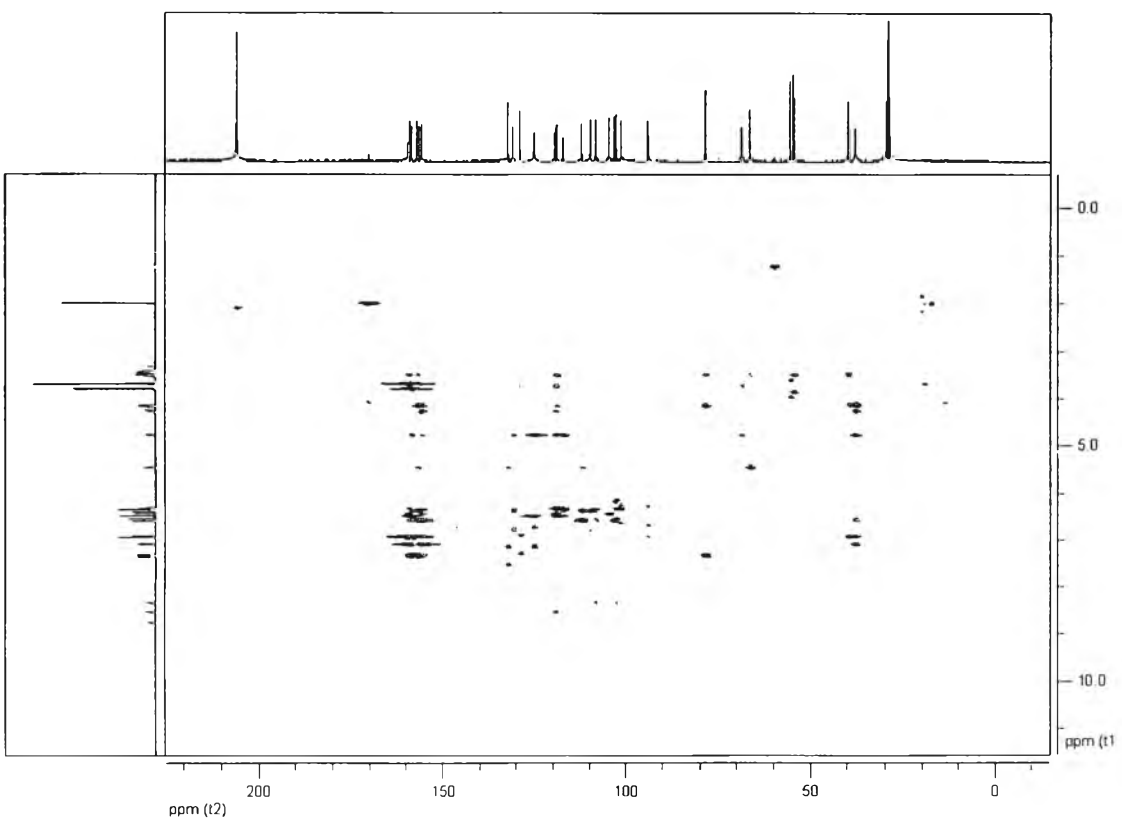

Figure 2.26 The HMBC spectrum of **D4**

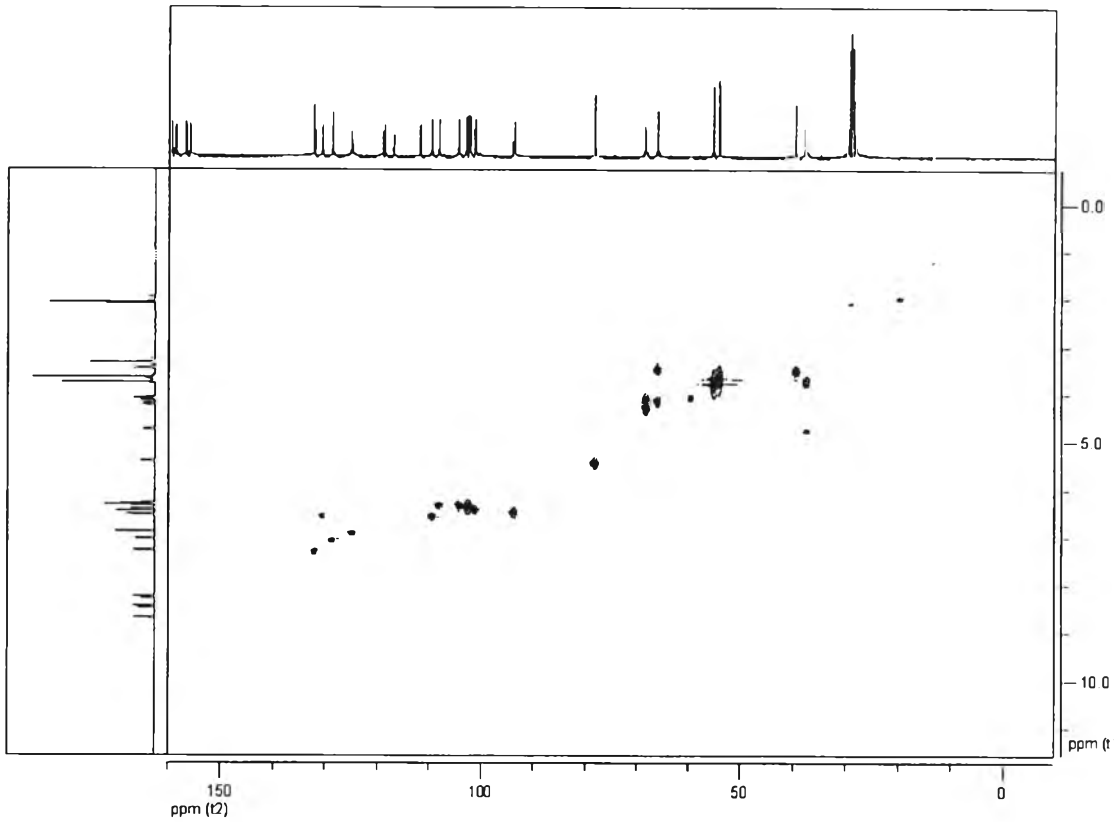

Figure 2.27 The HSQC spectrum of **D4**

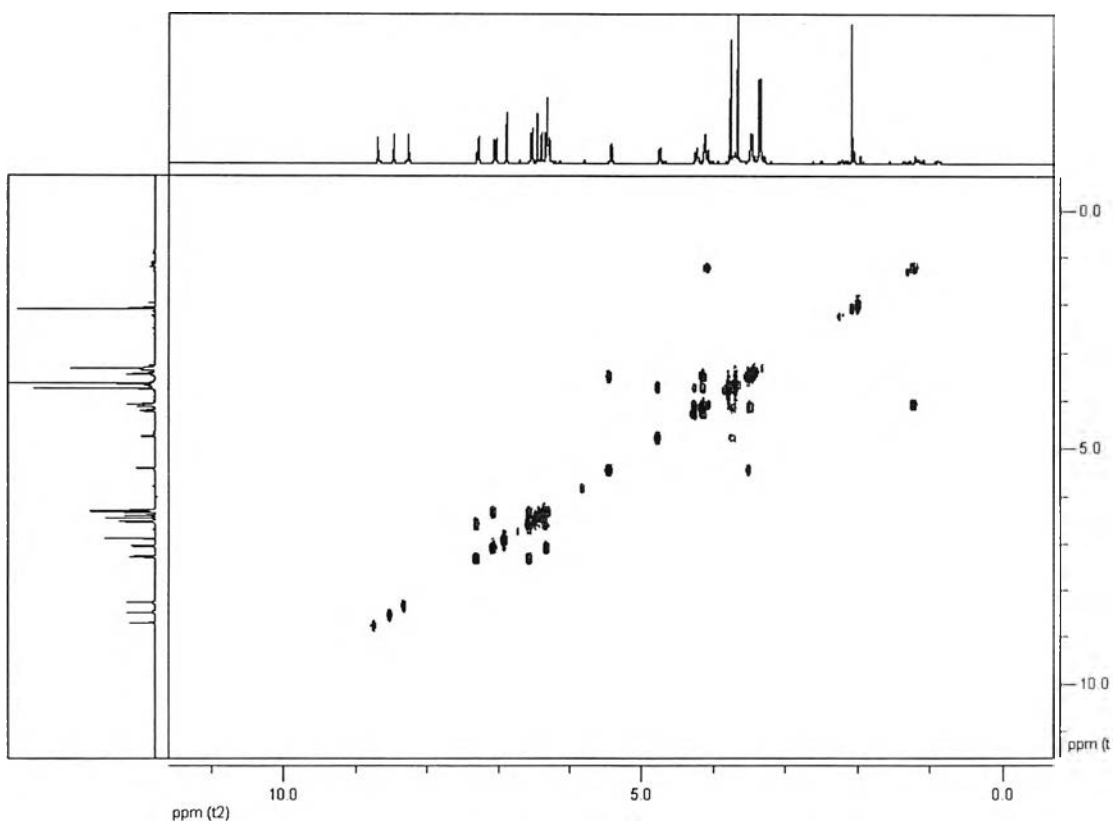

Figure 2.28 The COSY spectrum of **D4**

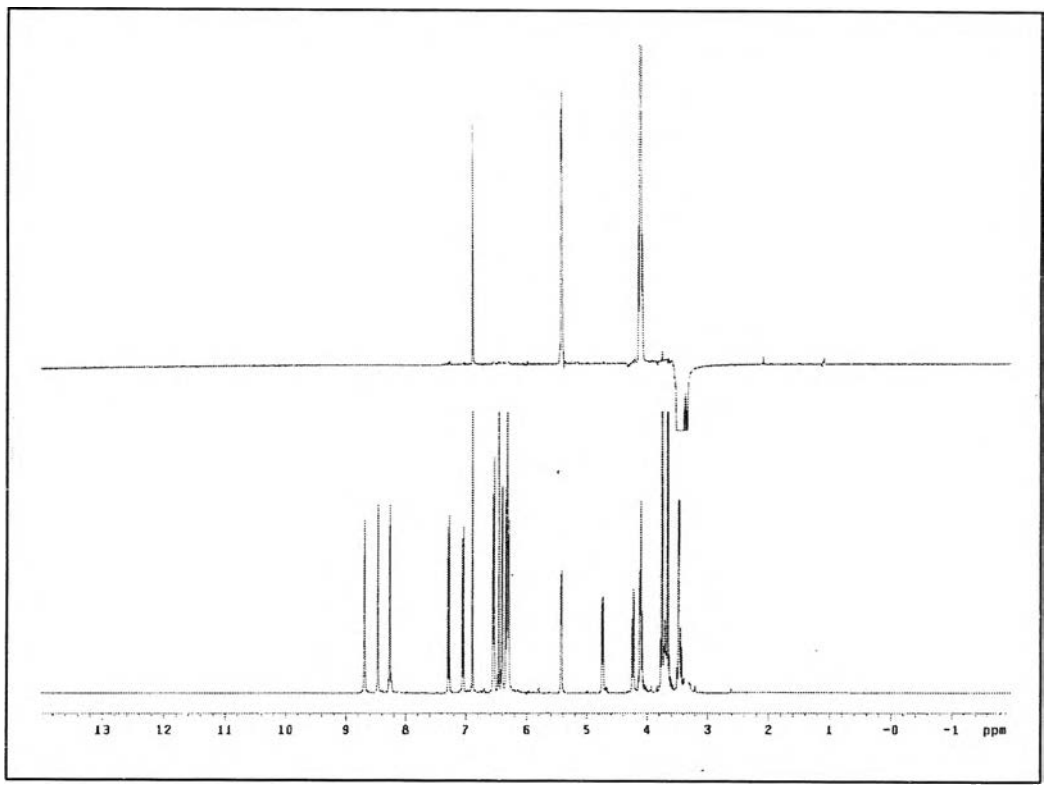

Figure 2.29 NOE DIFF of **D4** (irradiated at δ 3.49-3.51)

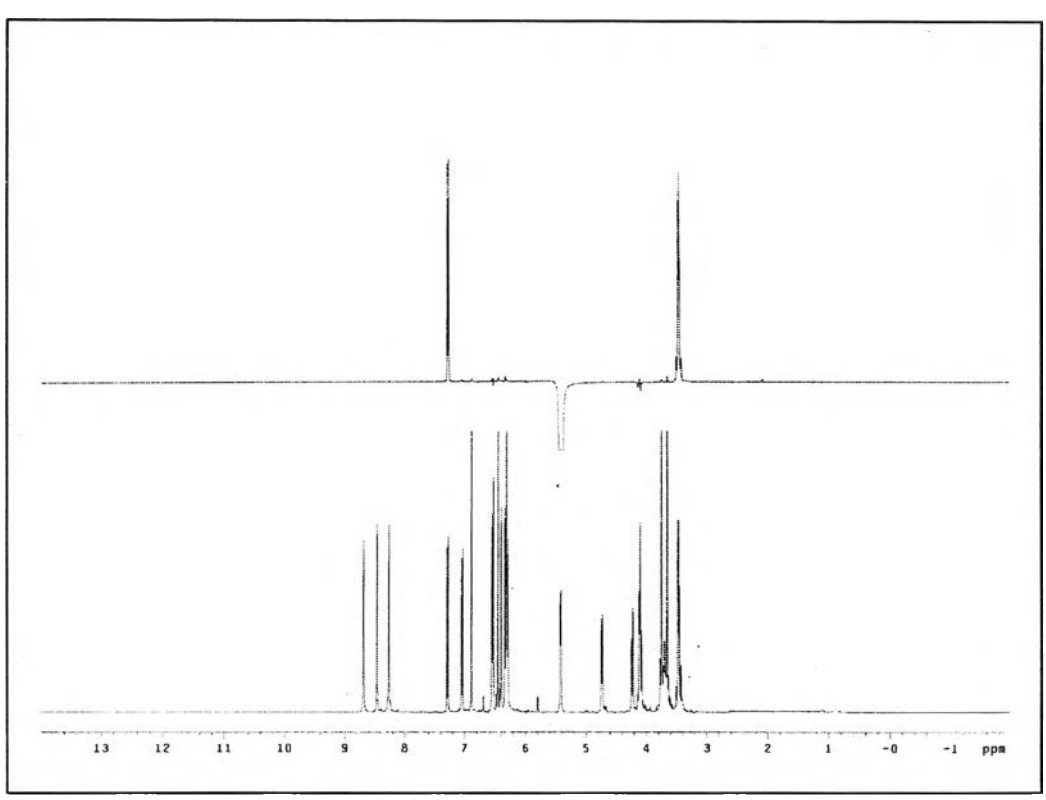

Figure 2.30 NOE DIFF of **D4** (irradiated at δ 5.46)

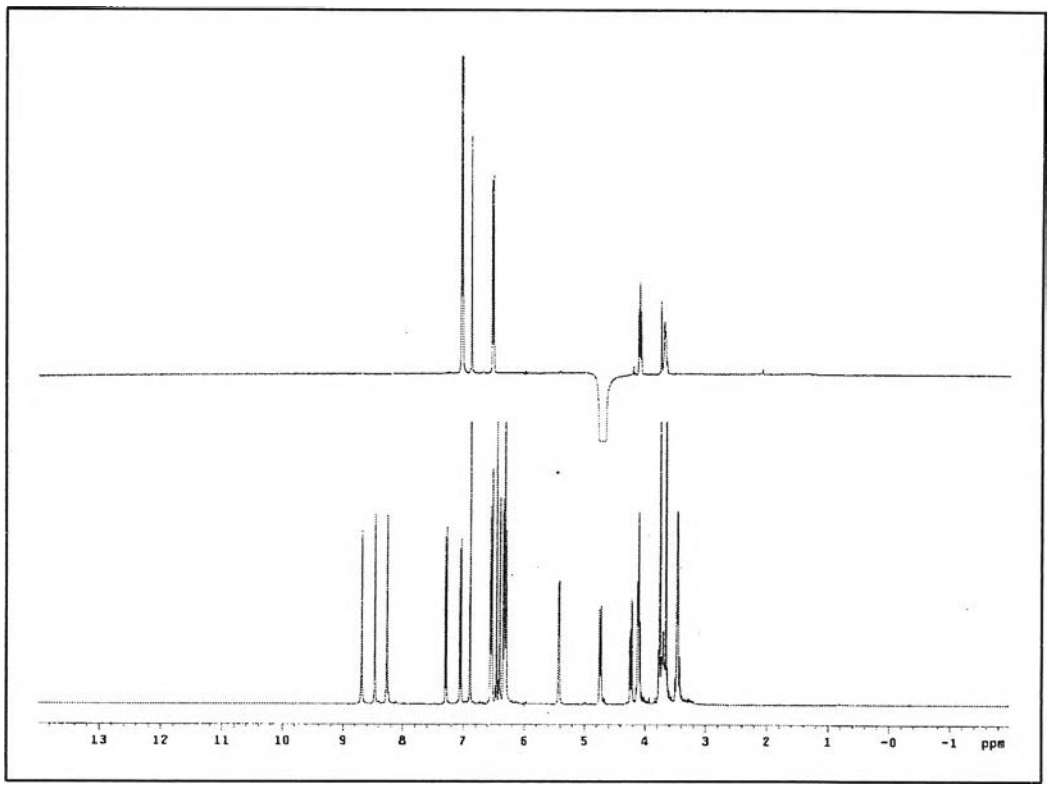

Figure 2.31 NOE DIFF of **D4** (irradiated at δ 4.78)

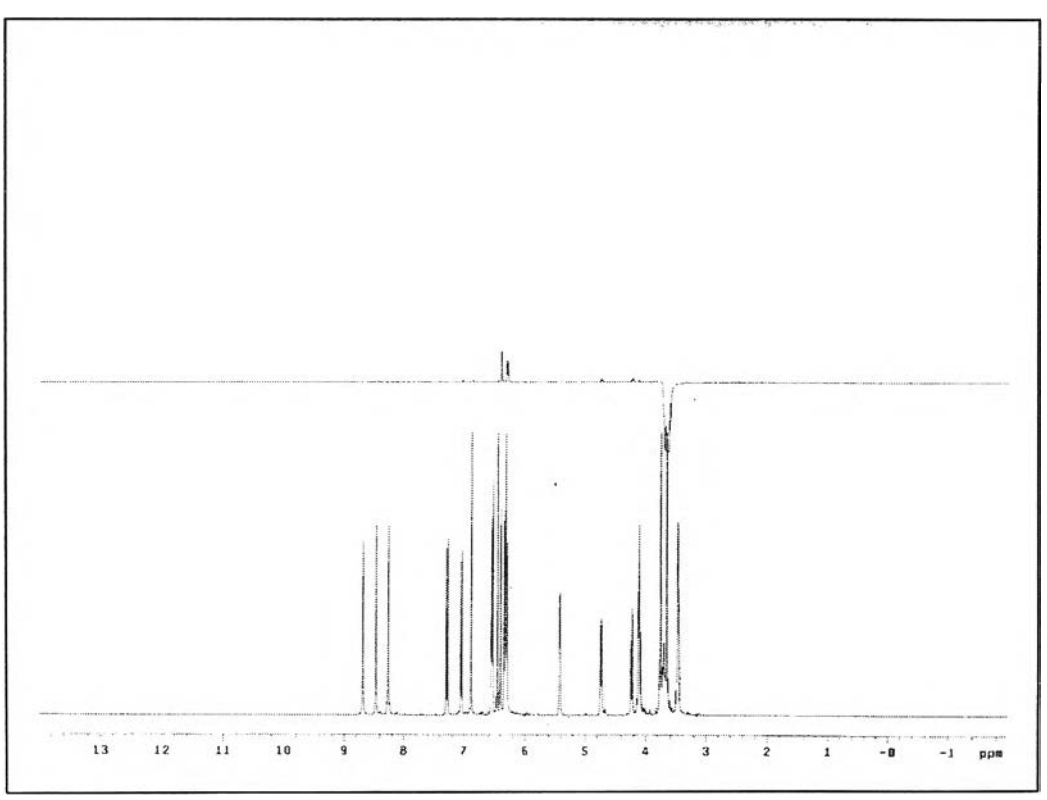

Figure 2.32 NOE DIFF of **D4** (irradiated at δ 3.70)

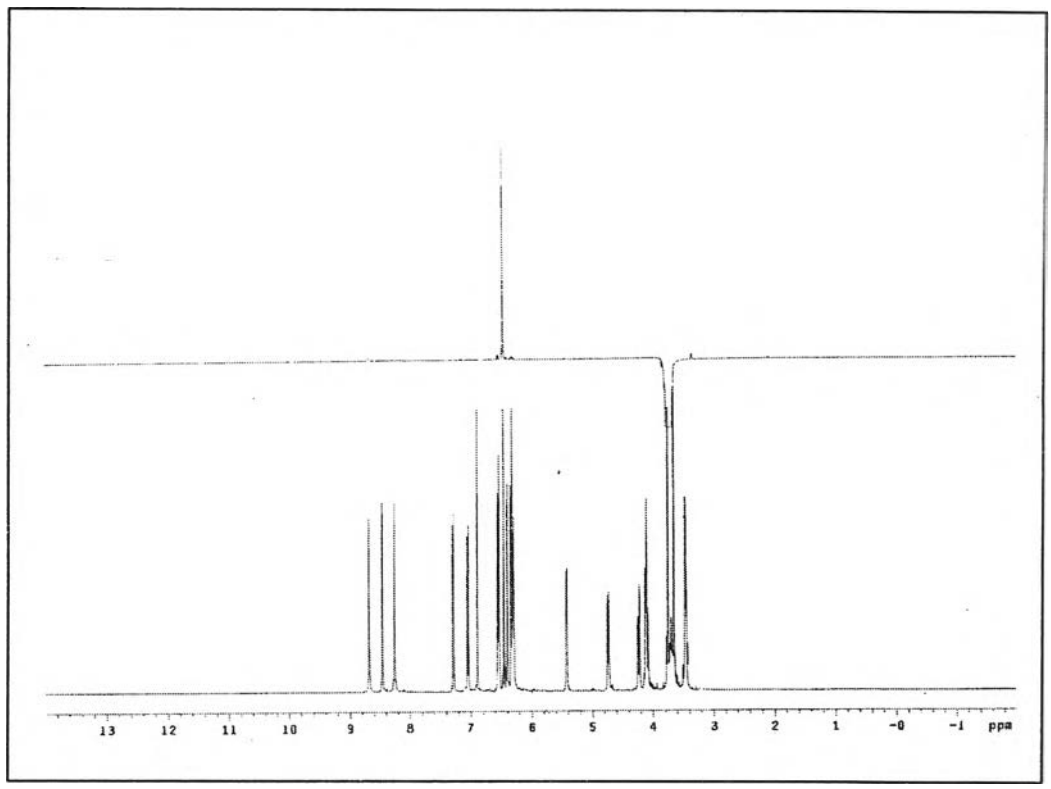

Figure 2.33 NOE DIFF of **D4** (irradiated at δ 3.79)

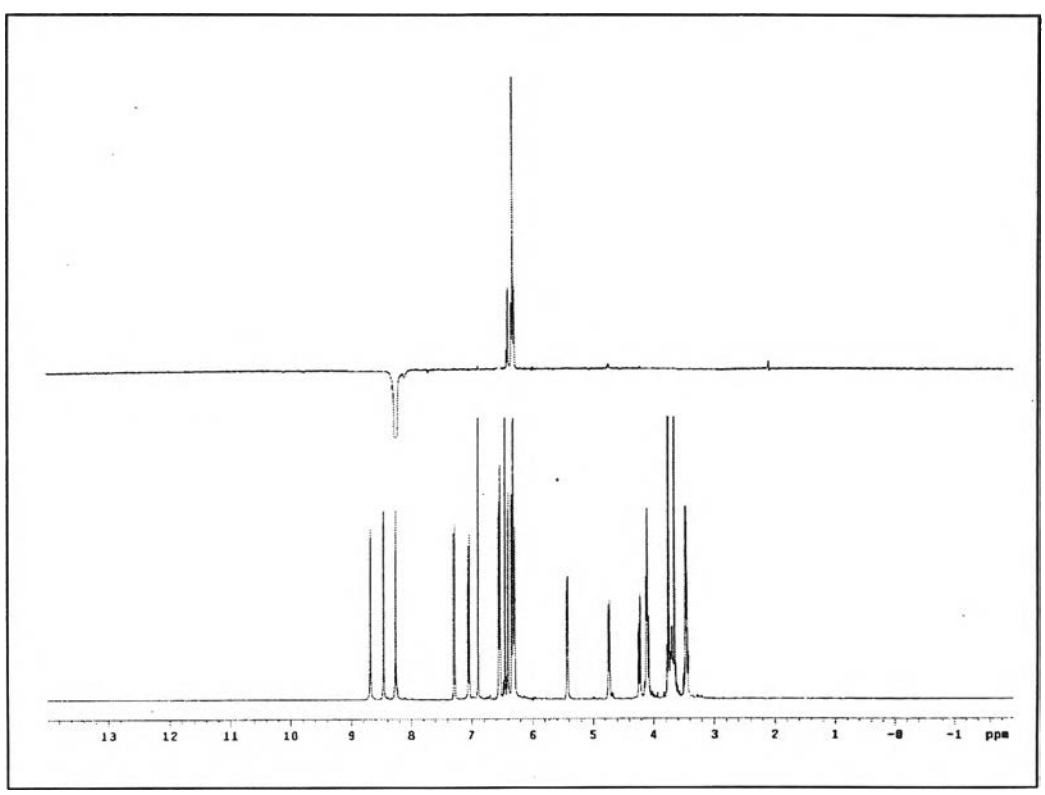

Figure 2.34 NOE DIFF of **D4** (irradiated at δ 8.33)

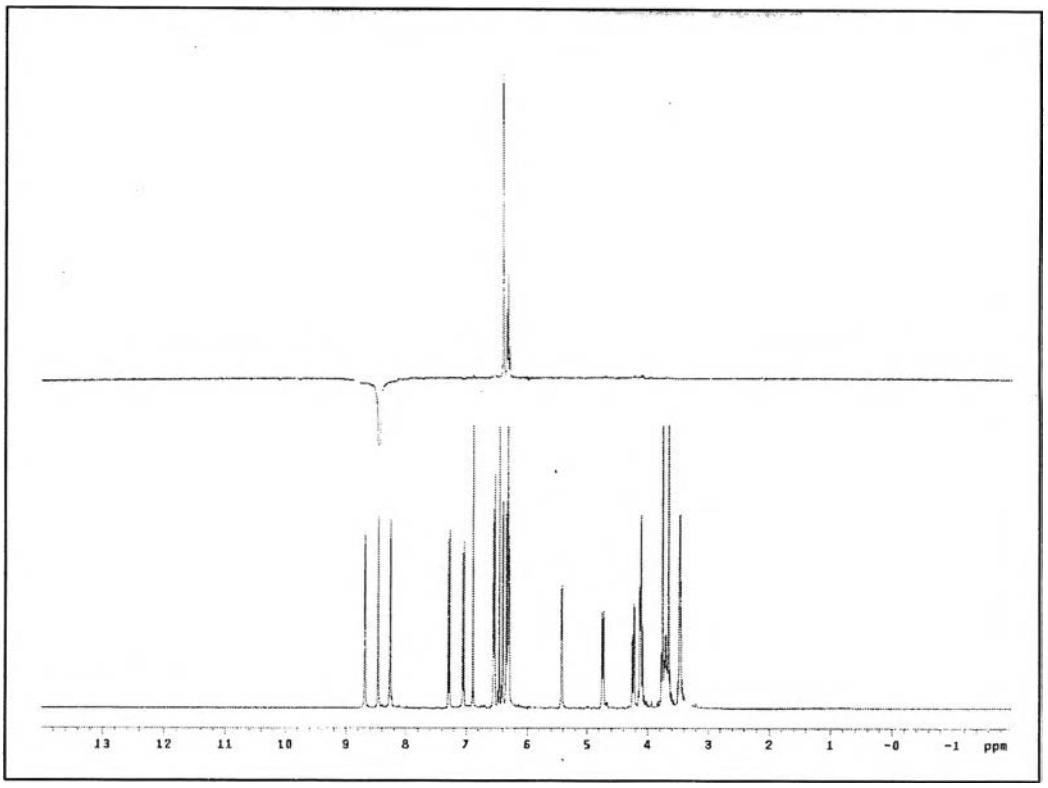

Figure 2.35 NOE DIFF of **D4** (irradiated at δ 8.53)

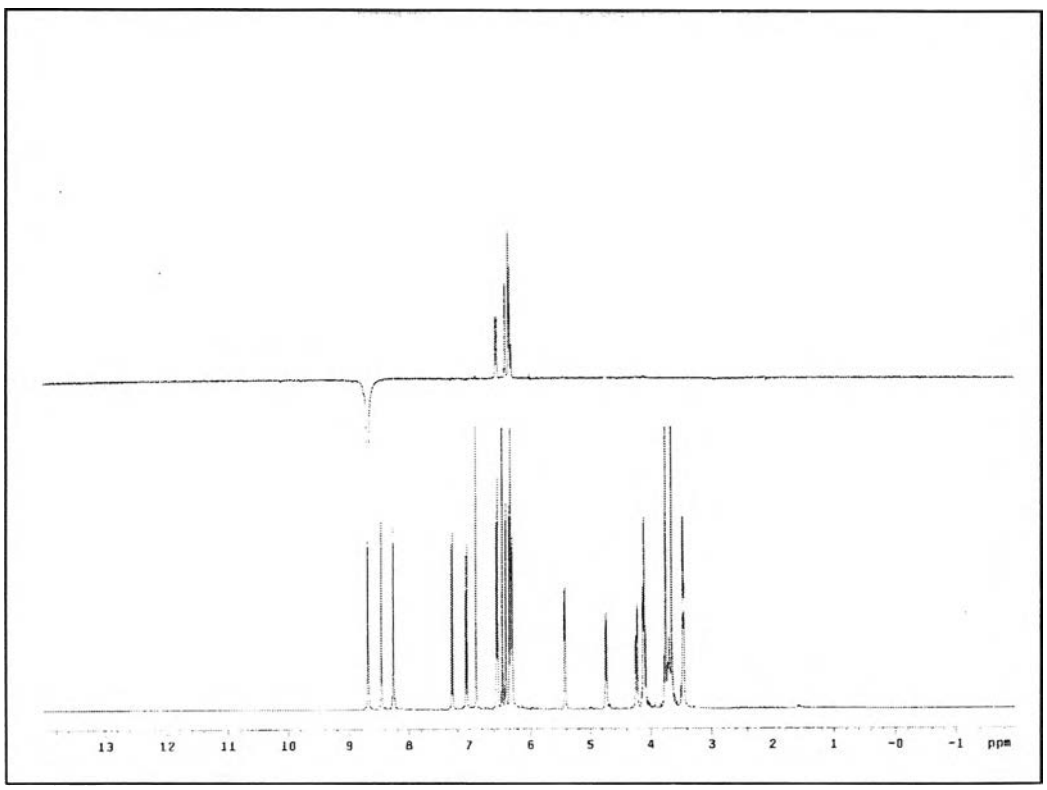

Figure 2.36 NOE DIFF of **D4** (irradiated at δ 8.75)

Separation of Fraction II

According to the monitoring fraction II (31.99 g) by thin TLC, this fraction exhibited similar spots as detected for **D2** and **D3** which were already isolated from fractions I and III, respectively. Therefore, there is rationalized not to separate and further explore this fraction. Moreover, from ^{1}H NMR spectrum of this fraction showed significant signals of both **D2** and **D3**. It showed the characteristic of methylenedioxy proton signal at δ 5.95 (2H, 2 overlapping d) of **D2** and showed doublet at 7.16 (J = 8.8 Hz) of H-7 of **D3** as presented in Figures 2.10 and 2.17, respectively.

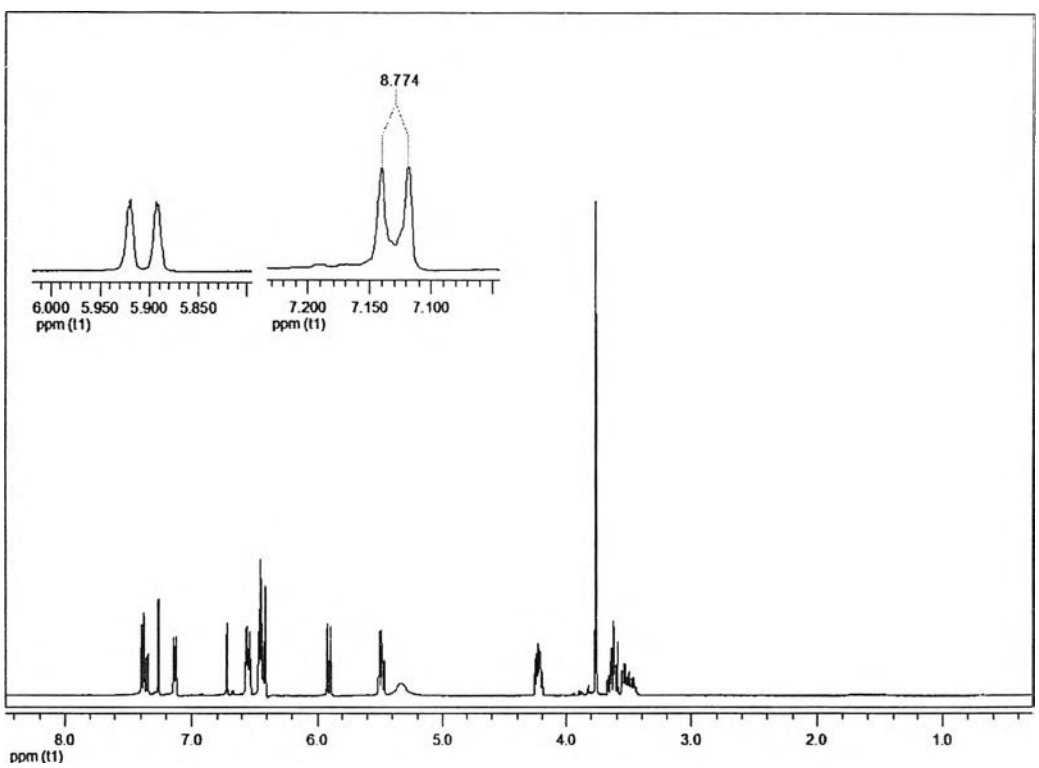

Figure 2.37 The ^{1}H-NMR spectrum of fraction II

Separation of Fraction IV

Fraction IV (7.52 g) was further separated by silica gel column chromatography, using gradient elution of 20% EtOAc in hexane to 100% EtOAc. Each fraction was collected approximately 50 mL and was monitored by TLC. The fraction demonstrated similar pattern on TLC plates were combined. The results of the separation of fraction IV are presented as shown below:

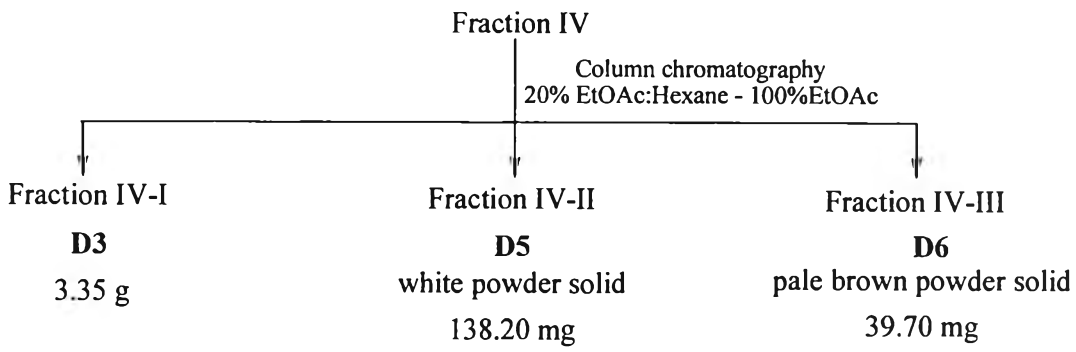

As aforementioned scheme, **D3**, white powder solid designated as **D5** and pale brown powder solid assigned as **D6** were achieved from fraction IV.

Structural elucidation of D5

D5 was obtained as white powder with m.p. 223.3-225.2°C (lit [72], 227°C) and R_f value 0.40 (40% EtOAc in hexane).

The mass spectrum (Figure 2.38) gave a molecular ion [M^+] peak at m/z 302 together with other fragment ion peaks at m/z 180, 168, 148, 133 and 123 consistent with a molecular formula of $C_{17}H_{18}O_5$. The possible fragmentation pattern of **D5** was proposed as shown in Scheme 2.5.

The IR spectrum (Figure 2.39) displayed absorption bands of hydroxyl group at 3517-3249 cm^{-1}, C-H stretching of CH_2 at 2999, 2939 and 2832 cm^{-1}. The C-H stretching of benzene ring was observed at 1618 and 1505 cm^{-1}.

The ^{1}H-NMR (acetone-d_6) spectrum (Figure 2.40) revealed a set of mutually coupled five protons (δ 2.80-2.85 (1H, m), 2.91-2.94 (1H, m), 3.45-3.52 (1H, m), 3.97 (1H, dd, J = 10.4 and 10.4 Hz) and 4.20-4.23 (1H, m)) suggested the presence of an isoflavan-type C ring assigned to H-4, H-3 and H-2. This spectrum further exhibited the presence of two methoxy groups (δ 3.86 and 3.90), two hydroxyl groups (δ 7.63 and 8.25) and a set of two *ortho*-coupled protons (δ 6.69 and 6.76, each d, J = 8.6 Hz).

Moreover, it also showed three protons in a ABC spin system 6.33 (d, J = 2.3 Hz, H-8), 6.40 (dd, J = 2.3 and 8.2 Hz, H-6) and 6.93 (d, J = 8.2 Hz, H-5).

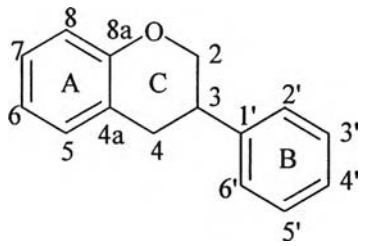

isoflavan skeleton

The ^{13}C-NMR (acetone-d_6) spectrum (Figure 2.41) revealed seventeen carbon signals of fifteen carbon skeleton and two substituted groups (flavonoid characteristic). This spectrum showed typical center-carbon signals of isoflavan skeleton type at δ 70.1 (C-2), 31.8 (C-3) and 31.2 (C-4). Two quaternary carbon signals occupied by an oxygen function (δ 156.7 and 155.1) displayed that ring A had a resorcinol oxidation pattern with a 7-hydroxy substitution. A set of *ortho*-couple protons (δ 6.69 and 6.76) in ^{1}H-NMR spectrum and three quaternary carbon signals attached to an oxygen function (δ 147.6, 145.9 and 139.5) in ^{13}C-NMR spectrum, simplified that ring B oxygenation pattern coincided to pyrogallol with a 2',3',4'-trisubstitution pattern. In addition, the chemical shifts of methoxy groups were observed at δ 55.6 and 60.0.

The optical rotation of **D5** was which was implied that the sign of optical rotation was ±, indicated that **D5** was optically inactive compound.

Hence, from the above-mentioned evidence, the structure of **D5** as (±)-3',7-dihydroxy-2',4'-dimethoxyisoflavan or (±)-mucronulatol could be deduced. The structure is shown below.

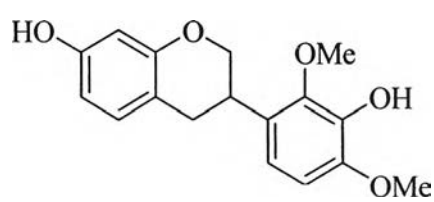

(±)-mucronulatol

The ^{1}H-, ^{13}C-NMR chemical shift assignments of **D5** compared with (*R*)-mucronulatol [73] are presented in Table 2.9.

Table 2.9 The ^{1}H-, ^{13}C-NMR chemical shift assignments of **D5** compared with (*R*)-mucronulatol [73]

Position	Chemical shift (ppm)		
	D5		(*R*)-mucronulatol
	^{13}C	^{1}H	^{1}H
2	70.1	3.97 (dd, *J* = 10.4, 10.4 Hz, H*ax*)	3.77-3.97 (m, H*ax*)
		4.20-4.23 (m, H*eq*)	4.15 (dd, *J* = 4.0, 9.0 Hz, H*eq*)
3	31.8	3.45-3.52 (m)	3.65-3.15 (m)
4	31.2	2.80-2.85 (m, H*eq*)	2.85 (d, *J* = 8.0 Hz)
		2.91-2.94 (m, H*ax*)	
4a	113.3	-	-
5	130.1	6.93 (d, *J* = 8.2 Hz)	6.83 (d, *J* = 7.0 Hz)
6	108.0	6.40 (dd, *J* = 2.3, 8.2 Hz)	6.37 (dd, *J* = 2.0, 7.0 Hz)
7	156.7	-	-
8	102.8	6.33 (d, *J* = 2.3 Hz)	6.27 (d, *J* = 2.0 Hz)
8a	155.1	-	-
1′	127.3	-	-
2′	147.6	-	-
3′	139.5	-	-
4′	145.9	-	-
5′	107.1	6.76 (d, *J* = 8.6 Hz)	6.60 (d, *J* = 8.0 Hz)
6′	116.6	6.69 (d, *J* = 8.6 Hz)	6.71 (d, *J* = 8.0 Hz)
OH		8.25 (s)	8.07 (s)
OH		7.63 (s)	7.41 (s)
OMe	55.6	3.86 (s)	3.81 (s)
OMe	60.0	3.90 (s)	3.87 (s)

ax: axial; *eq*: equatorial

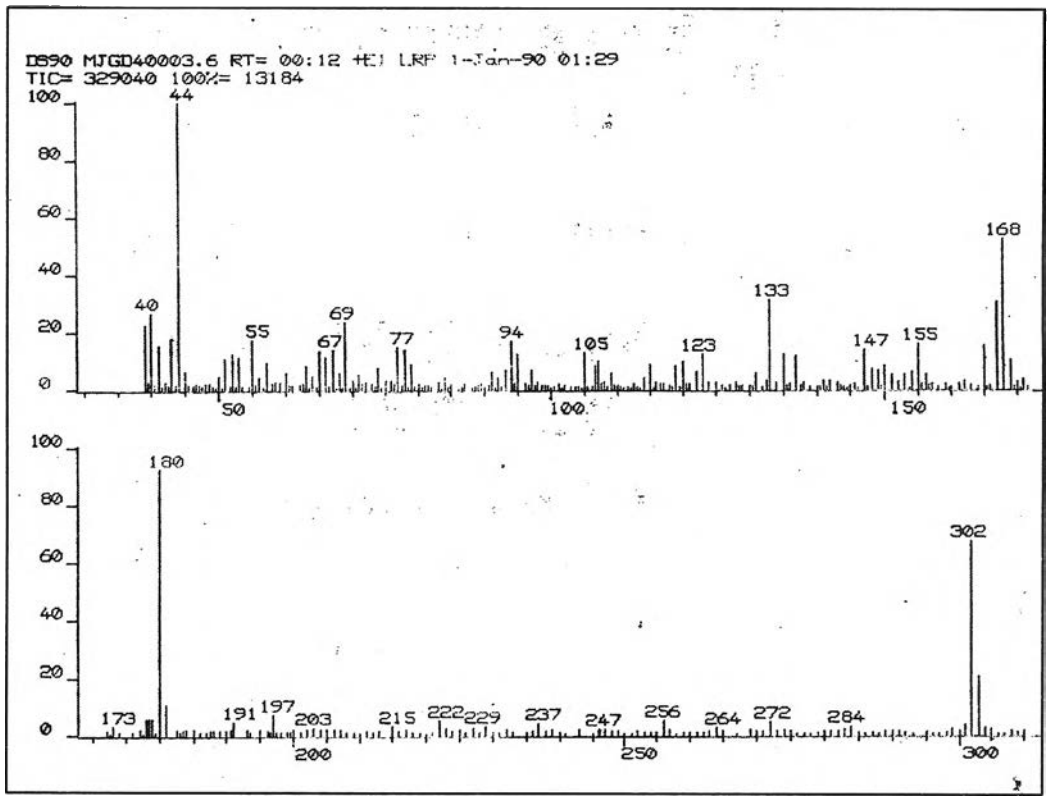

Figure 2.38 The mass spectrum of **D5**

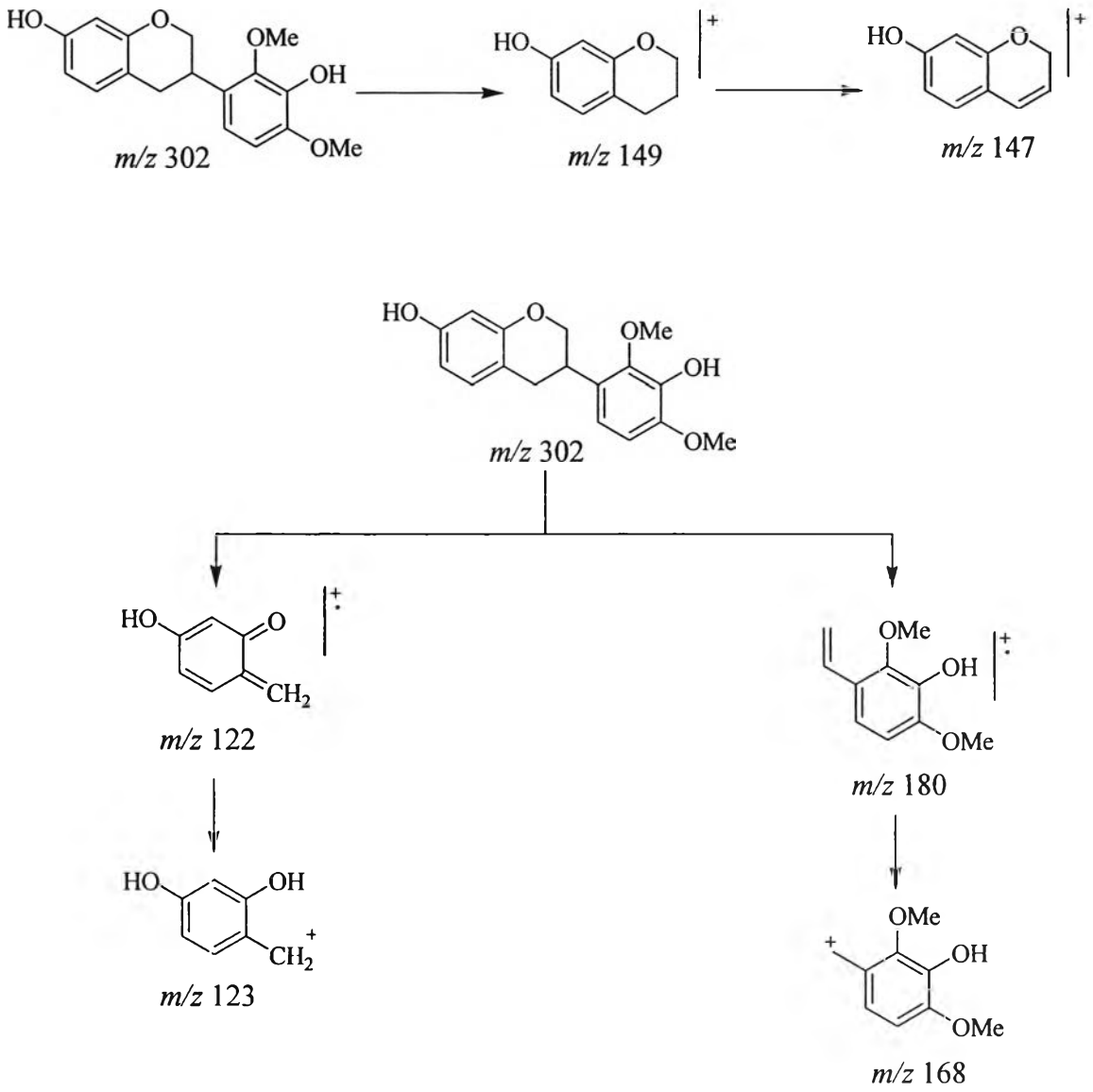

Scheme 2.5 Possible mass fragmentation pattern of **D5**

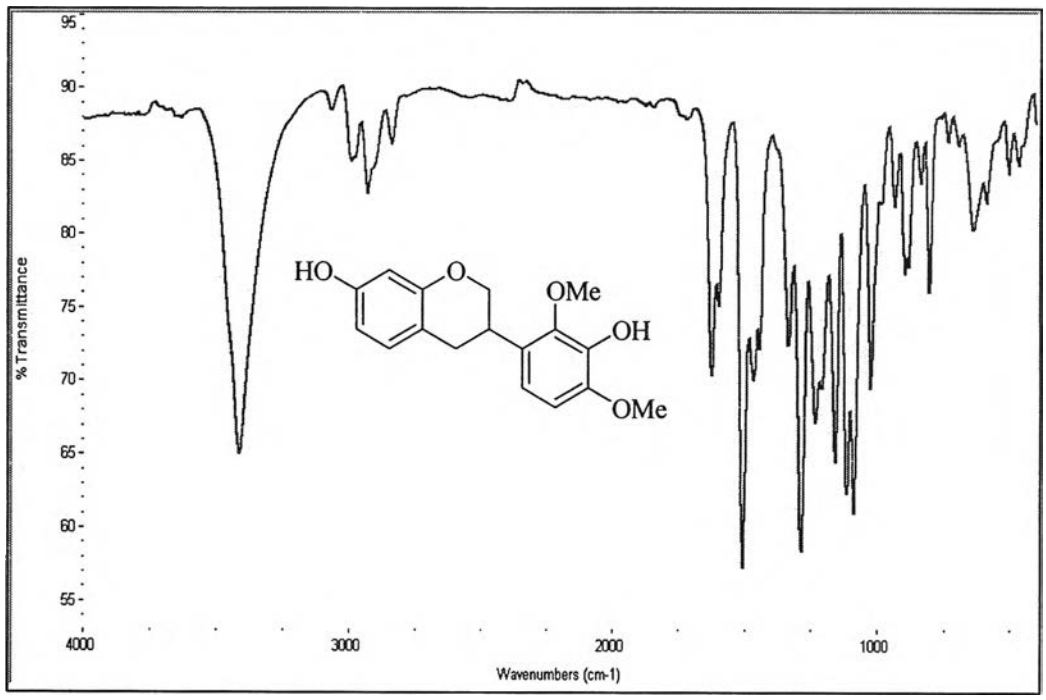

Figure 2.39 The IR spectrum of **D5**

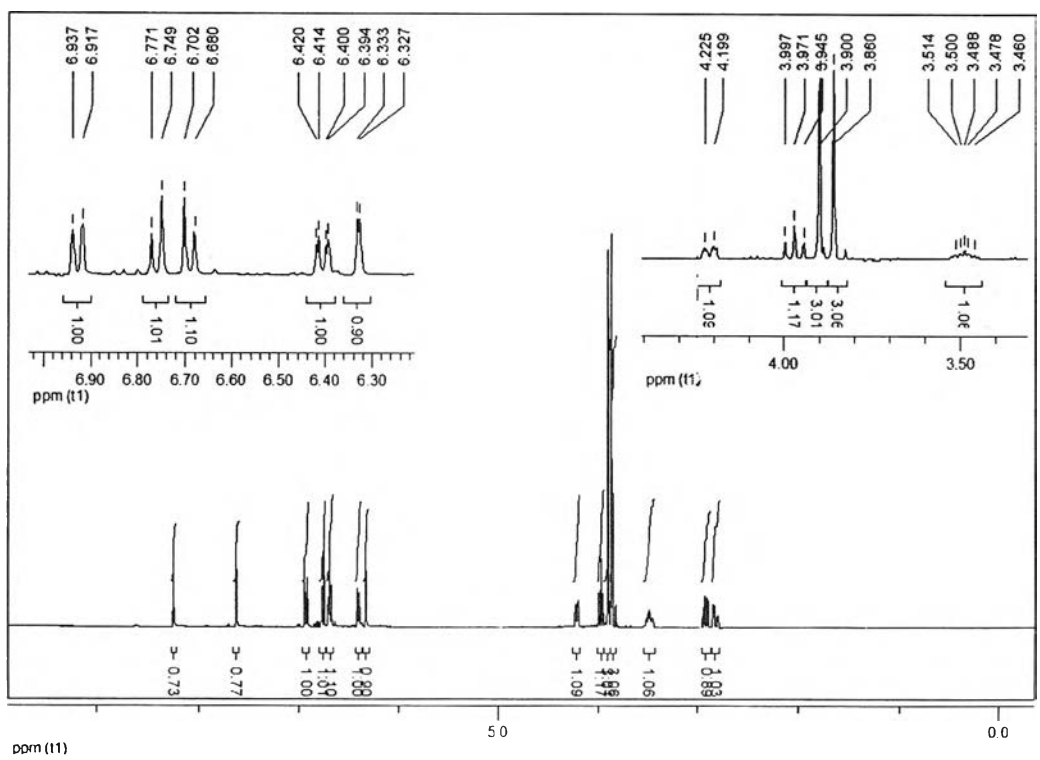

Figure 2.40 The ^{1}H-NMR spectrum of **D5**

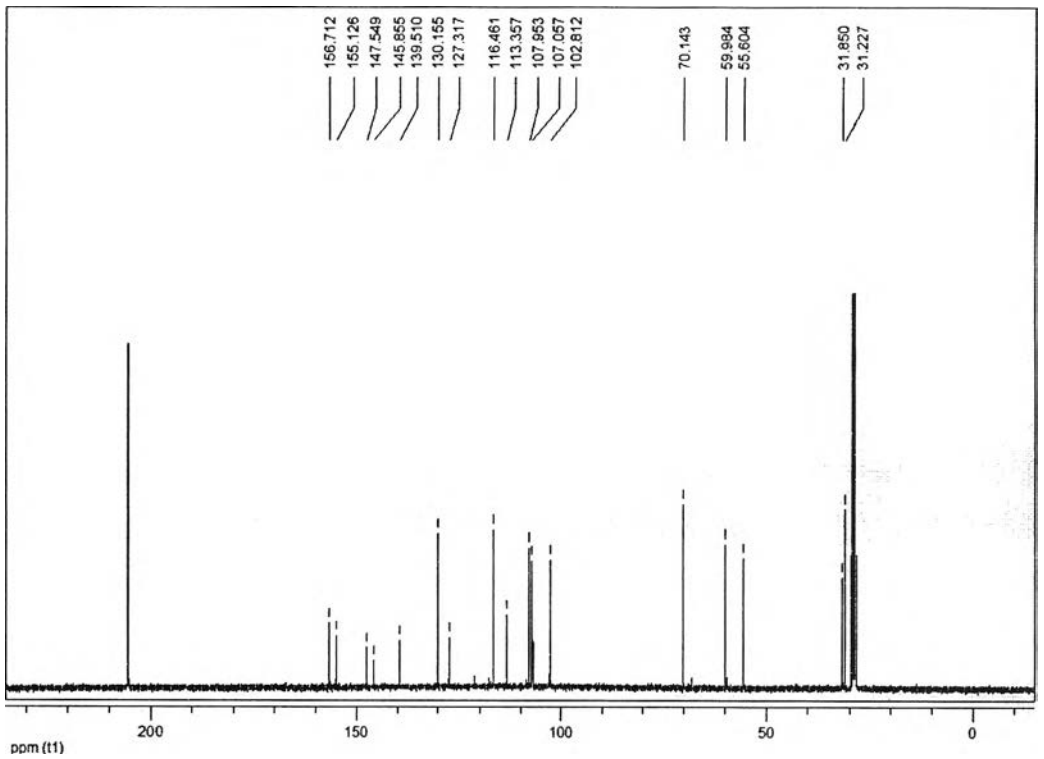

Figure 2.41 The ^{13}C-NMR spectrum of **D5**

Structural elucidation of D6

D6 was yielded as pale brown solid with m.p. 260.8-261.5°C (lit [74], 261°C). Its R_f value was 0.31 (40% EtOAc in hexane).

The formula of **D6** was established as $C_{16}H_{12}O_4$ by electron impact mass spectroscopy (EI-MS) (Figure 2.42). This spectrum exhibited the molecular ion peak at m/z 268 together with significant ions at m/z 253, 132 and 117. The possible fragmentation pattern was proposed as shown in Scheme 2.6.

The IR spectrum (Figure 2.43) showed the significant absorption band of hydroxyl group at 3011-3611 cm^{-1}, carbonyl group at 1606 cm^{-1} and C-H stretching of aromatic ring at 1517 and 1455 cm^{-1}.

The ^{1}H-NMR (DMSO-d_6) spectrum (Figure 2.44) revealed a low field singlet at δ 8.36, characteristic of the H-2 vinylic proton of isoflavone. Furthermore, it showed seven aromatic protons along with one methoxy group signal at δ 3.80. Two *ortho*-coupled protons to each other were assigned to H-5 (δ 7.99, d, J = 8.8 Hz) and H-6 (δ 6.96, dd, J = 2.2 and 8.8 Hz) and *meta*-coupled of H-8 (δ 6.89, d, J = 2.2 Hz) in ring A. The *para*-substitution of four aromatic protons at δ 7.52 (2H, d, J = 8.8 Hz, H-2' and H-6') and δ 7.01 (2H, d, J = 8.8 Hz, H-3' and H-5') in ring B.

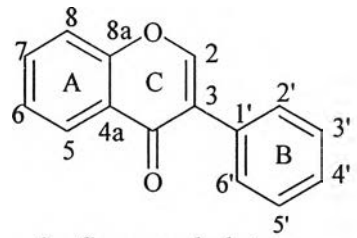

isoflavone skeleton

The ^{13}C-NMR (DMSO-d_6) spectrum (Figure 2.45) indicated sixteen carbon signals of fifteen carbon skeleton and one substituted group (flavonoid characteristic). This compound contained the characteristics of the C-2 vinylic carbon of isoflavone at δ 153.7, six quaternary carbons at δ 163.0 (C-7), 159.4 (C-4'), 157.9 (C-8a), 124.7 (C-1'), 123.6 (C-3) and 117.1 (C-4a), seven methane carbons at 130.6 (C-2' and C-6'), 127.8 (C-5), 115.7 (C-6), 114.1 (C-3' and C-5') and 102.6 (C-8), a methoxy carbon at δ 55.6 and a carbonyl carbon at δ 175.1 (C-4).

The position of the methoxy group at C-4' was affirmed by the NOE difference technique. To clarify this, the irradiation of the proton signal at δ 3.80 resulted in the enhancement of the proton signal at δ 7.01 (H-3' and H-5') (Figure 2.46). The NOE DIFF correlation of **D6** is shown below:

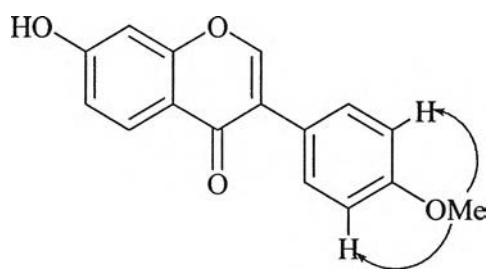

Based on all spectral data, the structure of **D6** was identified as 7-hydroxy-4'-methoxyisoflavone or formononetin. The structure is shown below.

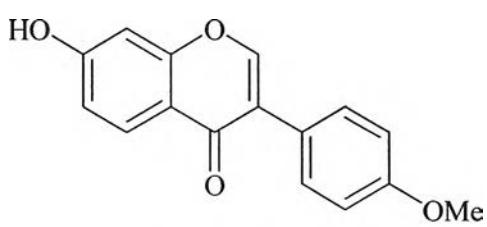

formononetin

The ^{1}H-, ^{13}C-NMR chemical shift assignments of **D6** compared with formononetin [75] are demonstrated in Table 2.10.

Table 2.10 The ^{1}H-, ^{13}C-NMR chemical shift assignment of **D6** compared with formononetin [75]

Position	Chemical shift (ppm)			
	D6		formononetin	
	^{13}C	^{1}H	^{13}C	^{1}H
2	153.7	8.36 (s)	152.9	8.30 (s)
3	123.6	-	124.3	-
4	175.1	-	174.5	-
4a	117.1	-	116.0	-
5	127.8	7.99 (d, J = 8.8 Hz)	127.9	7.95 (d, J = 9.0 Hz)
6	115.7	6.96 (dd, J = 2.2, 8.8 Hz)	115.6	6.92 (dd, J = 2.1, 8.7 Hz)
7	163.0	-	157.6	-
8	102.6	6.89 (d, J = 2.2 Hz)	102.0	6.84 (d, J = 1.8 Hz)
8a	157.9	-	158.9	-
1'	124.7	-	123.0	-
2', 6'	130.6	7.52 (d, J = 8.8 Hz)	130.0	7.49 (d, J = 8.4 Hz)
3', 5'	114.1	7.01 (d, J = 8.8 Hz)	113.5	6.97 (d, J = 8.7 Hz)
4'	159.4	-	163.7	-
OMe	55.6	3.80 (s)	55.1	3.76 (*s*)
OH	-	10.86 (s)	-	-

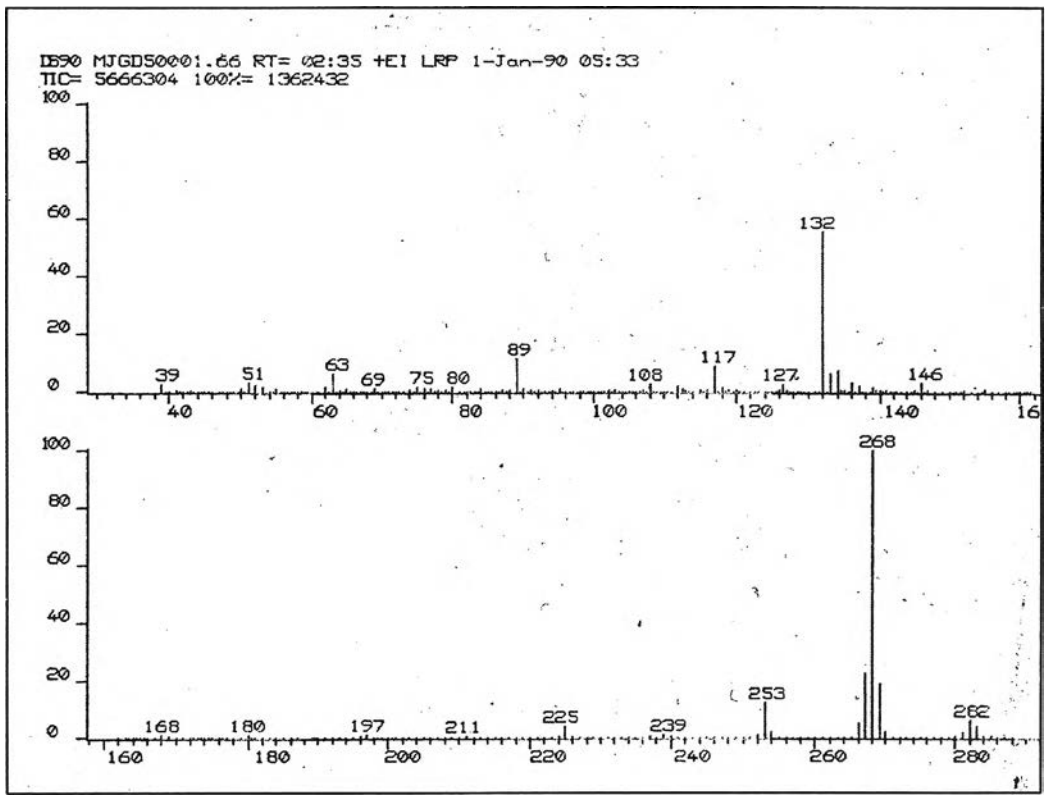

Figure 2.42 The mass spectrum of **D6**

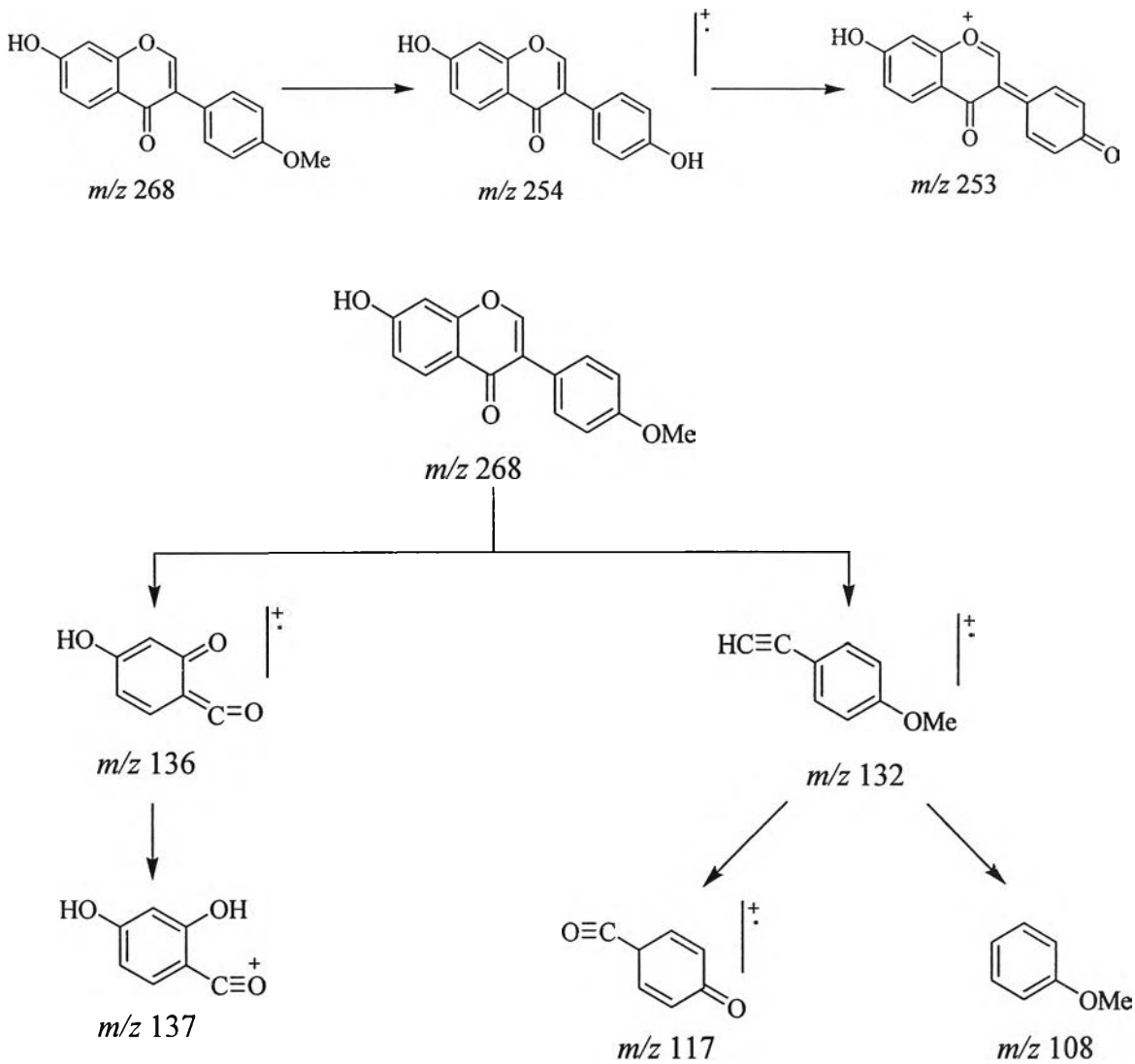

Scheme 2.6 Possible mass fragmentation pattern of **D6**

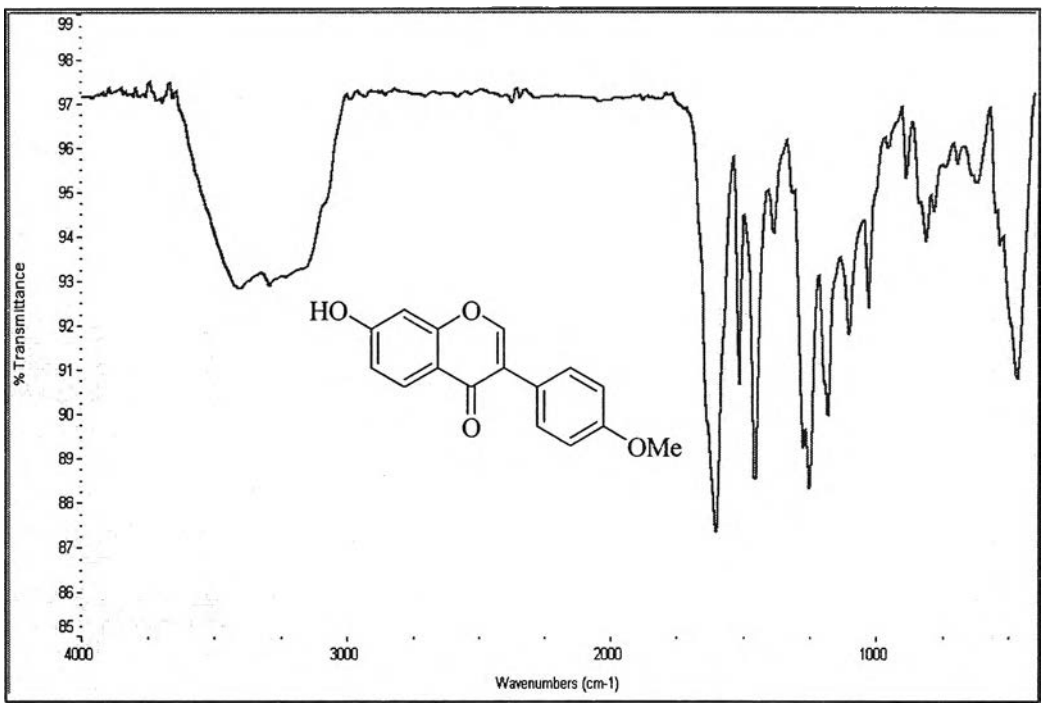

Figure 2.43 The IR spectrum of **D6**

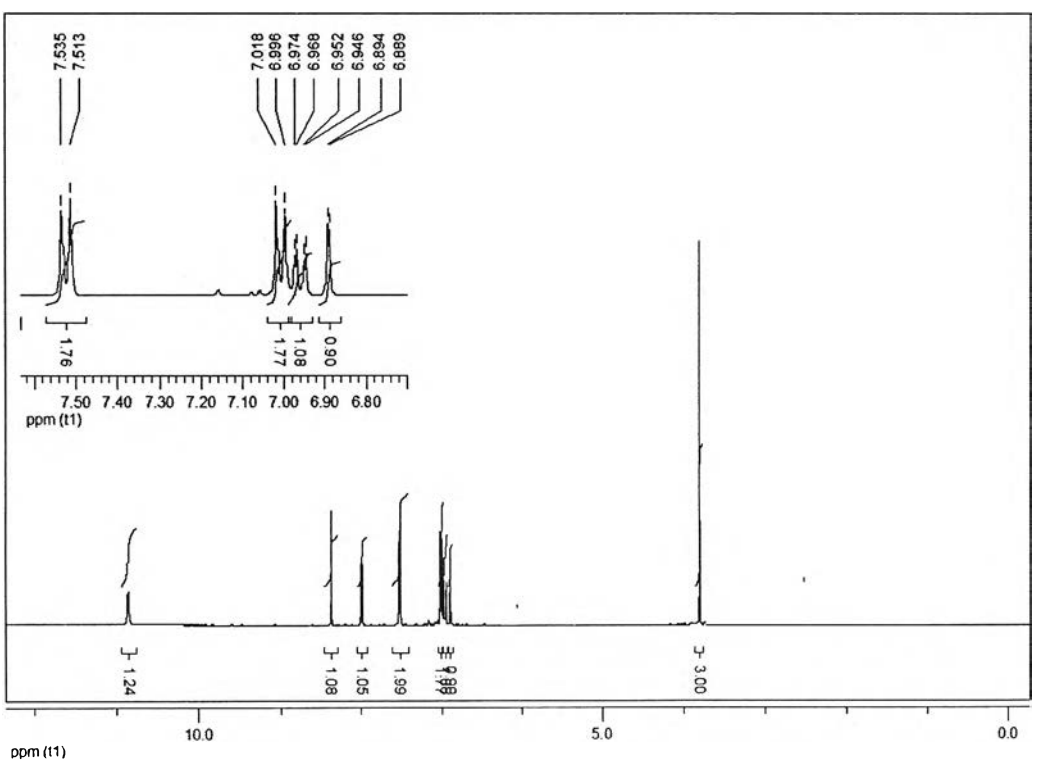

Figure 2.44 The ^{1}H-NMR spectrum of **D6**

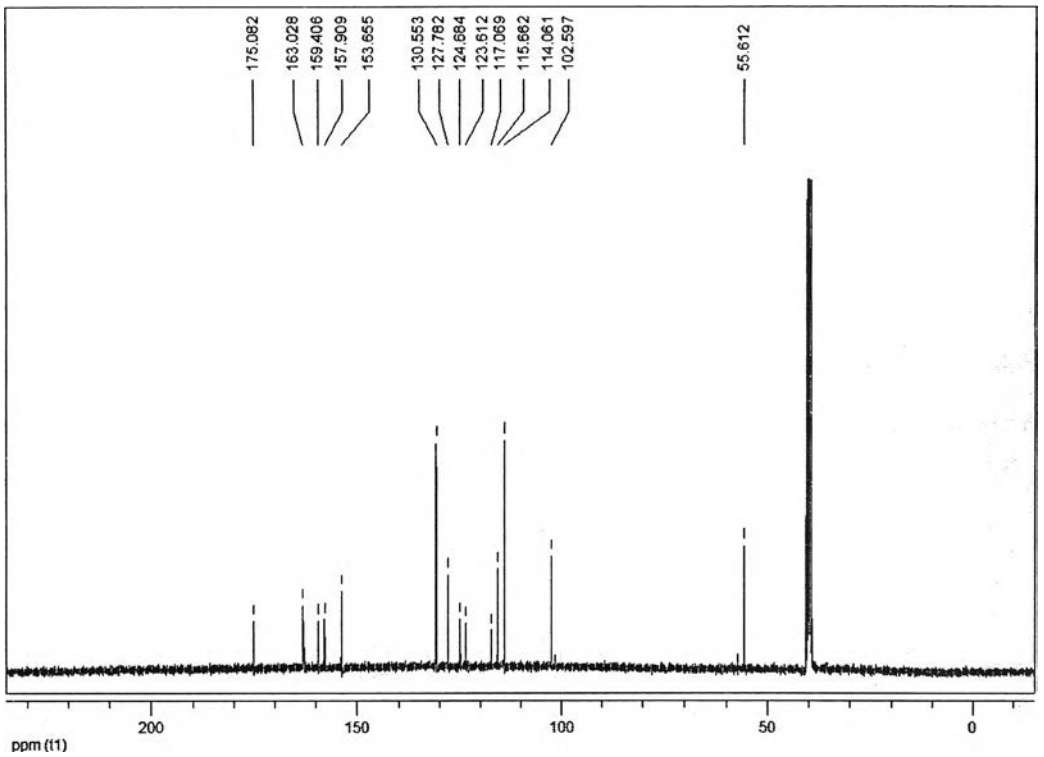

Figure 2.45 The ^{13}C-NMR spectrum of **D6**

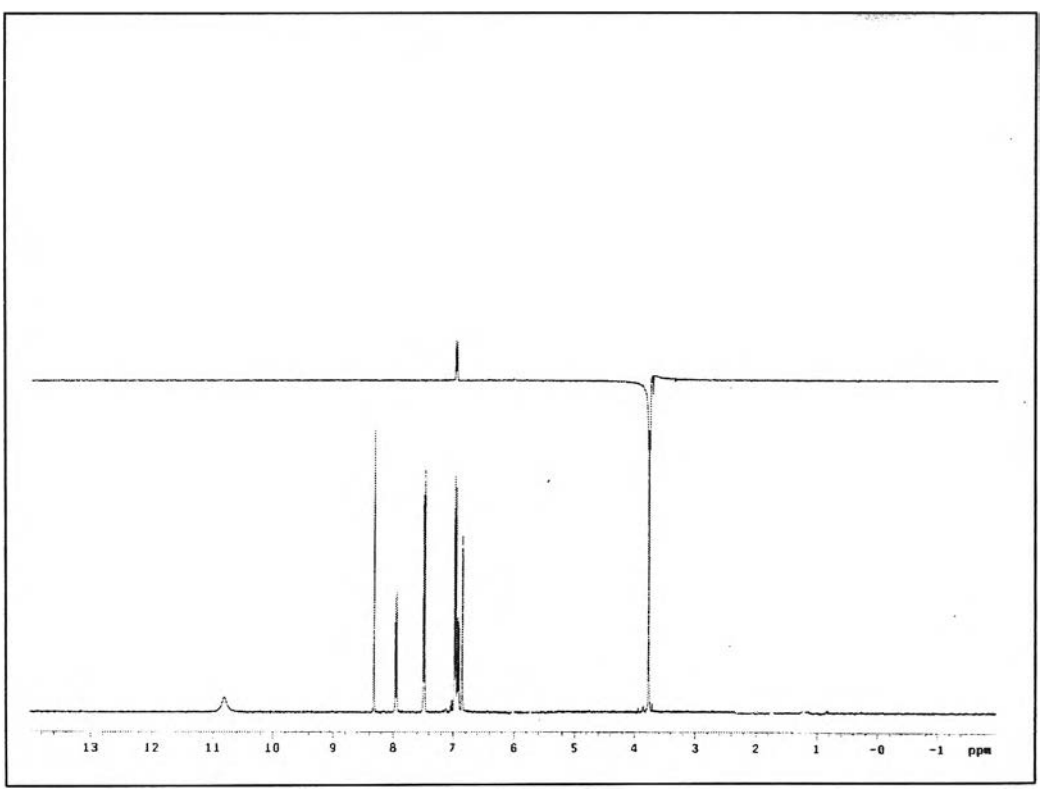

Figure 2.46 NOE DIFF of **D6** (irradiated at δ 3.80 ppm)

Separation of Fraction V

Fraction V (5.54 g) was subjected to silica column chromatography eluting with 100% CH_2Cl_2 to 5% EtOAc in CH_2Cl_2 to yield **D6** (329.20 mg).

Separation of Fraction VI

Fraction VI (14.12 g) was reseparated by silica gel column chromatography using gradient elution of 40% to 70% EtOAc in hexane to receive **D6**, white needle crystal designated as **D7** and fraction VI-III. Fraction VI-III was further purified by Sephadex LH20 column chromatography eluting with 50% MeOH in CH_2Cl_2 to oblige pale brown powder solid established as **D8**. The summary of the separation of fraction VI is disclosed as follows:

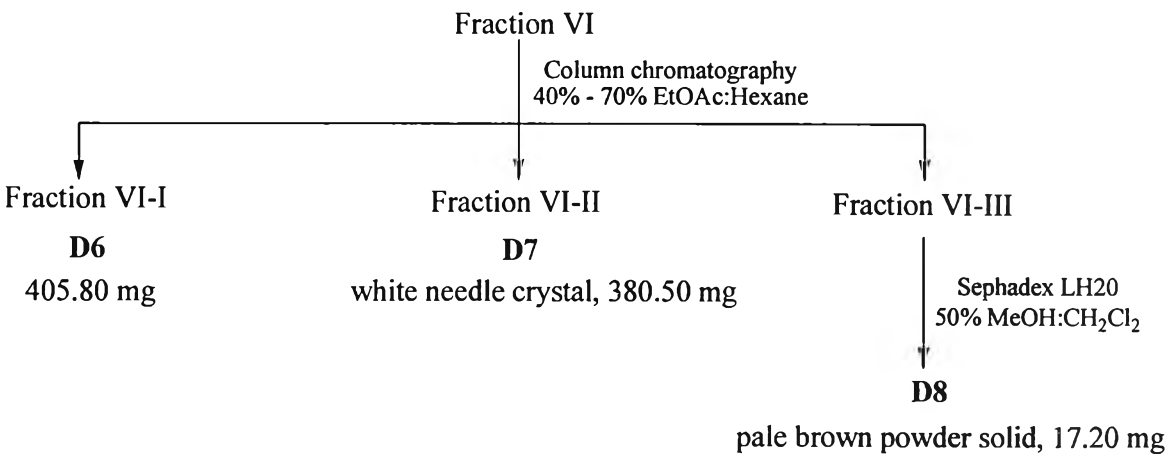

Structural elucidation of D7

D7 was isolated as white needle crystal (380.50 mg) with m.p. 204.3-206.2°C (lit [76], 204-206°C) and R_f value 0.49 (50% EtOAc in hexane).

D7 showed a molecular ion peak at m/z 316 (Figure 2.47) in EI-MS analysis, corresponding with the elemental formular $C_{17}H_{16}O_6$. In addition, it also revealed the other fragment ions at m/z 180, 165, 137 and 133. The possible fragmentation pattern was proposed as shown in Scheme 2.7.

The IR spectrum (Figure 2.48) signified the presence of hydroxyl group in region of 3179-3405 cm^{-1}, carbonyl group at 1669 cm^{-1} and C-H stretching of benzene ring at 1591 and 1494 cm^{-1}.

The ^{1}H-NMR (acetone-d_6) spectrum of **D7** (Figure 2.49) disclosed a set mutually coupled three protons at δ 4.48 (dd, J= 5.4 and 11.0 Hz, H-2*eq*), 4.62 (dd, J= 11.0 and 11.0 Hz, H-2*ax*) and 4.15 (dd, J = 5.4 and 11.0 Hz), clarifying that **D7** had an isoflavanone skeleton. The presence of two hydroxyl groups (δ 7.67 and 9.52 in rings A and C) and two methoxy groups (δ 3.81 and 3.85 in ring B) was supported by the ^{1}H-NMR spectrum and significant fragmentation ions (m/z 137 and 180). Two *ortho*-coupled protons to each other were assigned to H-5 (δ 7.82, d, J = 8.6 Hz) and H-6 (δ 6.61, m = overlapped) in ring A. Moreover, it also indicated a set of *ortho*-couple proton (δ 6.65 (H-6') and 6.71 (H-5')) in ring B.

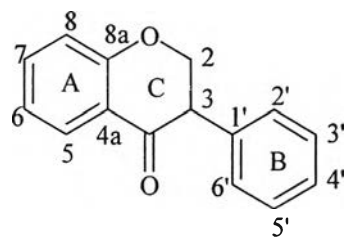

isoflavanone skeleton

The ^{13}C-NMR (acetone-d_6) spectrum of **D7** (Figure 2.50) exposed seventeen carbon signals of fifteen carbon skeleton and two substituent groups (characteristic of flavonoid). A set of three carbons at δ 190.5 (C-4), 71.2 (C-2) and 48.1 (C-3) was presented in this spectrum; simplifying that **D7** had an isoflavanone skeleton. Two quaternary carbon signals occupied by an oxygen function (δ 164.1 and 163.8) showed that ring A had a resorcinol oxidation pattern with a 7-hydroxyl substitution. Furthermore, three quaternary carbon signals attached to an oxygen function (δ 139.5, 146.0 and 148.3) in the ^{13}C-NMR spectrum, indicated that ring B oxygenation pattern corresponded to pyrogallol with a 2',3',4'-trisubstitution pattern. In addition, the chemical shifts of two methoxy groups were observed at δ 55.6 and 59.2.

The sign of optical rotation of **D7** was 0, indicating that **D7** was optically inactive compound.

All the above data suggested that the structure of **D7** could be concluded to (±)-3',7-dihydroxy-2',4'-dimethoxyisoflavanone or (±)-violanone. The ^{1}H-, ^{13}C-NMR chemical shift assignments of **D7** compared with 5,7,3'-trihydroxy-2',4'-dimethoxy-isoflavanone (secundiflorol H) [77] are demonstrated in Table 2.11. The structure of **D7** is shown below.

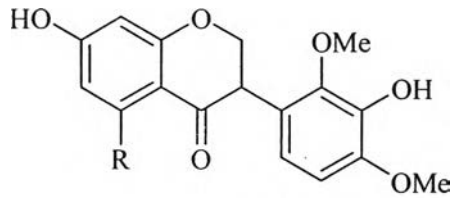

D7 R = H

secundiflorol H R = OH

Table 2.11 The ^{1}H-, ^{13}C-NMR chemical shift assignment of **D7** compared with secundiflorol H [77]

Position	Chemical shift (ppm)			
	D7		secundiflorol H	
	^{13}C	^{1}H	^{13}C	^{1}H
2	71.2	4.48 (dd, *Jeq* = 5.4, 11.0 Hz)	71.1	4.43 (dd, *Jeq* = 6, 11 Hz)
		4.62 (dd, *Jax* = 11.0, 11.0 Hz)		4.53 (dd, *Jax* = 11, 11 Hz)
3	48.1	4.15 (dd, *J* = 5.4, 11.0 Hz)	48.1	4.25 (dd, *J* = 6, 11 Hz)
4	190.5	-	198.2	-
4a	114.9	-	103.4	-
5	129.2	7.81 (d, *J* = 8.6 Hz)	165.7	-
6	110.4	6.61 (m= overlapped)	96.9	5.95 (m= overlapped)
7	164.1	-	169.1	-
8	102.6	6.45 (m= overlapped)	95.6	5.95 (m = overlapped)
8a	163.8	-	164.5	-
1'	122.2	-	122.1	-
2'	146.0	-	146.8	-
3'	139.5	-	140.3	-
4'	148.3	-	149.4	-
5'	106.5	6.71 (d, *J* = 8.9 Hz)	107.3	6.60 (d, *J* = 8 Hz)
6'	119.5	6.65 (d, *J* = 8.9 Hz)	120.2	6.70 (d, *J* = 8 Hz)
OH	-	7.67 (s)	-	8.00 (s)
OH	-	9.62 (s)	-	9.91 (s)
OH	-	-	-	12.4 (s)
OMe	55.6 s	3.85 (s)	56.5	3.83 (s)
OMe	59.2	3.81 (s)	60.1	3.84 (s)

ax: axial; *eq*: equatorial

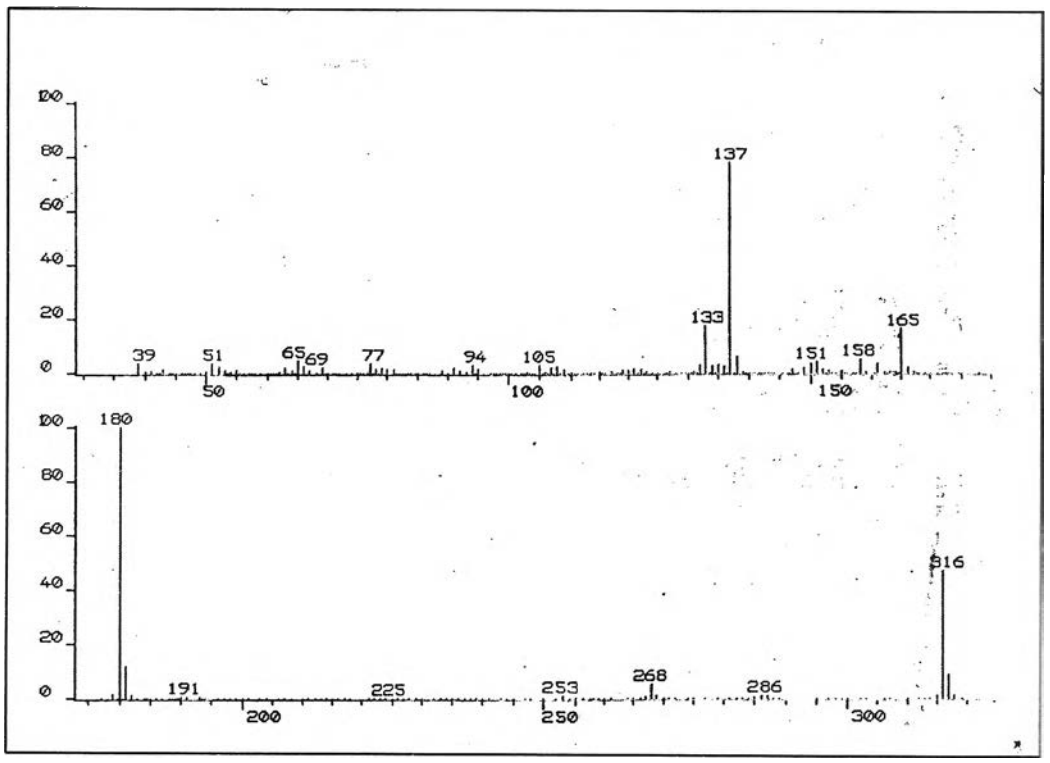

Figure 2.47 The mass spectrum of **D7**

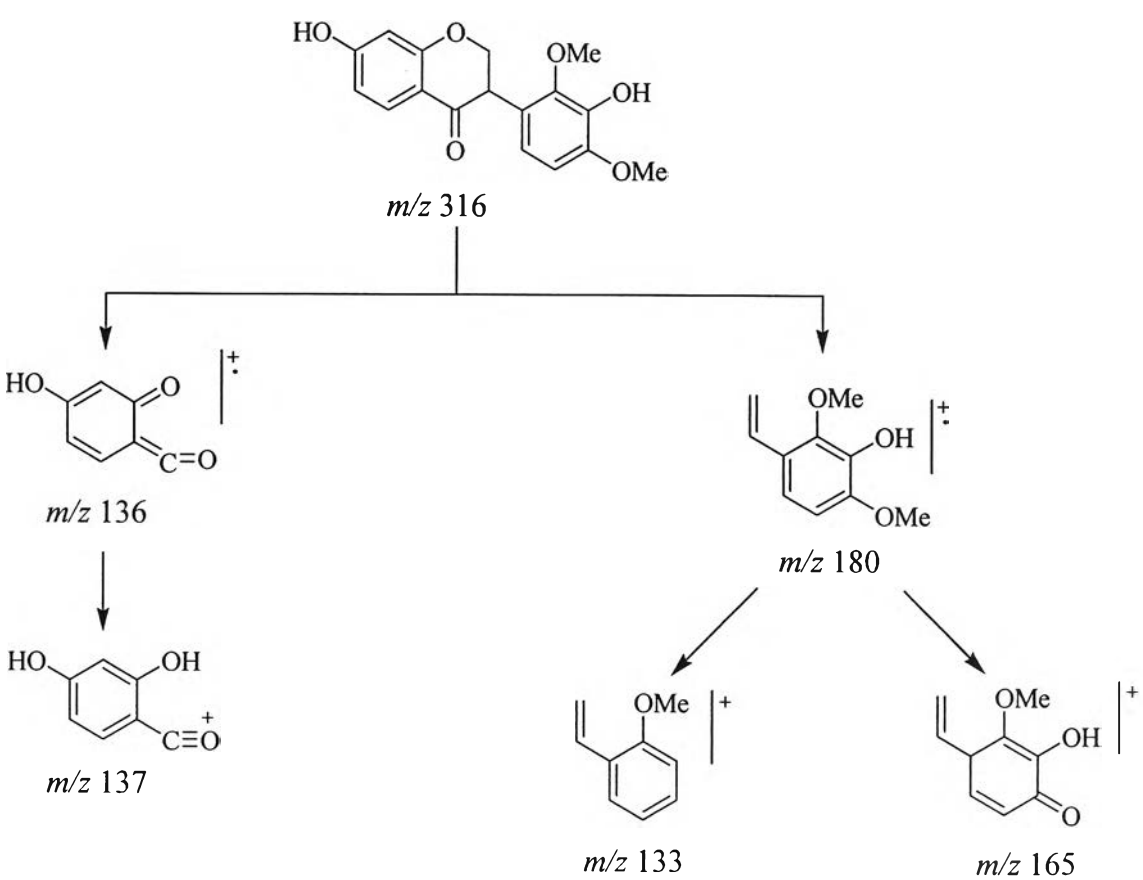

Scheme 2.7 Possible mass fragmentation pattern of **D7**

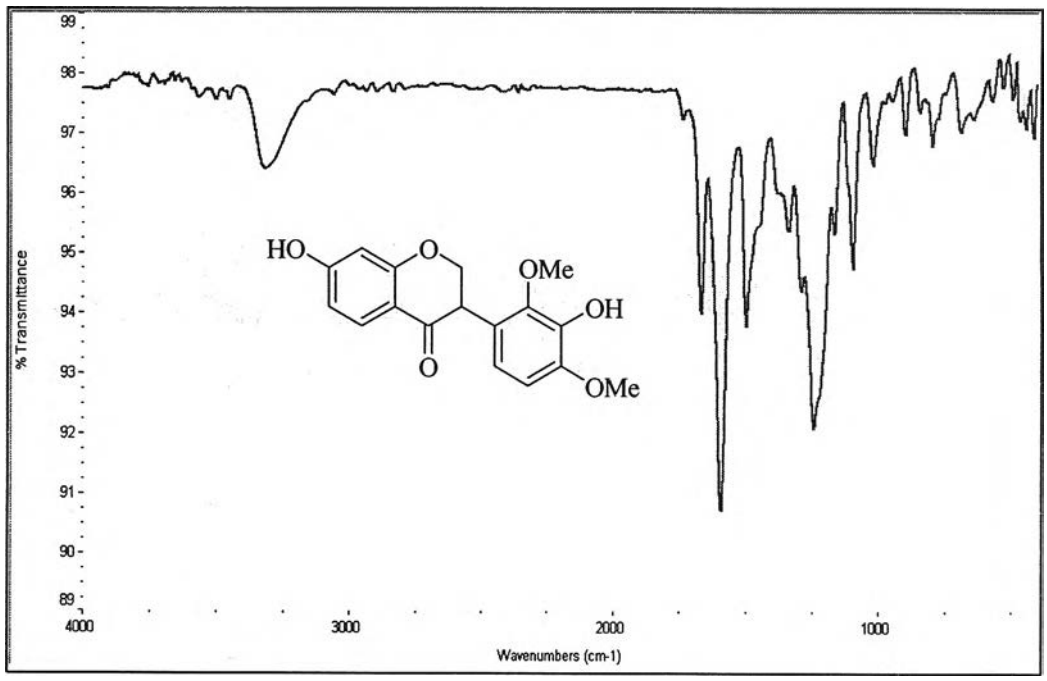

Figure 2.48 The IR spectrum of **D7**

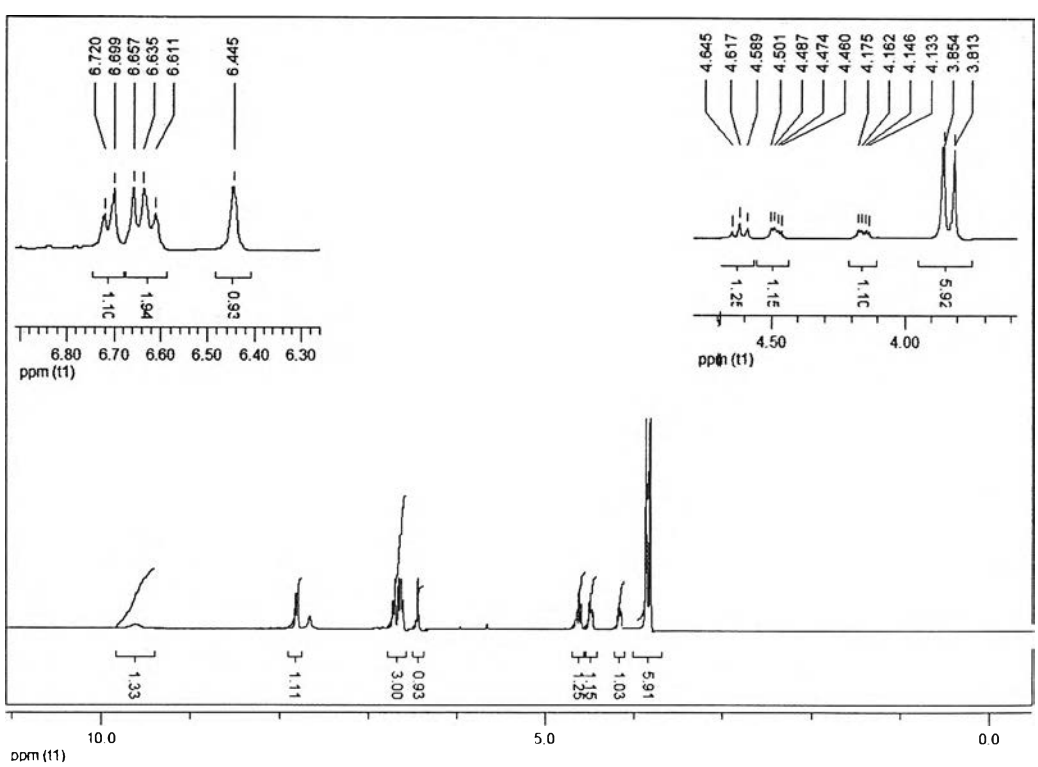

Figure 2.49 The ^{1}H-NMR spectrum of **D7**

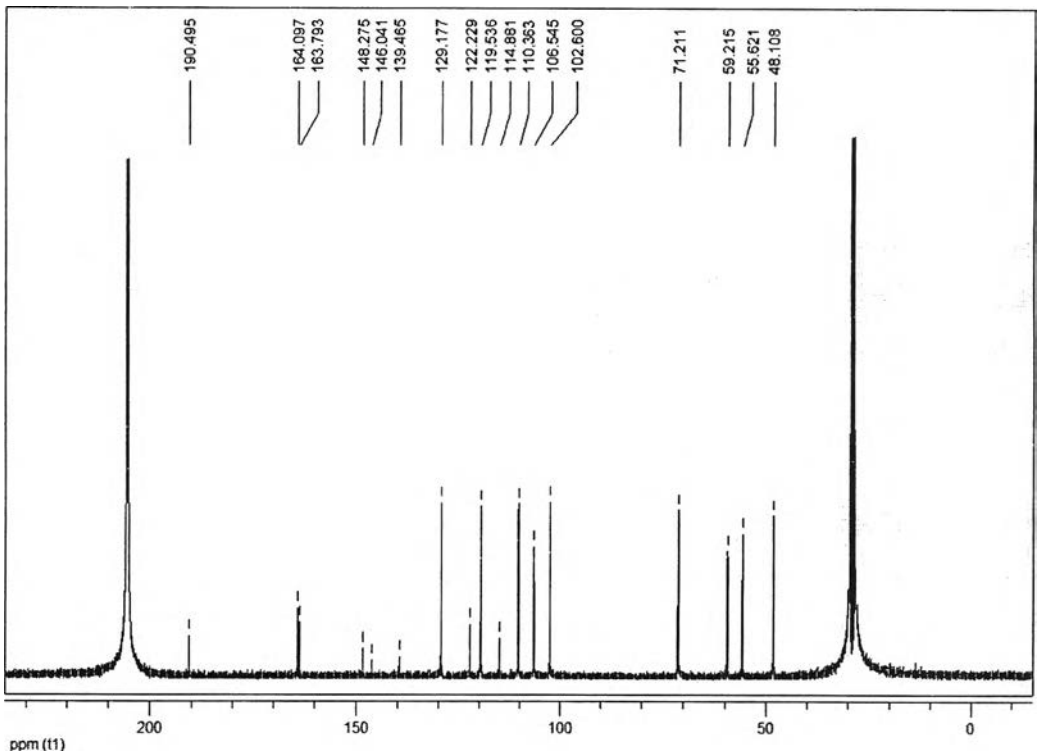

Figure 2.50 The ^{13}C-NMR spectrum of **D7**

Structural elucidation of D8

D8 was received as pale brown powder solid with m.p. 241-243°C (lit [78], 243-245°C) and R_f value 0.53 (100% EtOAc).

The IR spectrum (Figure 2.51) of this compound disclosed the significant absorption band of hydroxyl group at 3093-3323 cm^{-1}, carbonyl group at 1626 cm^{-1} and aromatic ring at 1568, 1513 and 1455 cm^{-1}.

The ^{1}H-NMR (acetone-d_6) spectrum of **D8** (Figure 2.52) exposed the characteristic signal of the H-2 vinylic proton of isoflavone as a low field singlet at δ 8.19. Six aromatic protons assigned at δ 8.10 (1H, d, J = 8.8 Hz, H-5), 7.19 (1H, d, J = 1.7 Hz, H-2'), 7.10 (1H, dd, J = 1.7, 8.0 Hz, H-6'), 7.04 (1H, dd, J = 1.8 , 8.8 Hz, H-6), 7.01 (1H, d, J = 8.1 Hz, H-5') and 6.93 (1H, d, J = 1.8 Hz, H-8) could be detected. Two *meta*-coupled protons showed a coupling constant of 1.8 and 1.7 Hz (H-8 and H-2', respectively). The coupling constant of 8.8 and 8.0 Hz showed *ortho*-coupled protons (H-5 and H-5', respectively). Two protons as doublet of doublet (J = 1.8, 8.8 Hz and J = 1.7, 8.0 Hz) should be derived from *meta*- and *ortho*-coupled to each other; thus could be assigned for H-6 and H-6', respectively. In addition, a

methoxy group present in this structure could be affirmed from the proton signal at δ 3.91 ppm.

The ^{13}C-NMR (acetone-d_6) spectrum of **D8** (Figure 2.53) signified sixteen carbons; fifteen carbons as for the characteristic skeleton of flavonoid and one substituent as a methoxy group. This compound also comprised the characteristic of the C-2 vinylic carbon of isoflavone at δ 152.6, seven quaternary carbons at δ 162.4 (C-7), 157.9 (C-8a), 147.4 (C-4'), 146.3 (C-3'), 125.4 (C-1'), 124.2 (C-3) and 117.7 (C-4a), six methine carbons at δ 127.6 (C-5), 120.0 (C-6'), 116.0 (C-2'), 114.8 (C-6), 111.2 (C-5') and 102.3 (C-8), a carbonyl carbon at δ 174.7 and a methoxy carbon at δ 55.4.

Furthermore, the location of the methoxy group on ring B at 4' position was established from the NOE experiment. Irradiation of the proton signal at δ 3.91 only caused the enhancement of the proton signal at δ 7.01 (H-2') (Figure 2.54). The NOE correlation of **D8** is shown below:

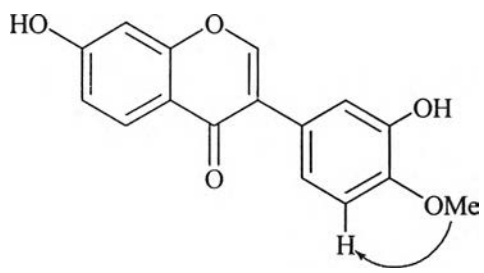

Gathering from the above results, the structure of **D8** is no doubt 3',7-dihydroxy-4'-methoxyisoflaone or calycosin. The structure of **D8** is shown below.

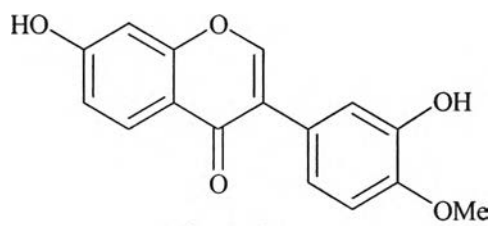

calycosin

The ^{1}H-, ^{13}C-NMR chemical shift assignments of **D8** compared with calycosin [78, 79] are demonstrated in Table 2.12.

Table 2.12 The ^{1}H-, ^{13}C-NMR chemical shift assignment of **D8** compared with calycosin [78, 79]

Position	Chemical shift (ppm)			
	D8		calycosin	
	^{13}C	^{1}H	^{13}C [78]	^{1}H [79]
2	152.6	8.19 (s)	153.0	8.09 (s)
3	124.2	-	123.3	-
4	174.7	-	174.5	-
4a	117.7	-	116.2	-
5	127.6	8.10 (d, J = 8.8 Hz)	127.3	8.00 (d, J = 8.4 Hz)
6	114.8	7.04 (dd, J = 1.8, 8.8 Hz)	115.1	6.87 (dd, J = 1.8, 8.7 Hz)
7	162.4	-	162.5	-
8	102.3	6.93 (d, J = 1.8 Hz)	102.2	6.76 (d, J = 1.8 Hz)
8a	157.9	-	157.3	-
1'	125.4	-	124.7	-
2'	111.2	7.19 (d, J = 1.7 Hz)	111.9	6.97 (br)
3'	146.2	-	146.0	-
4'	147.4	-	147.5	-
5'	116.0	7.01 (d, J = 8.0 Hz)	116.4	7.03 (s)
6'	120.0	7.10 (dd, J = 1.7, 8.0 Hz)	119.7	6.97 (br)
OMe	55.4	3.91 (s)	55.6	3.87 (s)

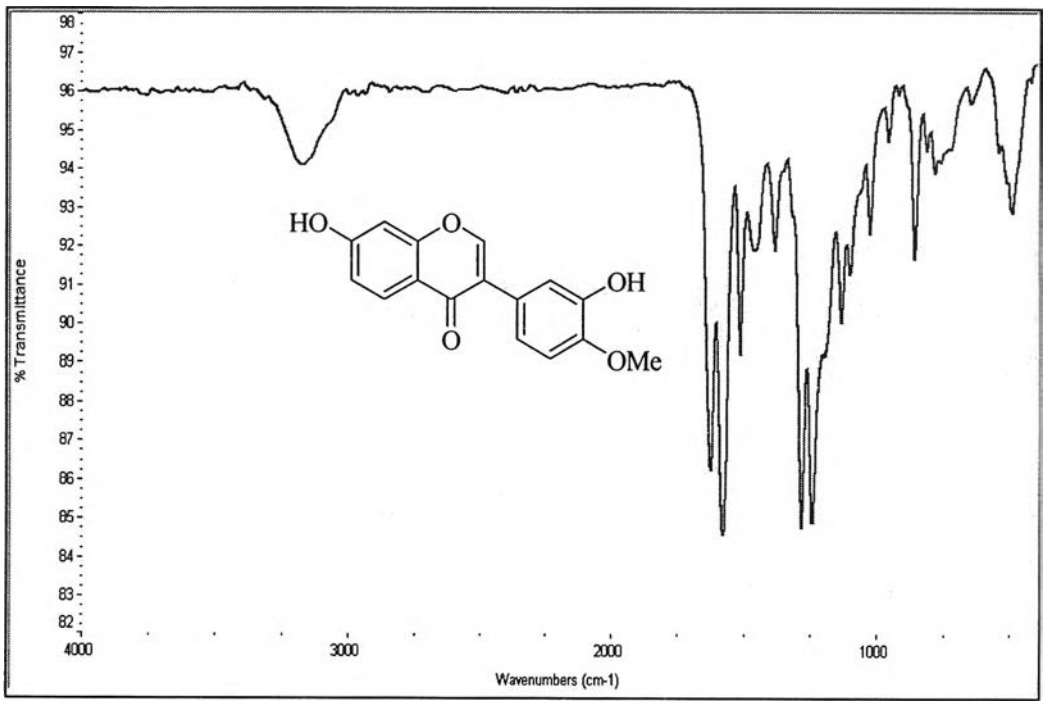

Figure 2.51 The IR spectrum of **D8**

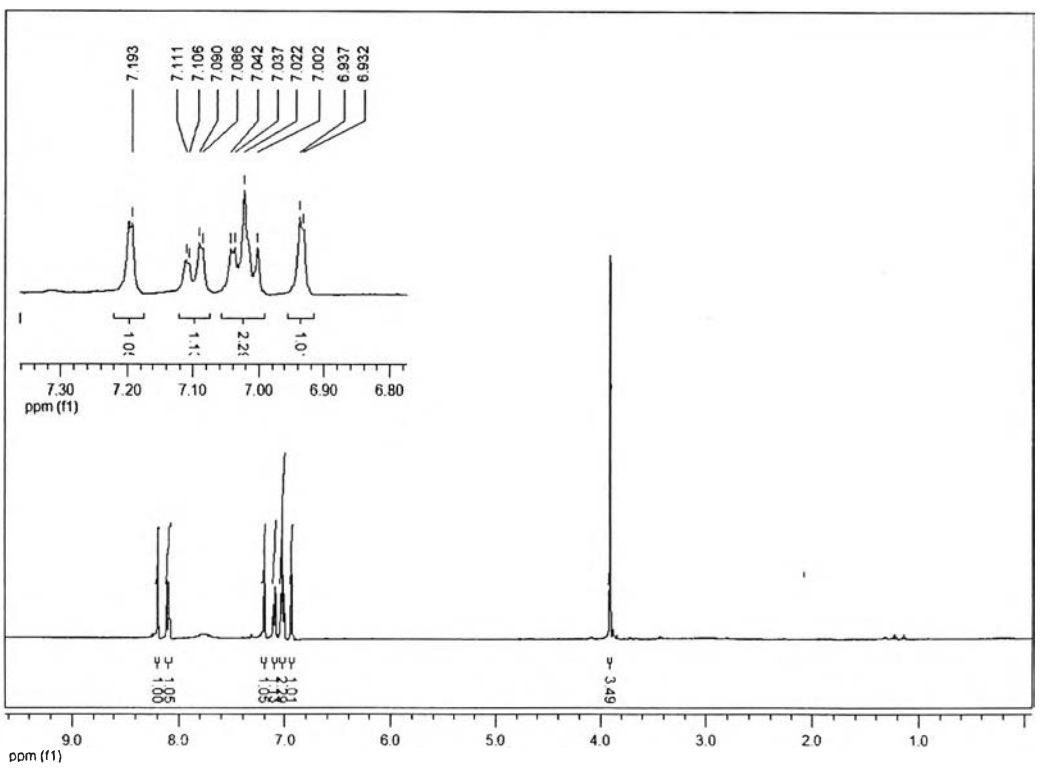

Figure 2.52 The ^{1}H-NMR spectrum of **D8**

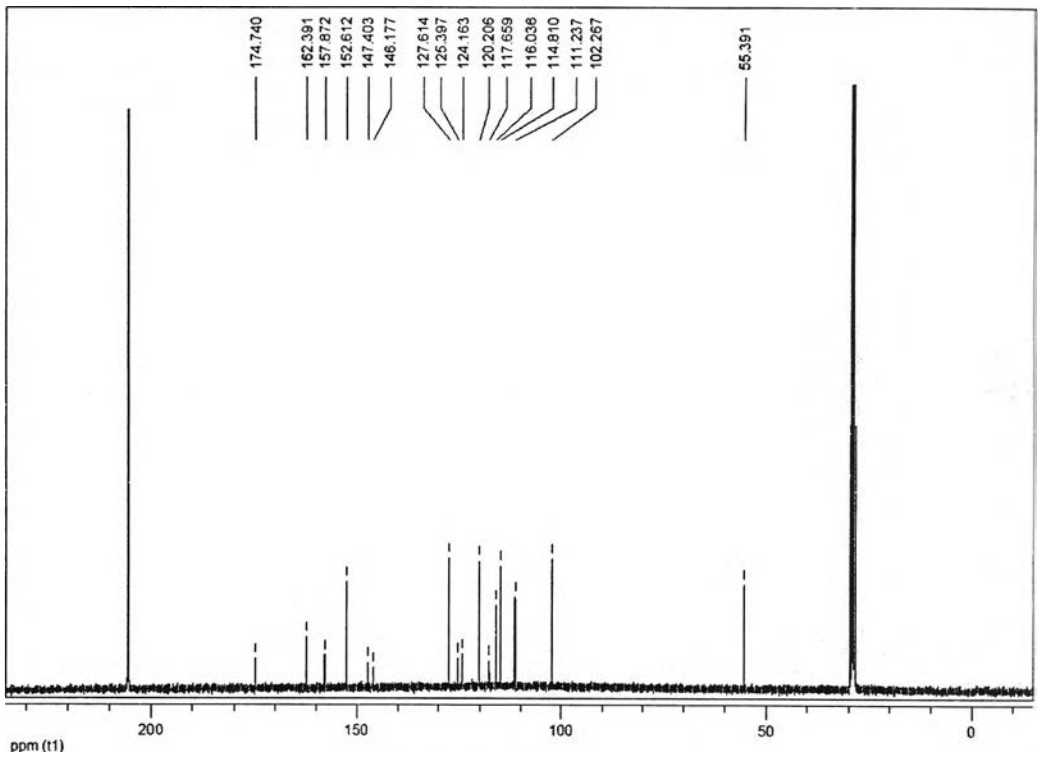

Figure 2.53 The ^{13}C-NMR spectrum of **D8**

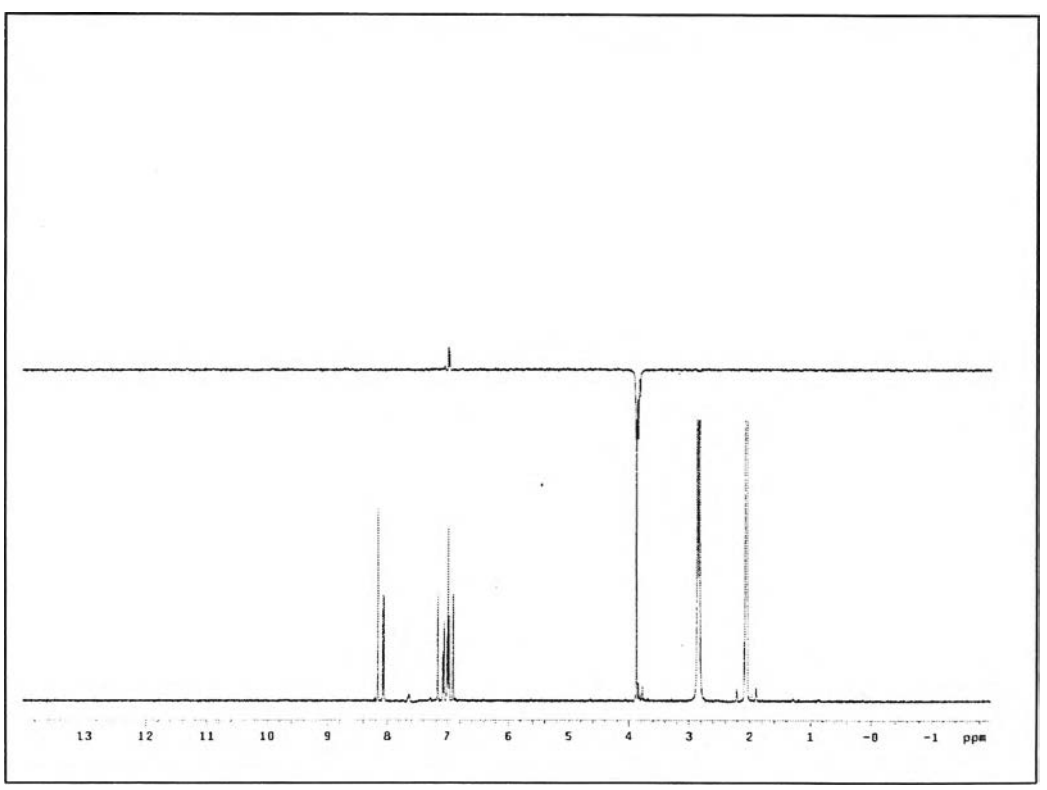

Figure 2.54 NOE DIFF of **D8** (irradiated at δ 3.91)

Separation of Fraction VII

Fraction VII (8.85 g) chromatographed on silica gel column, using gradient elution of 40% to 75% EtOAc in hexane to furnish **D6** and fraction VII-II (116.9 mg). The fraction VII-II was further purified by Sephadex LH20 eluting with 50% MeOH in CH_2Cl_2 as a solvent system to yield **D8**. The results of separation of fraction VII are shown below:

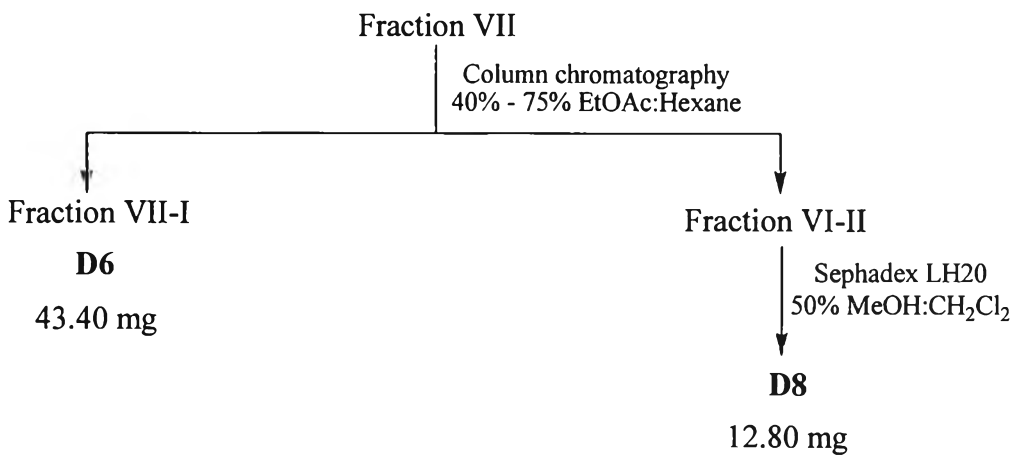

Separation of Fraction VIII

Fraction VIII (24.60 g) was reseparated by silica gel column chromatography eluting gradient solvent system with 40% EtOAc in hexane to 100% EtOAc to achieve **D8** (69.20 mg).

In summary, eight compounds could be isolated from fraction I-IX of the CH_2Cl_2 extract. The isolation diagram of all substances was summarized in Scheme 2.8.

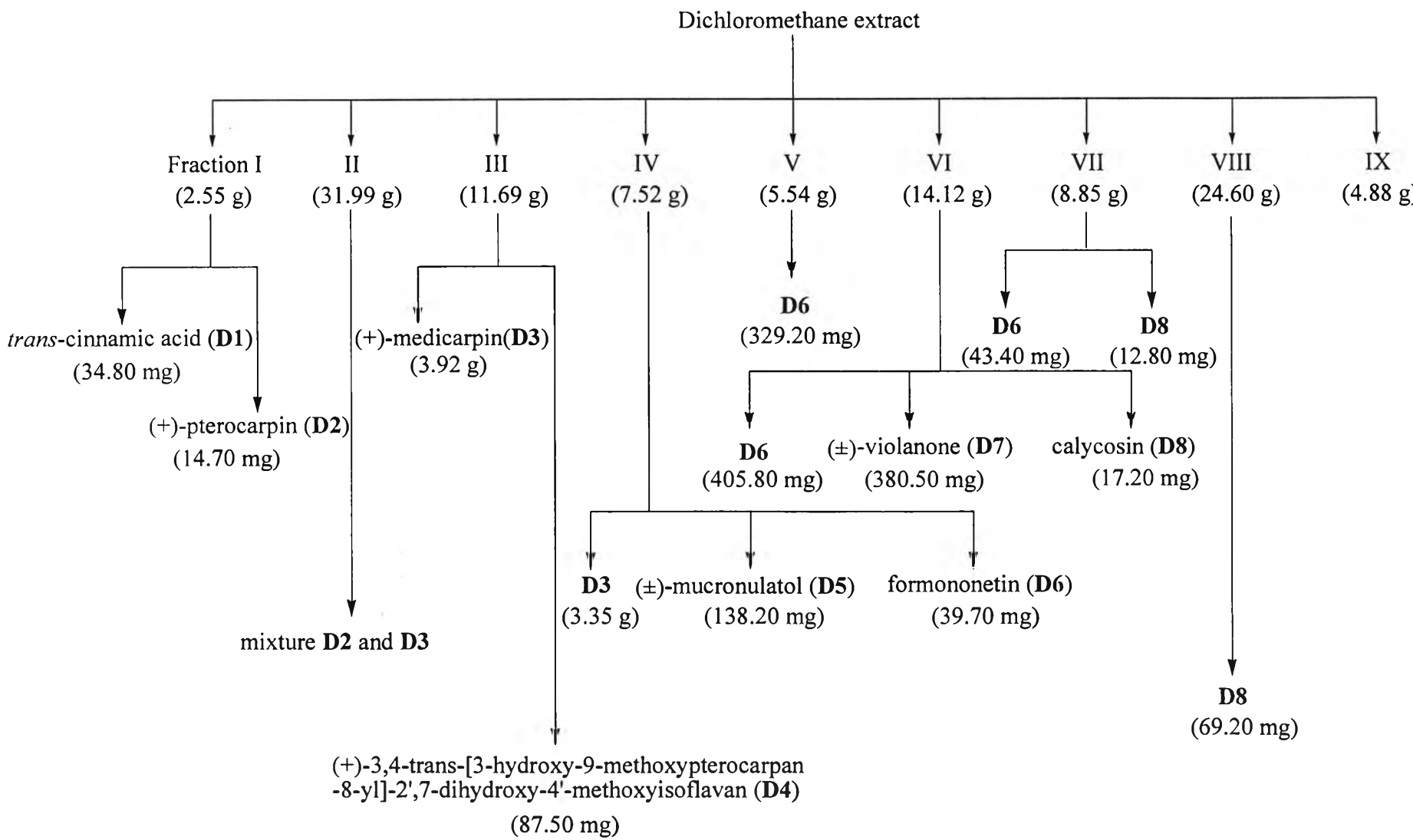

Scheme 2.8 Isolation diagram of the CH_2Cl_2 extract from the heartwoods of *D. oliveri*

2.3.3 The Separation of Hexane Extract

During the evaporation of solvent from hexane extract (4.0 g), it was noticed that some white powder solid deposited. These solids were filtered and recrystalized with hexane to furnish **HC1** as white powder. The remaining hexane extract was further concentrated to afford yellow material, which was further fractioned using silica gel (No. 7734) column chromatography eluting by gradient eluent with increasing polarity of hexane, CH_2Cl_2 in hexane and finally CH_2Cl_2 in EtOAc, respectively. The eluted solution was collected approximately 250 mL. Every fraction collected was concentrated to a small volume and then monitored by TLC. The fractions which contained similar components were combined. The separation of hexane extract afforded 3 fractions (I-III) as presented in Table 2.13.

Table 2.13 The separation of hexane extract

Fraction	Solvent system	Remarks	Weight (g)
I	100% Hexane- 40% CH_2Cl_2:Hexane	Yellow oil	0.38
II	50% CH_2Cl_2:Hexane- 100% CH_2Cl_2	Yellow syrup	0.80
III	2% EtOAc:CH_2Cl_2- 20% EtOAc:CH_2Cl_2	Dark brown syrup	0.67

During the evaporation of solvent, it was observed that some white crystal and needle crystal deposited from fraction I and II, respectively. These crystals were filtered and designated as **HC2** and **HC3**, respectively. The results of separation are shown in Scheme 2.9.

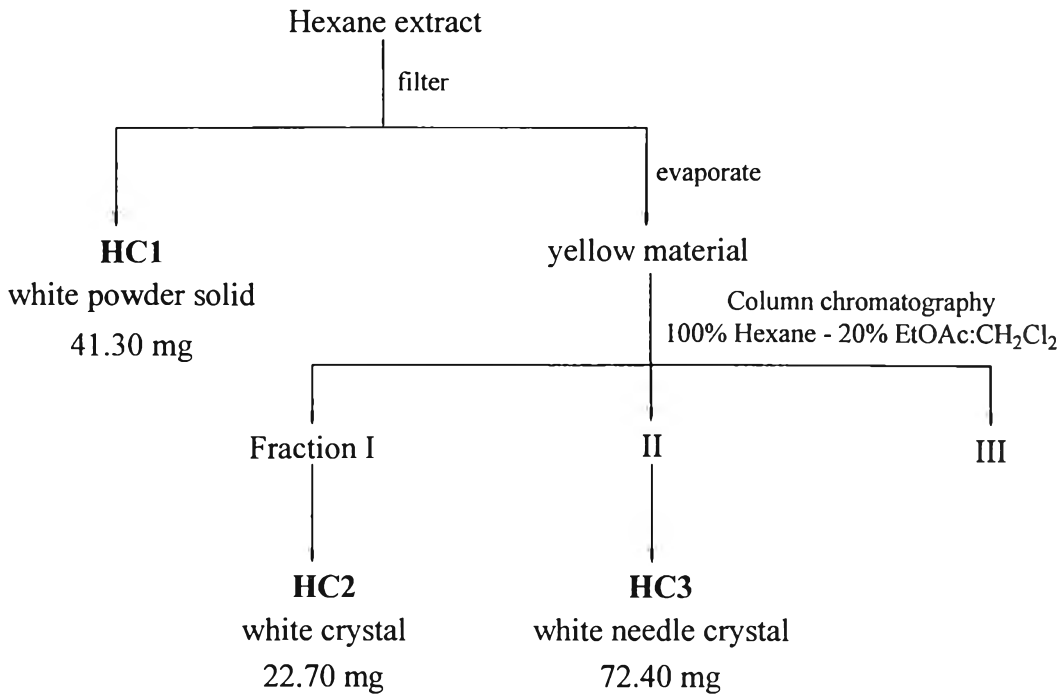

Scheme 2.9 The separation of hexane extract

Structural elucidation of HC1

HC1 was obtained as white powder solid (41.30 mg) with m.p. 79-80°C and R_f value 0.77 (20% EtOAc in hexane). This compound was soluble in chloroform, CH_2Cl_2 and EtOAc. According to the spectroscopic study, the IR spectrum (Figure 2.55) of this compound disclosed the significant absorption band of carbonyl group at 1708 cm^{-1} of ketone or aldehyde and C-H stretching vibration of CH_2 and CH_3 at 2848 and 2928 cm^{-1}. Concerning with the ^{1}H-NMR ($CDCl_3$) spectrum of **CH1** (Figure 2.56), it exhibited a high intensity signal at δ 1.27 suggesting several interlinking of methylene group in a molecule. The signal of the methylene group connecting to a carbonyl group was detected at δ 2.35. The signal of a methyl group was detected at δ 0.89. Moreover, the characteristic peak of aldehyde proton at δ 9-10 was not appeared in the ^{1}H-NMR spectrum. It was thus considered that this compound was ketone. This postulation was confirmed by the ^{13}C-NMR ($CDCl_3$) spectrum (Figure 2.57) which displayed a significant signal at δ 179.6 of a carbonyl group.

Based on all spectral data, the structure of **HC1** was clarified as a long chain saturated ketone.

$$H_3C_n(H_2C)-\overset{\overset{\displaystyle O}{\|}}{C}-(CH_2)_nCH_3$$

long chain saturated ketone

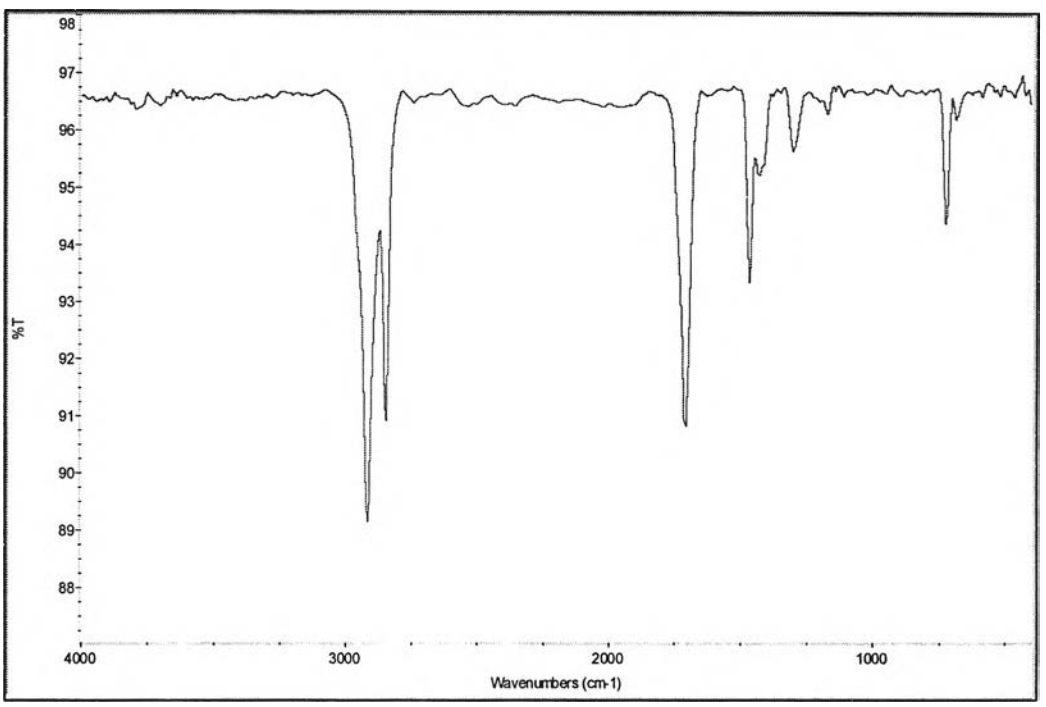

Figure 2.55 The IR spectrum of **HC1**

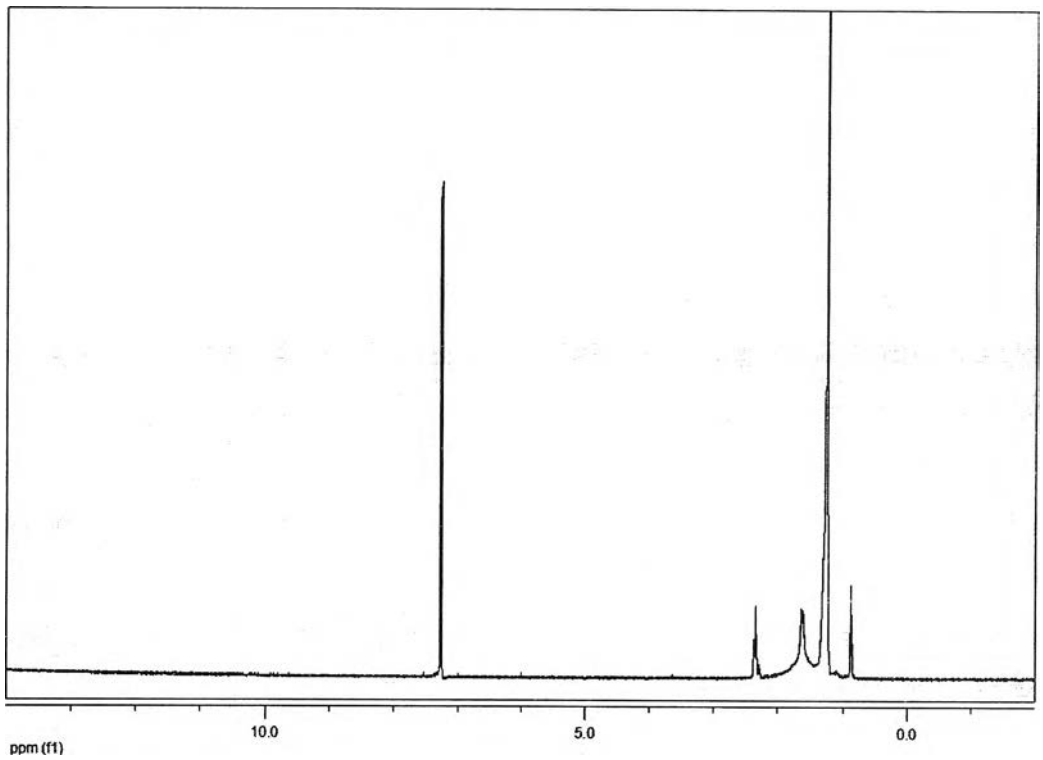

Figure 2.56 The ^{1}H-NMR spectrum of **HC1**

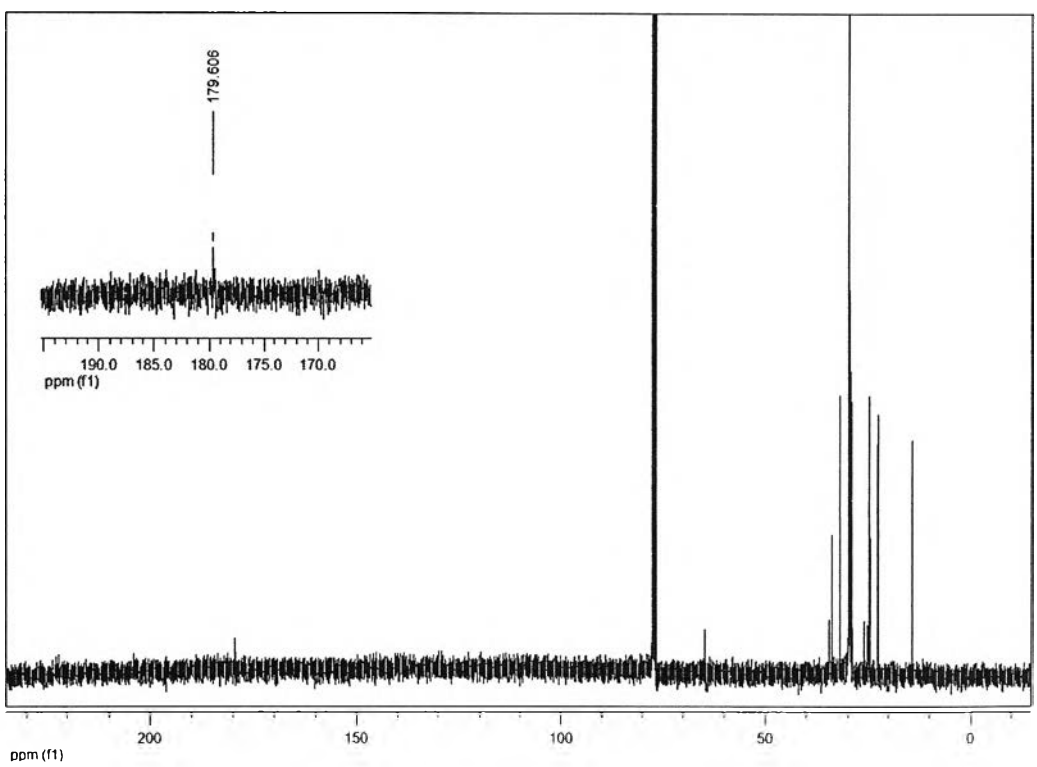

Figure 2.57 The ^{13}C-NMR spectrum of **HC1**

Structural elucidation of HC2

HC2 was yielded as white crystal (22.70 mg) with m.p. 81-82°C and R_f value 0.74 (40% EtOAc in hexane). This compound was soluble in chloroform, and CH_2Cl_2. It could not be detected on TLC under UV light, but can be detected with 10% H_2SO_4 in EtOH indicated that there was not of a conjugated double bond in this molecule. In addition, this compound showed a positive violet color with Liebermann-Burchard's reagent. Therefore, this compound was presumed to contain a triterpenoid nucleus. According to the spectroscopic data, the IR spectrum (Figure 2.58) of this compound gave the significant absorption peaks of a hydroxyl group at 3268-3626 cm^{-1}, carbonyl group at 1734 cm^{-1}, C=C stretching vibration at 1466 cm^{-1} and C-H stretching vibration of CH_2 and CH_3 at 2852 and 2918 cm^{-1}. Concerning with the ^{1}H-NMR ($CDCl_3$) spectrum of **CH2** (Figure 2.59), it exhibited a significant intensity signal at δ 0.61-2.25 (m) of methine, methylene and methyl groups in a molecule. The signal of three olefinic protons was discovered at δ 4.53 (m), 5.07 (m) and 5.30 (m). The signals of olefinic carbons at δ 122.6, 129.2, 138.3 and 139.7, respectively could also be endorsed previous observation. The carbonyl group could also be observed at δ 173.3 in the ^{13}C-NMR ($CDCl_3$) spectrum (Figure 2.60).

Gathering from the above data, the structure of **HC2** is no doubt a mixture of triterpenoid ester.

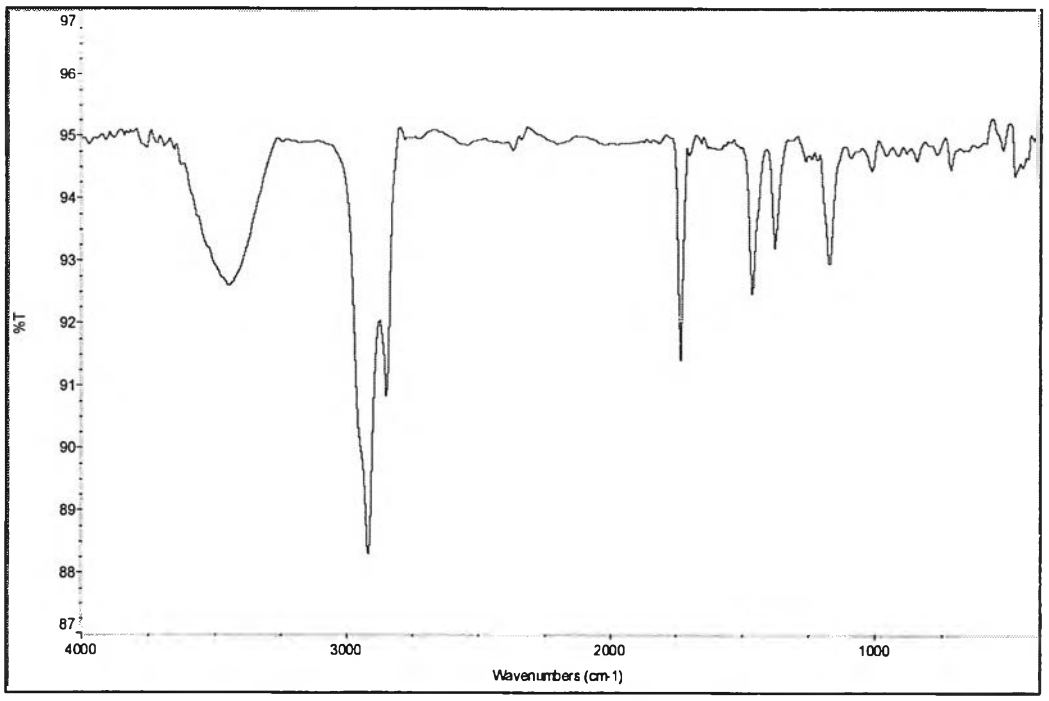

Figure 2.58 The IR spectrum of **HC2**

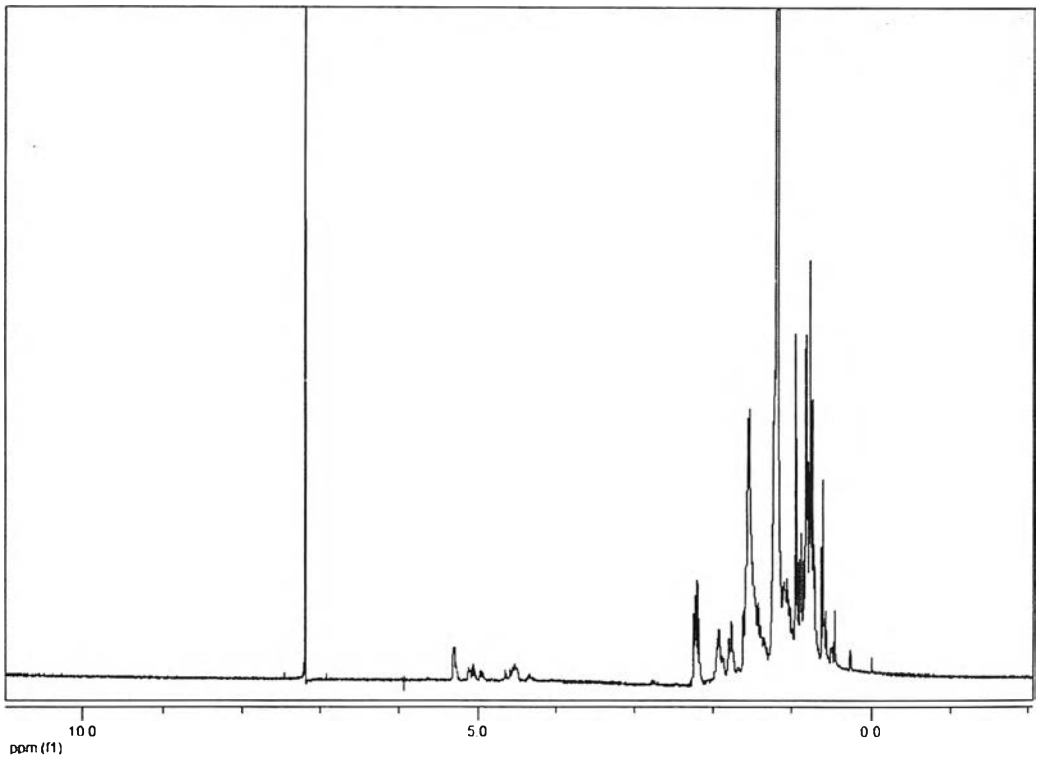

Figure 2.59 The ^{1}H-NMR spectrum of **HC2**

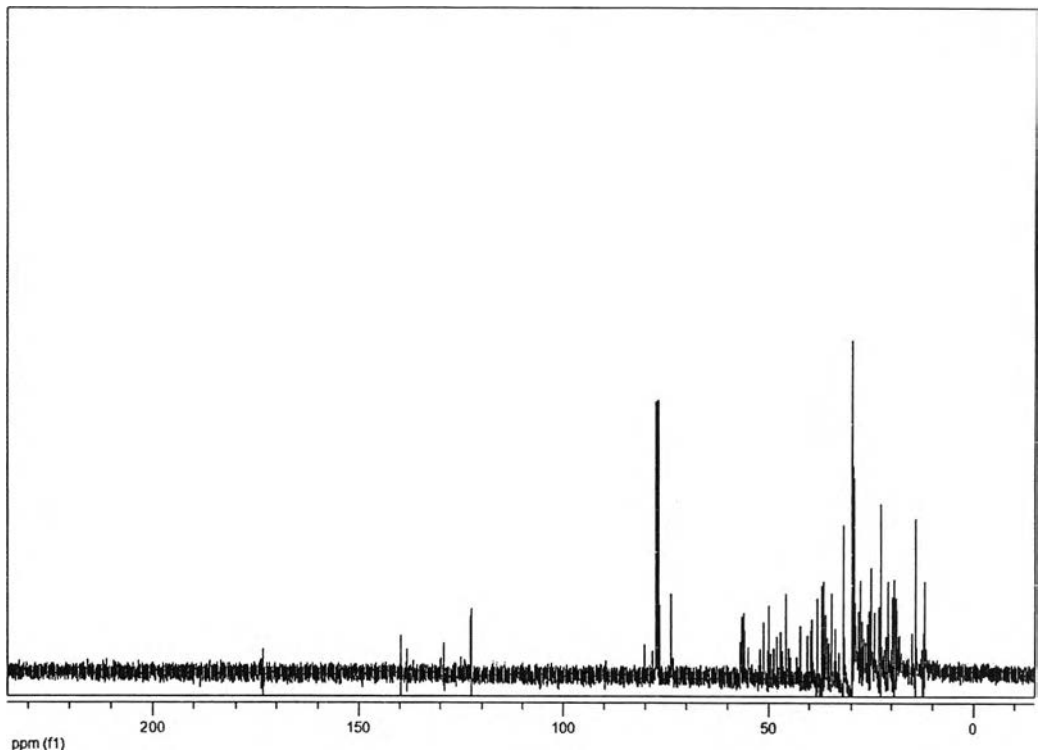

Figure 2.60 The ^{13}C-NMR spectrum of **HC2**

Structural elucidation of HC3

HC3 was acquired as white needle crystal (72.40 mg) with m.p. 132-134°C and R_f value 0.47 (40% EtOAc in hexane). This compound was soluble in chloroform, and CH_2Cl_2. It could not be detected on TLC under UV light, but can be detected with 10% H_2SO_4 in EtOH indicated that no conjugated double bond in this molecule was present. In addition, this compound showed a positive greenish blue solution with Liebermann-Burchard's reagent. This compound therefore contained a steroidal nucleus. According to the spectroscopic data, the IR spectrum (Figure 2.61) of this compound gave the significant absorption peaks of hydroxyl group at 3089-3687 cm^{-1}, C=C stretching vibration at 1459 cm^{-1} and C-H stretching vibration of CH_2 and CH_3 at 2867 and 2937cm^{-1}. Concerning with the ^{1}H-NMR ($CDCl_3$) spectrum of **CH3** (Figure 2.62), it exhibited a significant intensity signal at δ 0.68-2.35 (m) of methine, methylene and methyl groups in a molecule. The signal of three olefinic protons was detected at δ 5.04-5.02 (m), 5.12-5.18 (m) and 5.35 (m). The signal of the proton connecting to a hydroxyl group was detected at δ 3.52. Furthermore in good agreement with ^{1}H-NMR data, the signal of four olefinic carbons could be detected at δ 121.7, 129.2, 138.3 and 140.7, respectively in the ^{13}C-NMR ($CDCl_3$) spectrum

(Figure 2.63). In addition, this compound showed the R_f value corresponding to an authentic stigmasterol, the common steroid found in plants.

As a result of its physical properties and spectroscopic data, it could be noticeably concluded that this compound was stigmasterol.

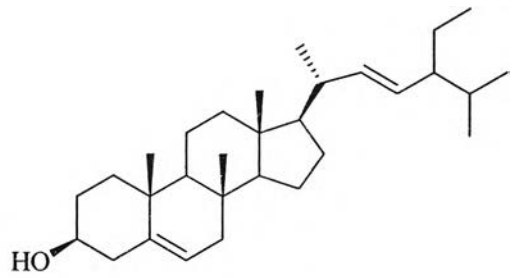

stigmasterol

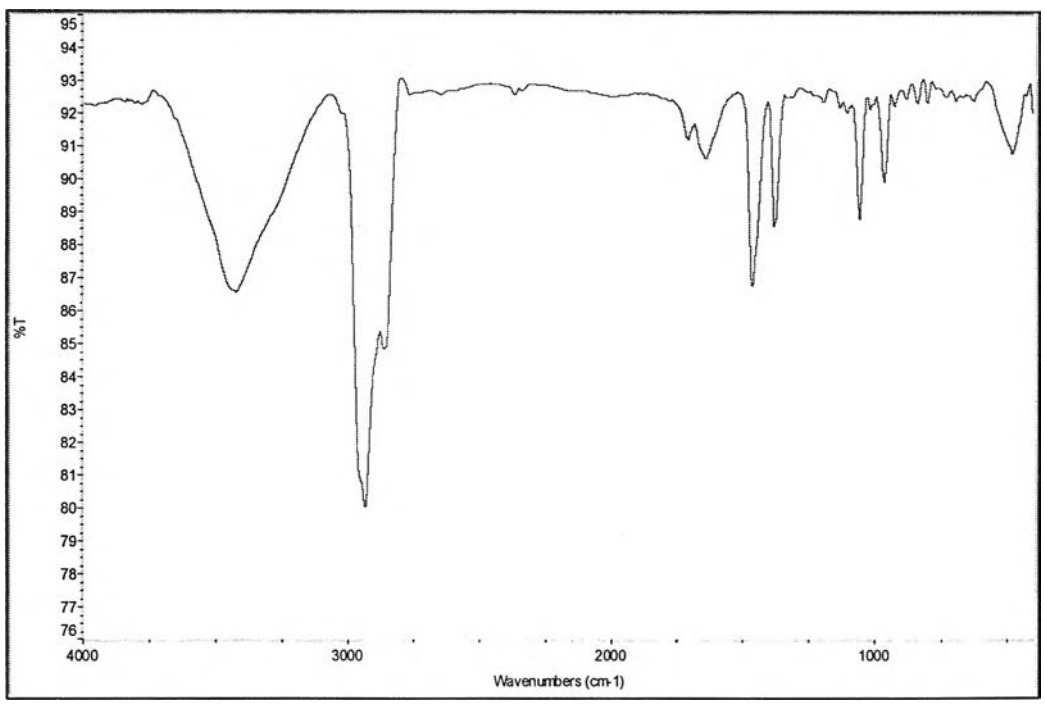

Figure 2.61 The IR spectrum of **HC3**

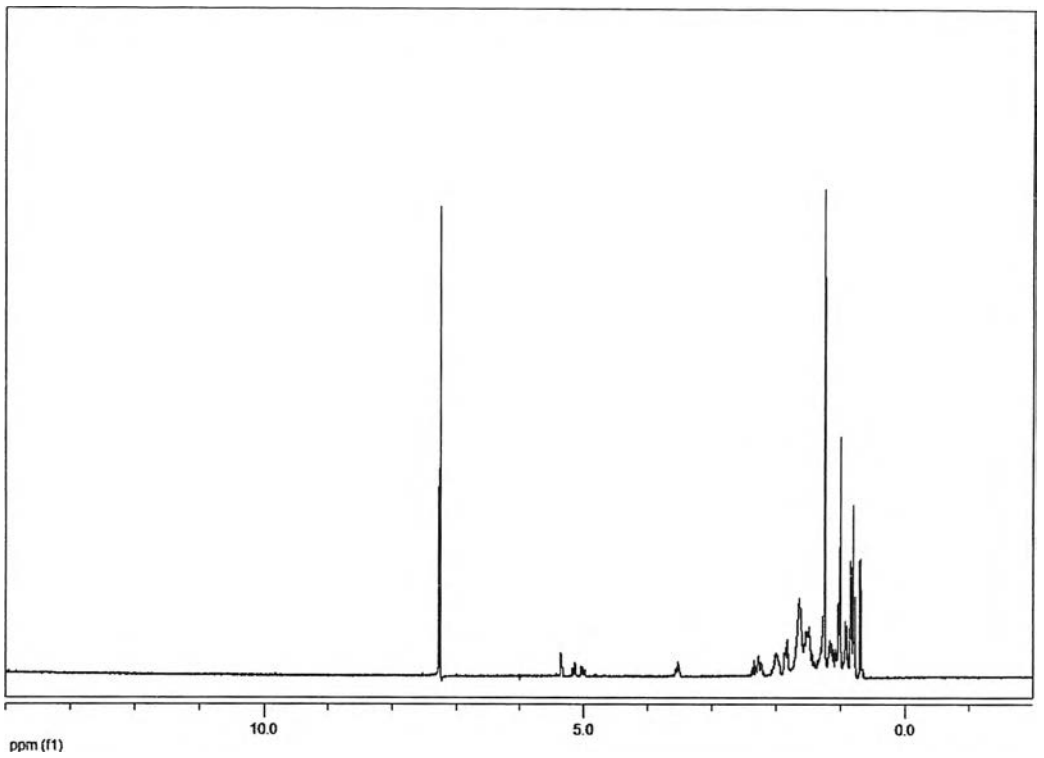

Figure 2.62 The ^{1}H-NMR spectrum of **HC3**

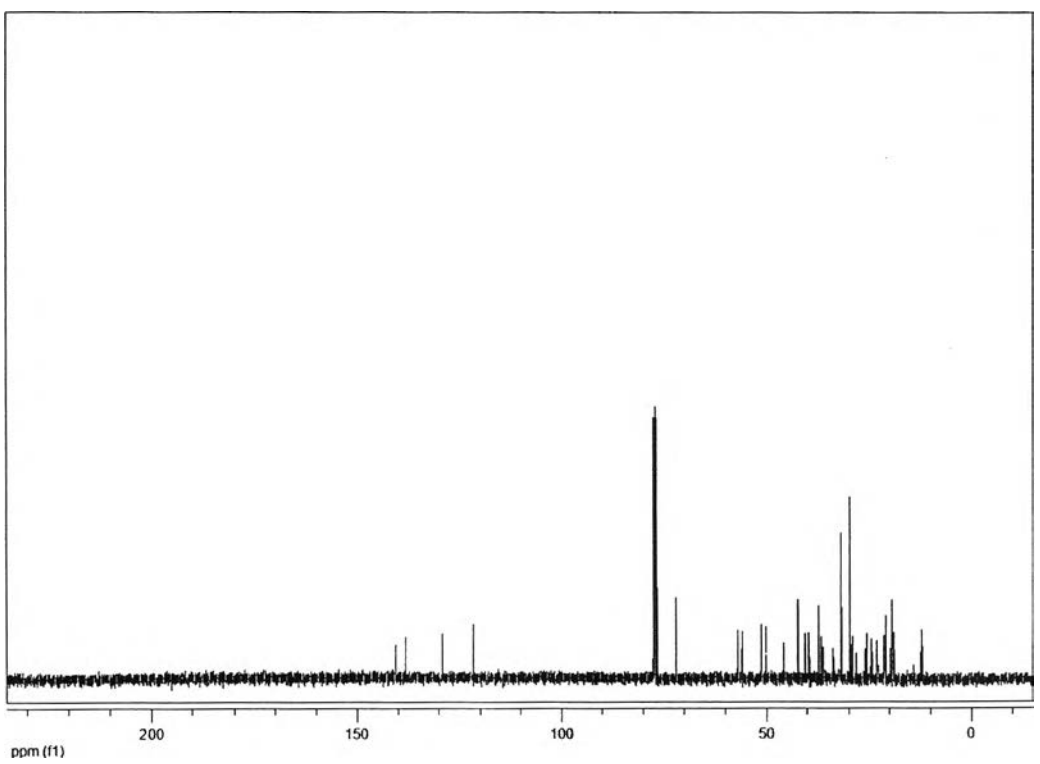

Figure 2.63 The ^{13}C-NMR spectrum of **HC3**

In summary, three substances, long chain saturated ketone, a mixture of triterpenoid ester and stigmasterol, could be isolated from fraction I-III of the hexane extract from *D. oliveri* heartwoods.

2.3.4 The Separation of EtOAc Extract

According to the monitoring of EtOAc extract (150 g) by TLC, this extract displayed similar spots as detected for CH_2Cl_2 extract. Therefore, the chemical constituents of EtOAc extract should be resembled to those of CH_2Cl_2 extract. The EtOAc extract as a dark brown material was fractioned using silica gel (< 45 μm, cat No. 7731) column chromatography eluting by gradient eluent with increasing polarity of CH_2Cl_2, EtOAc in CH_2Cl_2 and finally MeOH in EtOAc, respectively. The eluted solution was collected approximately 2000 mL. Every fraction collected was concentrated to a small volume and then monitored by TLC. The fractions which contained similar components were combined. The results of separation are shown in Scheme 2.10 and Table 2.14.

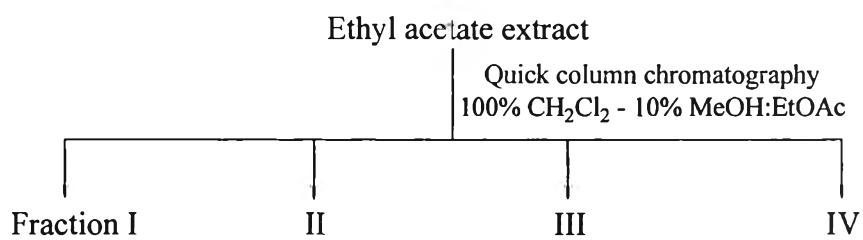

Scheme 2.10 The separation of EtOAc extract

The separation of EtOAc extract using gradient eluent started form 100% CH_2Cl_2 until 10% MeOH in EtOAc afforded 4 fractions (I-IV).

Table 2.14 The separation of EtOAc extract

Fraction	Solvent system	Remarks	Weight (g)
I	100% CH_2Cl_2 10% EtOAc:CH_2Cl_2	Yellow syrup	25.63
II	20% EtOAc:CH_2Cl_2- 30% EtOAc: CH_2Cl_2	Yellow syrup	6.36
III	40% EtOAc:CH_2Cl_2- 50% EtOAc: CH_2Cl_2	Dark brown syrup	19.71
IV	60% EtOAc: CH_2Cl_2 10% MeOH:EtOAc	Dark brown syrup	32.68

Separation of Fraction I

According to the results of monitoring fraction I (25.63 g) by TLC, this fraction exhibited the major spot with the same R_f value as that detected for **D3**. Therefore, it is rationalized not to separate and to further explore this fraction. During the evaporation of solvent from this fraction, it was noticed that some white needle crystal deposited. These crystals were filtered and later comprehended that they were **D3** (87.40 mg).

Separation of Fraction II

Fraction II contained some white powder solid and pale brown solid. These solids were filtered to obtain white powder solid (43.00 mg) and pale brown solid (641.20 mg). Monitoring these solids by TLC compared with the constituents obtained from CH_2Cl_2 extract, these solids exhibited the same R_f values as those of the compounds previously isolated and characterized as **D5** and **D6**, respectively.

Separation of Fraction III

This fraction comprised some white powder solid and pale brown powder solid which were filtered to furnish white powder solid (400.40 mg) and pale brown powder (1.97 g). Pursuing these solids by TLC compared with the constituents obtained from CH_2Cl_2 extract, these solids exhibited similar spots with the same R_f

values detected for **D6** and a mixture of **D6** and **D8**, respectively. After evaporation of the solvent, dark brown material was afforded which was further separated by silica gel column chromatography using gradient elution of 40% to 60% EtOAc in hexane to furnish **D6** (57.30 mg) and **D8** (133.80 mg).

Separation of Fraction IV

Monitoring fraction IV (32.68 g) by TLC revealed that this fraction exhibited similar R_f values of the spots as detected for **D6** and **D8**. This fraction was thus inattentive to separate and further explore. Some pale brown powder solid was noticed during the evaporation the solvent. These solids were filtered and later comprehended that they were a mixture of **D6** and **D8** (9.12 g).

In conclusion, most chemical constituents in EtOAc extract from *D. oliveri* heartwoods were quiet similar to that found in CH_2Cl_2 extract. The isolation diagram of all substances was summarized in Scheme 2.11.

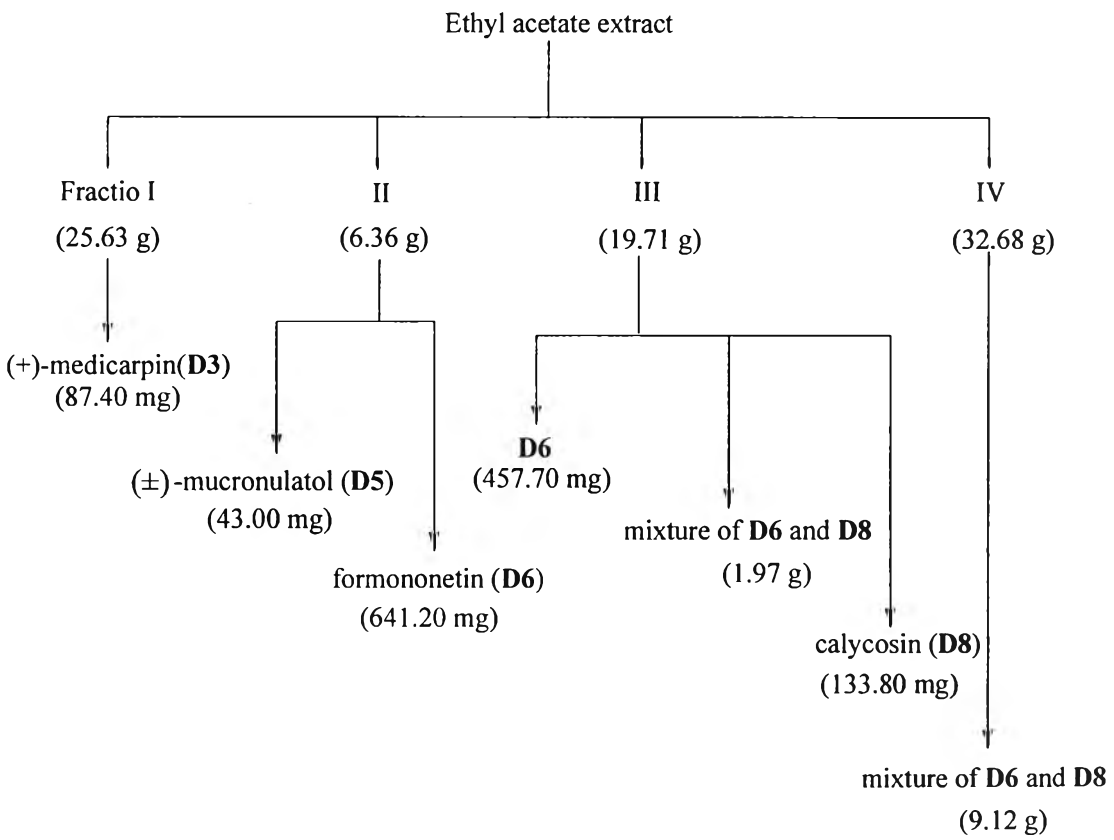

Scheme 2.11 Isolation diagram of the EtOAc extract from the heartwoods of *D. oliveri*

2.3.5 Biological Activity Study of Isolated Compounds from the CH_2Cl_2 Extract of *D. oliveri* Heartwoods

As aforementioned discussion, the separation of CH_2Cl_2 extract from *D. oliveri* heartwoods led to the isolation of eight substances. The isolated substances were further studied for biological activity. The radical scavenging effect on DPPH radical, antifungal activity, antimicrobial activity and cytotoxicity were selected for exploration followed the protocols described in Section 2.2.5.

2.3.5.1 Scavenging Effect on DPPH Radical

The DPPH radical scavenging activity by TLC method of isolated substances revealed that **D4**, **D5**, **D7** and **D8** showed significant activity toward DPPH radical. The results of scavenging effect on DDPH by TLC assay are presented in Table 2.15.

Table 2.15 TLC autography assay for DPPH radical scavenger

Sample	Antioxidant Activity
D1	-
D2	-
D3	-
D4	++
D5	+++
D6	-
D7	+++
D8	++

+++ : positive results observed immediately
++ : positive results observed after 5 minutes

The quantitative analysis for determination IC_{50} values of those substances was then performed using spectrophotometric method as described in Section 2.2.5.1. The results of scavenging effect on DPPH by spectrophotometric assay of each compound are presented in Appendix. The curve between the percentage of radical scavenging and the concentration of each sample was plotted. Figure 2.64 as an instance shows the curve of radical scavenging effect for **D5**.

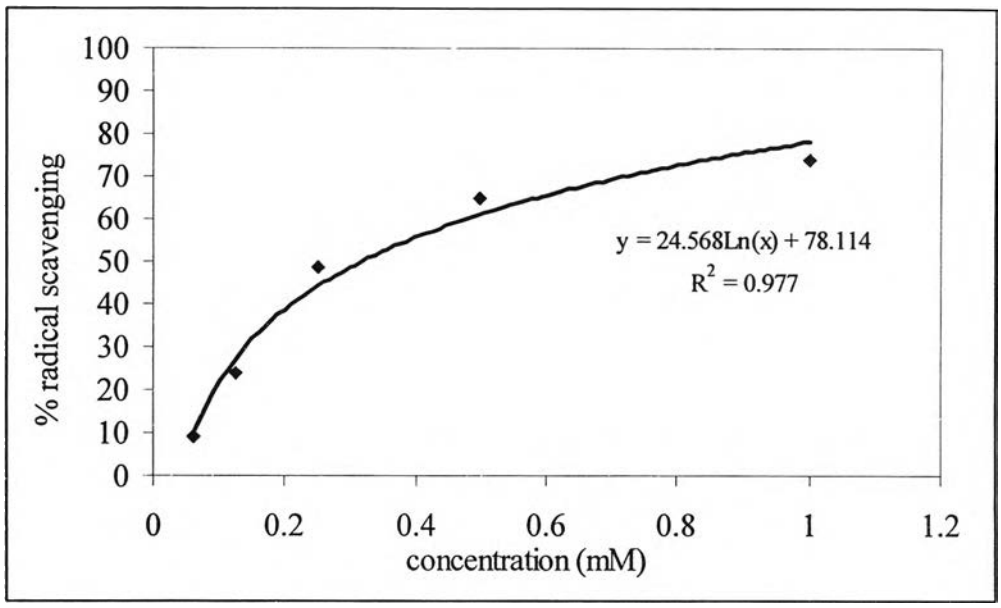

Figure 2.64 DPPH radical scavenging effect of **D5**

The IC_{50} values of each substance were calculated from the logarithmic equation of each curve and are tabulated in Table 2.16.

Table 2.16 IC_{50} values of radical scavenging effect on DPPH radical

Substances	Structure	IC_{50} (mM)
D4	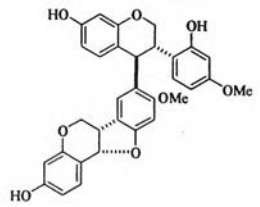	> 1.00
D5	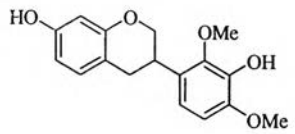	0.32
D7	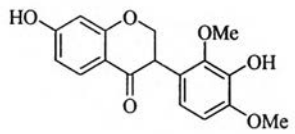	0.48
D8	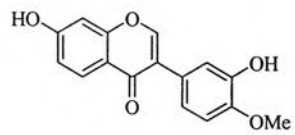	0.54
BHA	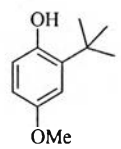	0.12

From the result of radical scavenging effect on DPPH radical spectrophotometric assay, it was found that **D5** ((±)-mucronulatol) showed the highest activity whereas **D7** (±)-violanone and **D8** and (calycosin) exhibited moderate activity. **D4** ((+)-3,4-*trans*-[3-hydroxy-9-methoxypterocarpan-8-yl]-2',7-dihydroxy-4'-methoxyisoflavan) displayed low activity among all tested substances. From the comparison with BHA (butylated hydroxyanisole), a commercial antioxidant, the activity of all tested substances was compatible with BHA.

As the comparison with preliminary result of CH_2Cl_2 extract, it was believed that the active components which scavenged the DPPH radical on TLC should be **D5**, **D7** and **D8**. Therefore, this inference was ensured by spectrophotometric method. The IC_{50} values of each substance pointed out that **D5** gave the lowest IC_{50} among those substances tested. By this reason, it could obviously conclude that **D5** was responsible as the active antioxidant agent from the CH_2Cl_2 extract of *D. oliveri* heartwoods.

2.3.5.2 Antifungal Activity

Eight isolated substances from the CH_2Cl_2 extract from the heartwoods of *D. oliveri* were investigated for antifungal activity. Two phytophatogenic fungi *Fusarium oxysporum* and *Colletotrichum gloeosporioides* were employed. The TLC plate containing spot of each substance was sprayed with spore suspension of those two mentioned fungi and incubated in a moisture chamber at 25°C for 2 days. The inhibition was observed by clear zone of active component against blue background.

Table 2.17 The antifungal activity of isolated substances

Samples	Fungi	
	Fusarium oxysporum	***Colletotrichum gloeosporioides***
D1	+	+
D2	-	-
D3	+	+
D4	-	-
D5	+	+
D6	-	-
D7	+	+
D8	-	-

+ : positive - : negative

When the TLC plate was sprayed with spore suspension of *F. oxysporum* and *C. gloeosporioides*, **D1** (*trans*-cinnamic acid), **D3** ((+)-medicarpin)), **D5** ((±)-mucronulatol) and **D7** ((±)-violanone) showed inhibitory effect as presented in Table 2.16. It should thus be denoted that those compounds had tendency to inhibit the fungal growth. Therefore, these compounds were further investigated the minimum amount required for the inhibition of fungal growth on TLC as described in Section 2.2.5.2. The phytophatogenic fungi of *Fusarium oxysporum* and *Alternaria brassicicola* were employed for the minimum amount required for the antifungal assay. The results of minimum amount required for the antifungal assay are deduced as shown in Table 2.18.

Table 2.18 The minimum amount required for the inhibition of fungal growth on TLC plates

Substances	Antifungal activity (μg)	
	Fusarium oxysporum	*Alternaria brassicicola*
D1	1.0	1.0
D3	0.5	0.5
D5	0.5	>10
D7	1.0	>10
Iprodion	0.1	0.1
Captan	0.1	0.1

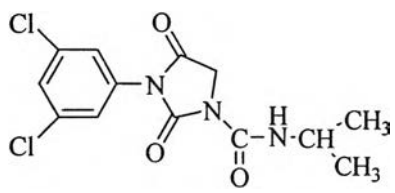

Iprodion

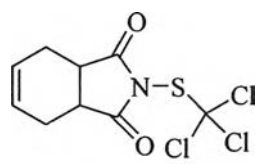

Captan

According to the results presented above, the minimum amount required for the antifungal assay: **D3** displayed the highest activity (0.5 μg) against both *F. oxysporum* and *A. brassicicola* whereas **D5** exposed the highest activity against only *F. oxysporum* and **D7** disclosed the lowest activity (>10 μg) against *A. brassicicola* among of those substances. **D1** indicated medium activity (1 μg) against both *F. oxysporum* and *A. brassicicola*. Furthermore, **D7** showed moderate activity toward *F. oxysporum*.

From the comparison with iprodione and captan, commercial antifungal agent, the activity of **D3** was compatible. By this result, it could manifestly conclude that **D3** was the active antifungal activity against *F. oxysporum* and *A. brassicicola* from the CH_2Cl_2 extract of *D. oliver* heartwoods.

In addition, in 2004 Deesamer and co-workers [80] investigated the α-glucosidase inhibitory activity of *trans*-cinnamic acid and its derivatives. 4-Methoxy-*trans*-cinnamic acid and 4-methoxy-*trans*-cinnamic acid ethyl ether showed the highest potent inhibitory activity among of *trans*-cinnamic acid

derivatives. The presence of substitutents at 4-position of *trans*-cinnamic acid altered the α-glucosidase inhibitory activity. Increasing of bulkiness and the chain length of 4-alkoxy substituents as well as the increasing of electron withdrawing group has been shown to decrease the inhibitory activity. 4-Methoxy-*trans*-cinnamic acid was a noncompetitive inhibitor for α-glucosidase, whereas, 4-methoxy-*trans*-cinnamic acid ethyl ester was a competitive inhibitor. These results indicated that *trans*-cinnamic acid derivatives could be classified as a new group of α-glucosidase inhibitorys. Moreover, Thedpitak [81] evaluated antifungal activity of *trans*-cinnamic acid derivatives against four phytopathogenic fungi: *Alternaria porri*, *Fusarium oxysporum*, *Pestalotiopsid* sp. and *Phytophthora parasitica*, in order to define a possible structure activity relationship (SAR). 2,6-Dichloro-*trans*-cinnamic acid showed strong activity among fifty *trans*-cinnamic acid derivatives and may be suitable compounds for an application to plants. In addition, 2,6-dichloro-*trans*-cinnamic acid was much more effective than captan and iprodione, a conventional chemical fungicide, and therefore can be an antifungal agent, particularly to control *Pestalotiopsid* sp. and *Phytophthora parasitica*.

2.3.5.3 Antimicrobial Activity

The antimicrobial activity against *Escherichia coli* (CIP 54127), *Staphylococcus aureus* (CIP 53124) and *Saccharomyces cerevisiae* (CIP 28383) was performed by Laboratoie Synthese et Etude de Substances Naturelles a Activites Biologiques, Faculte des Sciences et Techniques de St Jerome, Marseille, France as described in Section 2.2.5.3. Streptomycin and econazole were employed as commercial antimicrobial agents in this assay. The antimicrobial activity results are concluded as presented in Table 2.19.

Table 2.19 Antimicrobial activity of isolated compounds

Samples	Antimicrobial activity* (μg/mL)		
	E. coli (CIP 54127)	*S. aureus* (CIP 53124)	*S. cerevisiae* (CIP 28383)
D1	>100	>100	>100
D2	>100	>100	>100
D3	>100	>100	>100
D4	>100	>100	>100
D5	>100	>100	>100
D6	>100	>100	>100
D7	>100	>100	>100
D8	>100	>100	>100
Streptomycin	6-12	6-12	-
Econazole	-	-	<3

*: The minimum inhibitory concentration was evaluated as the microbial agent concentration inhibiting 80% of absorbance regarding to the reference (no agent added)

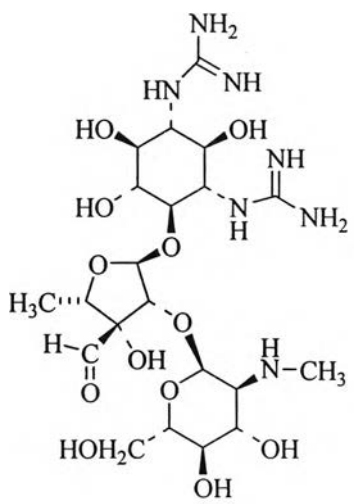

Streptomycin

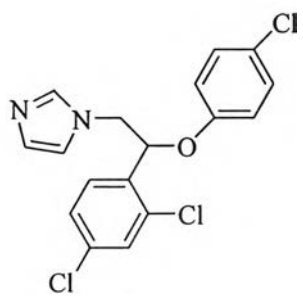

Econazole

As the results presented in Table 2.18, it was found that all isolated substances (**D1-D8**) did not show antimicrobial activity against *E. coli*, *S. aureus* and *S. cerevisiae*.

2.3.5.4 Cytotoxicity against HepG2

Eight isolated substances were also evaluated for cytotoxicity against HepG2. IC_{50} implied the concentration of samples that killed 50% of human liver tumor cells. The results of cytotoxicity against HepG2 are deduced as shown in Table 2.20.

Table 2.20 Cytotoxicity of isolated compounds against HepG2

Samples	IC_{50} (μg/mL)
D1	10.5
D2	2.3
D3	2.3
D4	11.1
D5	3.7
D6	10.5
D7	4.7
D8	11.1

From the above results, among isolated compounds, **D2** and **D3** displayed significant cytotoxicity against HepG2 cells with IC_{50} values of 2.3 μg/mL. **D5** and **D7** showed moderate cytotoxicity against HepG2 cells with IC_{50} values of 3.7 and 4.7 μg/mL, respectively whereas the other compounds disclosed low cytotoxicity against HepG2 cells with IC_{50} values of >10 μg/mL.

In addition, cytotoxicity studies of **D3**, a major constituent, were reported in the literature [82, 83]. It showed moderate cytotoxicity against KB human oral epidermoid cell line with EC_{50} value of 2.4 μg/mL [82] and HL-60 human leukemia cells with IC_{50} value of 18 μmol [83].

2.3.5.5 Cytotoxicity against Diamondback Moth

Four isolated substances (**D1**, **D3**, **D6** and **D7**) were selected to evaluate for cytotoxicity against diamondback moth, *Plutella xylostella*, as described in Section 2.2.3.5. LC_{50} and LC_{95} implied the concentration of samples that killed 50% and 95% of diamondback moth, respectively. The results of cytotoxicity against diamondback moth are concluded as shown in Table 2.21.

Table 2.21 Cytotoxicity of isolated compounds against diamondback moth

Samples	LC_{50} (ppm)	LC_{95} (ppm)
D1	172	3192
D3	99	1142
D6	102	1652
D7	92	794

According to the results presented above, **D7** showed high cytotoxicity against diamondback moth with LC_{50} and LC_{95} values of 92 and 794 ppm, respectively. **D3** and **D6** displayed moderate cytotoxicity against diamondback moth with LC_{50} values of 99 and 102 ppm, respectively and **D1** disclosed low cytotoxicity against diamondback moth with LC_{50} value of 172 ppm.

2.3.5.6 Cytotoxicity against Mosquito Larvae

D1, **D3**, **D6** and **D7** were selected to evaluate for cytotoxicity against mosquito larvae, *Aedes aegypti*, as described in Section 2.2.3.6. LC_{50} and LC_{95} implied the concentration of samples that killed 50% and 95%, respectively of mosquito larvae. The results of cytotoxicity against mosquito larvae are deduced as shown in Table 2.22.

Table 2.22 Cytotoxicity of isolated compounds against mosquito larvae

Samples	LC_{50} (ppm)	LC_{95} (ppm)
D1	210	3906
D3	200	1374
D6	162	1482
D7	121	1048

As the results presented in Table 2.22, **D7** showed high cytotoxicity against mosquito larvae with LC_{50} and LC_{95} values of 121 and 1048 ppm, respectively. **D6** displayed moderate cytotoxicity against mosquito larvae with LC_{50} and LC_{95} values of 162 and 1482 ppm, respectively. **D1** and **D3** displayed low cytotoxicity against diamondback moth with LC_{50} values of 210 and 200 ppm, respectively.

2.3.6 Biosynthesis of the Flavonoid Derivatives

All flavonoids are derived from a chalcone precursor, the product of the condensation of 4-coumaroyl CoA (a product of the central phenylpropanoid pathway) and three molecules of malonyl CoA (formed from acetate *via* a cytoplasmic form of acetyl CoA carboxylase) by the enzyme chalcone synthase (CHS) and chalcone reductase (CHR) [40, 84]. The pathways leading to the major classes of flavonoid derivatives are summarized in Scheme 2.12.

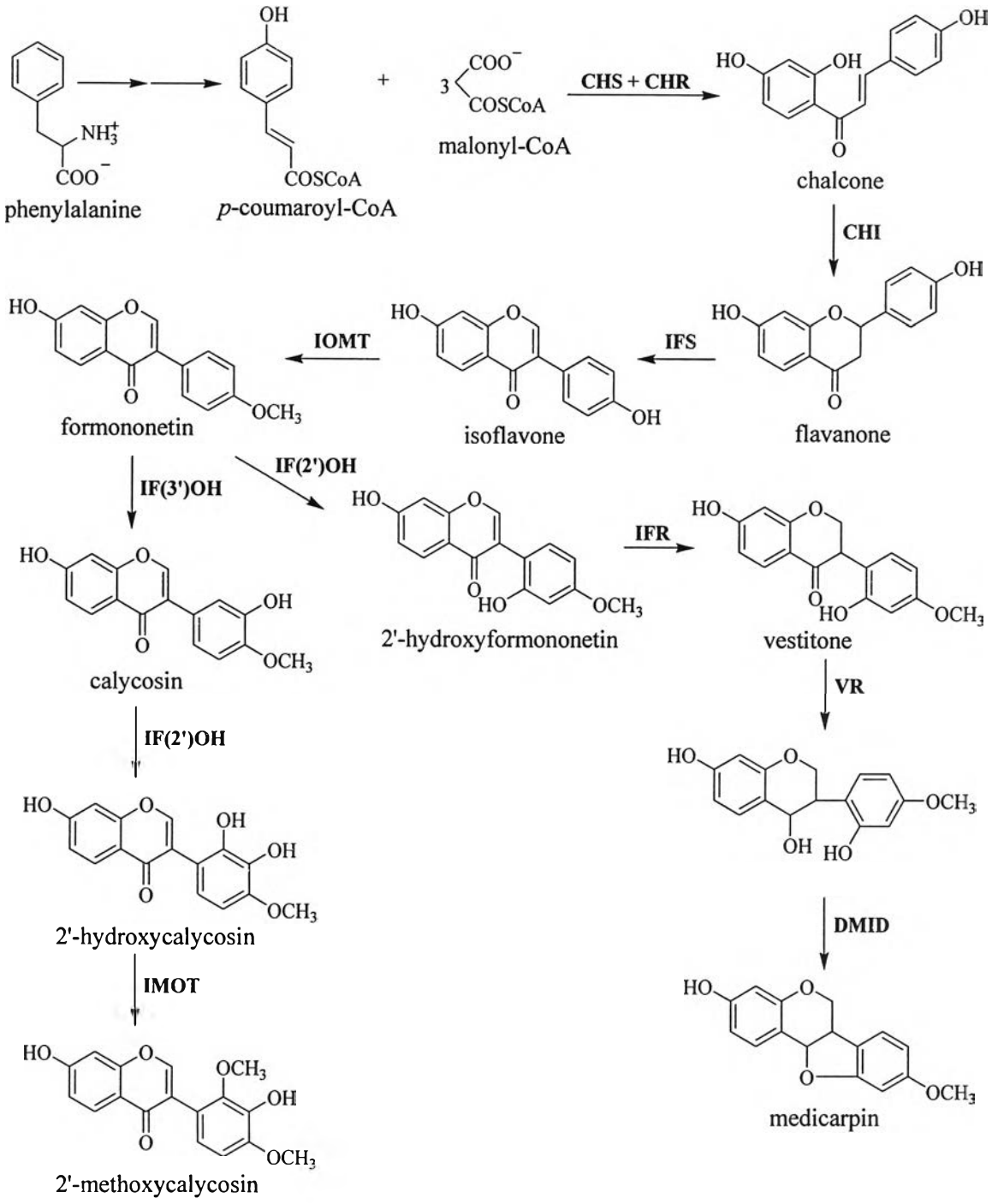

Scheme 2.12 The biosynthesis of flavonoid derivatives. The names of the enzymes catalyzing each step are abbreviated as follows: CHS, chalcone synthase; CHR, chalcone reductase; CHI, chalcone isomerase; IFS, isoflavone synthase; IOMT, isoflavone *O*-methyl transferase; IFOH, isoflavone hydroxylase; IFR, isoflavone reductase; VR, vesitone reductase; DMID, dehydratase; PTOH, pterocarpan hydroxylase and PTOMT, pterocarpan *O*-methyl transferase.

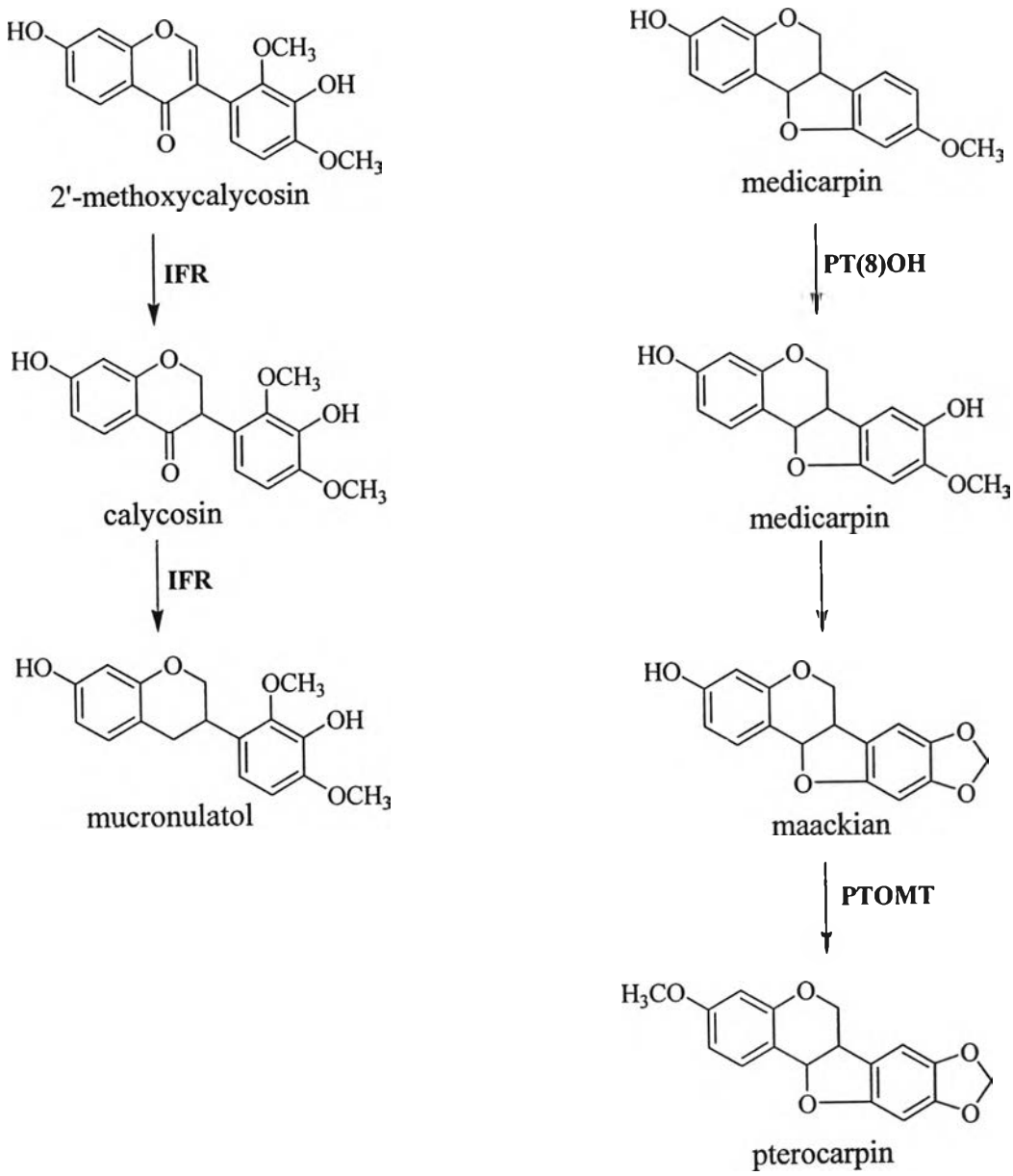

Scheme 2.12 (continued)

2.4 CONCLUSION

During the course of this research focusing on the search for bioactive constituents, four Thai plants in Leguminosae family were accumulated for preliminary insecticidal activity against common cutworm, *Spodoptera litura*, and radical scavenging effect on DPPH radical screening. As the results of screening test, the extract from the heartwoods of *Dalbergia oliveri* exhibited significant radical scavenging effect on DPPH radical. Therefore, chemical constituents and biological activity of the extracts form *D. oliveri* heartwoods were thoroughly examined. Three substances, long chain saturated ketone, a mixture of triterpenoid ester and stigmasterol were isolated from the hexane extract. After fractionation and purification, eight pure compounds (**D1-D8**) were obtained from the CH_2Cl_2 extract. Concerning with the EtOAc extract, most chemical constituents (**D3**, **D5**, **D6** and **D8**) in this extract were similar to those found in CH_2Cl_2 extract. All isolated substances were further elucidated by means of their physical properties and spectroscopic evidences. The structures of isolated substances are summarized as presented in Table 2.23.

Table 2.23 Isolated substances from the CH_2Cl_2 extract of *D. oliveri* heartwoods

Substance	Weight	% Yield*	Structure	Remark
Compound **D1**: 3-phenylpropenoic acid (*trans*-cinnamic acid)	34.80 mg	8.7×10^{-4}	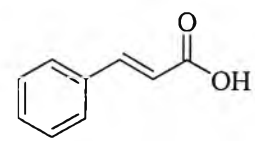	White crystal
Compound **D2**: (+)-3-methoxy-8,9-methylenedioxypterocarpan ((+) (*6aS,11aS*)-pterocarpin)	14.70 mg	3.7×10^{-4}	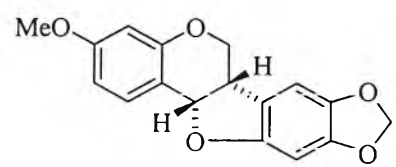	Yellow needle crystal
Compound **D3**: (+)-3-hydroxy-9-methoxypterocarpan ((+) (*6aS,11aS*)-medicarpin)	7.36 g	1.8×10^{-1}	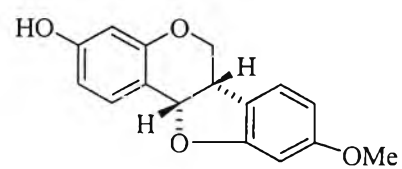	White needle crystal

Table 2.23 (continued)

Substance	Weight	% Yield*	Structure	Remark
Compound **D4**: (+)-3,4-*trans*-[3-hydroxy-9-methoxypterocarpan-8-yl]-2',7-dihydroxy-4'-methoxyisoflavan	87.50 mg	2.2 x10^{-3}		Brown solid
Compound **D5**: (±)-3',7-dihydroxy-2',4'-dimethoxyisoflavan ((±)-mucronulatol)	181.20 mg	4.5 x 10^{-3}		White powder solid
Compound **D6**: 7-hydroxy-4'-methoxyisoflavone (formononetin)	1.92 g	4.8 x 10^{-2}		Pale brown powder solid

Table 2.23 (continued)

Substance	Weight	% Yield*	Structure	Remark
Compound **D7**: (±)-3',7-dihydroxy-2',4'-dimethoxyisoflavanone ((±)-violanone)	380.50 mg	9.5×10^{-3}	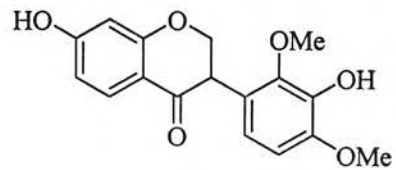	White needle crystal
Compound **D8**: 3',7-dihydroxy-4'-methoxyisoflaone (calycosin)	233.00 mg	5.8×10^{-3}	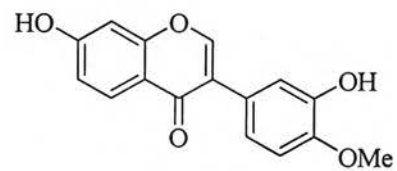	Brown powder solid

*The percentage yield of isolated substances was calculate based on the dried *D. oliveri* heartwoods (4 kg)

Isolated substances were further bioassayed. The selected bioactivity assays are as follows: scavenging effect on DPPH radical, antiplantpathogenic fungal activity, antimicrobial activity and cytotoxicity activity. **D2** ((+)-pterocarpin) displayed high cytotoxicity against HepG2 cells with IC_{50} value of 2.3 μg/mL. **D3** ((+)-medicarpin), a major constituent, displayed significant antifungal activity against both *Fusarium oxysporum* and *Alternaria brassicicola* and cytotoxicity toward human hepatocellular carcinoma (HepG2) cells and medium and low cytotoxicity against diamondback moth and mosquito larvae with LC_{50} values of 99 and 200 ppm, respectively. **D5** ((±)-mucronulatol) exhibited the highest scavenging activity toward DPPH radical as well as the highest antifungal activity against *F. oxysporum* and the medium cytotoxicity against HepG2 whereas the minimum amount of this compound required to inhibit growth of the fungus *Alternaria brassicicola* was determined as >10 μg. **D7** ((±)-violanone) revealed high cytotoxicity against diamondback moth and mosquito larvae with LC_{50} values of 92 and 121 ppm, respectively, medium antifungal activity against *F. oxysporum*, scavenging activity toward DPPH radical and cytotoxicity against HepG2 and low antifungal activity against *A. brassicicola.*

Concerning with bioactivities of the other substances, **D1** (*trans*-cinnamic acid) showed moderate antifungal activity against both *F. oxysporum* and *A. brassicicola* and low cytotoxicity against HepG2, diamondback moth and mosquito larvae. **D4** ((+)-isoflavan-ptercarpan) exposed low cytotoxicity against HepG2 with IC_{50} value of 11.1 μg/mL. **D6** (formononetin) displayed moderate cytotoxicity against diamondback moth and mosquito larvae with LC_{50} values of 102 and 162 ppm, respectively and low cytotoxicity against HepG2 with IC_{50} value of 10.5 μg/mL. **D8** (calycosin) disclosed moderate scavenging activity toward DPPH radical with IC_{50} value of 0.54 mM and low cytotoxicity against HepG2 with IC_{50} value of 11.1 μg/mL. Concerning with antimicrobial activity against *Escherichia coli*, *Staphylococcus aureus* and *Saccharomyces cerevisiae*, all isolated substances revealed insignificant result.

The scavenging effect on DPPH radical, antifungal activity and antimicrobial activity and cytotoxicity of chemical constituents of the extract from *D. oliveri* heartwoods was addressed for the first time in chemical literature. In addition, **D4** was found for the first time in natural products.

In conclusion, it could be clearly seen that the heartwood of *D. oliveri* Gamble could be used as a good source of (+)-medicarpin, a significant antifungal substance.